The role of neprilysin in ocular surface homeostasis and corneal wound healing

Genova, Rachel Marie

Genova, R. M. (2020). The role of neprilysin in ocular surface homeostasis and corneal wound healing [University of Iowa]. https://doi.org/10.17077/etd.005281

THE ROLE OF NEPRILYSIN IN OCULAR SURFACE HOMEOSTASIS AND CORNEAL WOUND HEALING

by

Rachel Marie Genova

A thesis submitted in partial fulfillment
of the requirements for the Doctor of Philosophy degree in
Molecular Physiology and Biophysics in the Graduate College of
The University of Iowa

May 2020

Thesis Committee: Andrew Pieper, Thesis Supervisor
Michael G. Anderson
Matthew Harper
Andrew Russo Mark
Stamnes Michael
Welsh

ABSTRACT

The cornea is a transparent, dome-shaped structure that transmits and refracts light, and serves as a physical barrier against ocular pathogens. As the outermost tissue of the eye, the cornea is vulnerable to injury, an underreported and globally significant cause of vision loss. While superficial wounds stimulate rapid regeneration of the corneal epithelium, extensive injury can delay or overwhelm the ability of the cornea to heal completely. Even with our current medical and surgical treatment strategies, visual prognosis after severe corneal injury often remains guarded. Increasing our understanding of corneal wound healing mechanisms is therefore critical for development of improved therapies for corneal injury.

The work in this dissertation employs a mouse model of corneal injury to investigate wound healing mechanisms that we hypothesize could be targeted to accelerate recovery in human patients. We focus on the role of neprilysin (NEP), a widely distributed ectoenzyme that modulates inflammation by catalyzing the degradation of vasoactive and neuroinflammatory peptides. Though NEP has been identified in the human cornea, the function of this enzyme in the cornea is unknown. Using genetic and pharmacologic approaches, we characterized the contribution of NEP to homeostatic maintenance of the uninjured cornea and to repair of the chemically injured cornea.

We first established functional expression of NEP in the mouse cornea, where the enzyme most strongly immunolocalizes to the epithelial layer. Clinical examination, *in vivo* ocular surface imaging, and histological analysis of corneal tissue reveal no differences between NEP-deficient ($NEP^{-/-}$) and wild-type (WT) control mice in circumcorneal vasculature, corneal thickness, epithelial cellularity, or gross appearance of the ocular surface. However, $NEP^{-/-}$ mice have increased corneal innervation compared to WT controls. Collectively, these data indicate that loss of NEP activity does

not disrupt corneal homeostasis but may influence development or maintenance of corneal innervation.

To investigate the effect of NEP on corneal wound healing, we modeled chemical corneal injury and evaluated wound healing with slit lamp imaging over 1 week. By 3 days post-injury, $NEP^{-/-}$ mice had significantly smaller corneal defects compared to WT controls. We extended these findings by showing that daily intraperitoneal administration of the NEP inhibitor thiorphan also accelerates corneal epithelial wound healing in WT mice by 1 week post-injury without increasing inflammation, scarring, or neovascularization. Interestingly, *in vitro* wound healing assays with the TKE2 mouse corneal epithelial cell line suggest that thiorphan does not affect cell migration. Overall, these results provide insight into corneal wound healing mechanisms and identify NEP as a potential therapeutic target for treating severe corneal injury.

PUBLIC ABSTRACT

The cornea is a transparent, dome-shaped structure that focuses incoming light and provides a physical barrier against infection and damage to the eye. As the outermost tissue of the eye, the cornea is vulnerable to injury, an underreported and globally significant cause of vision loss. While superficial wounds are easily and rapidly repaired, extensive injury can overwhelm the ability of the cornea to heal normally. This can result in scarring, ulceration, and ultimately, compromised visual acuity. Depending on the extent of injury, both medical and surgical interventions may be required to restore corneal transparency. However, visual prognosis after severe corneal injury often remains guarded, even with our current treatment strategies. Increasing our understanding of corneal wound healing mechanisms is therefore critical for development of improved therapies for corneal injury.

The work in this dissertation employs a mouse model of corneal injury to investigate wound healing mechanisms that we hypothesize could be targeted to accelerate recovery and improve outcomes in human patients. We focus on the role of neprilysin (NEP), an enzyme involved in modulating inflammation throughout the body. Using genetic and pharmacologic approaches, we characterize the contribution of NEP to maintenance of the uninjured cornea and to repair of the chemically injured cornea. Overall, we provide insight into corneal wound healing mechanisms and identify NEP as a potential therapeutic target for treating severe corneal injury.

TABLE OF CONTENTS

LIST OF FIGURES vi

CHAPTER 1: INTRODUCTION 1

Overview of the Ocular Surface 1

Anatomy and Histology of the Cornea 1

Corneal Epithelial Homeostasis 9

Corneal Wound Healing: Uncomplicated Epithelial Injury 12

Corneal Wound Healing: Severe Injury and Its Complications 15

Neprilysin 20

Thesis Overview 27

CHAPTER 2: CONSTITUTIVE LOSS OF NEP ACTIVITY DOES NOT DISRUPT HOMEOSTASIS IN THE UNINJURED CORNEA 30

Background and Rationale 30

Materials and Methods 32

Results 39

Discussion 46

CHAPTER 3: CONSTITUTIVE LOSS OR PHARMACOLOGICAL INHIBITION OF NEP ACCELERATES CORNEAL EPITHELIAL WOUND HEALING 53

Background and Rationale 53

Materials and Methods 54

Results 61

Discussion 72

CHAPTER 4: CONCLUSIONS AND FUTURE DIRECTIONS 79

Conclusions 79

Future Directions 80

Final Thoughts 85

ABBREVIATIONS 86

REFERENCES 88

LIST OF FIGURES

Figure 1. Expression of NEP protein in mouse cornea 38

Figure 2. Full length immunoblot for NEP protein in mouse cornea..... 39

Figure 3. Localization of NEP in the mouse cornea 40

Figure 4. NEP enzyme activity in mouse cornea 40

Figure 5. Constitutive genetic disruption of NEP activity does not affect morphological development of the ocular surface..... 41

Figure 6. *In vivo* measurement of central corneal thickness in WT and $NEP^{-/-}$ mice 42

Figure 7. NEP deficiency does not alter corneal epithelial cellularity..... 43

Figure 8. NEP deficiency does not alter limbal vasculature 44

Figure 9. $NEP^{-/-}$ mice have increased corneal innervation at the level of the subbasal plexus..... 44

Figure 10. NEP deficiency does not alter substance P levels in the cornea..... 45

Figure 11. NEP deficiency does not alter neurokinin-1 receptor expression in the cornea..... 46

Figure 12. Broad-beam slit lamp image of the alkali-injured cornea..... 62

Figure 13. Corneal wound healing after alkali burn in WT and $NEP^{-/-}$ mice..... 63

Figure 14. Effect of topical thiorphan on NEP activity in the cornea 64

Figure 15. Effect of systemic thiorphan on NEP activity in the cornea and trigeminal ganglia 65

Figure 16. Corneal wound healing after alkali burn with thiorphan administration in WT mice 67

Figure 17. Corneal perforation in alkali-injured WT mice 68

Figure 18. Thiorphan administration does not significantly affect CD45, CD31, or α-smooth muscle actin expression in alkali-injured WT corneas at one week 69

Figure 19. Expression of NEP protein in TKE2 cell line..... 70

Figure 20. Thiorphan does not affect migration of TKE2 cells after wounding *in vitro*..... 71

CHAPTER 1: INTRODUCTION

Overview of the Ocular Surface

The tunica fibrosa oculi comprises the outermost layer of the eye. In humans, five-sixths of this surface is occupied by the sclera, an opaque white collagenous shell that provides structural integrity to the globe and physical protection to the delicate neural structures within. The remaining one-sixth of the ocular surface, situated anterior to the iris and pupil and interacting most directly with the environment, constitutes the cornea, and the epithelial transition between the two is termed the sclerocorneal limbus (Foster et al. 2004).

The cornea, though collagenous like the sclera, is transparent. Specialized to transmit light, the dome-like cornea refracts incident rays through the lens and onto the retina, accounting for two-thirds of the total ocular refractive power in humans (Kaufman et al. 2011). While the lens is shielded by the cornea, the cornea is exposed to the environment and vulnerable to a host of traumatic and infectious insults. Indeed, damage to this critical region of the visual system is the second most common cause of blindness worldwide (Whitcher et al. 2001), lending urgency to the need for increased understanding of corneal physiology.

Anatomy and Histology of the Cornea

The human cornea is approximately 0.5 mm thick centrally and 1 mm thick peripherally, arranged throughout in five histologic layers: epithelium, Bowman's layer, stroma, Descemet's membrane, and endothelium, from superficial to deep (Foster et al. 2004). Each differs in structure, function, and proliferative capacity, as detailed below.

Endothelium

Facing the aqueous humor within the anterior chamber, the cornea is lined by a low cuboidal endothelium. This monolayer of hexagonal cells maintains corneal clarity by controlling fluid flow into the stroma (Foster et al. 2004). While the endothelium permits paracellular diffusion of aqueous humor into the cornea, stromal hydration is tightly and actively regulated by sodium-potassium and bicarbonate-dependent magnesium ATPase pumps clustered in the lateral membranes of endothelial cells (Hodson and Miller 1976; Maurice 1972; Stiemke et al. 1991). Failure of this pump action leads to excess fluid accumulation, or stromal edema, and consequent loss of corneal transparency (Hull et al. 1977). Unfortunately, the human corneal endothelium has insufficient proliferative potential to replace cells lost to injury or senescence and instead responds by lateral spreading to cover any exposed basement membrane (Bourne et al. 1997; Joyce et al. 2002). While the corneal endothelium grows thinner and less dense with age, its basement membrane, named Descemet's membrane after the physician Jean Descemet, is continuously synthesized throughout life, reaching up to 12 μm in late adulthood (Foster et al. 2004). The reason for its unusual heft is unknown.

Stroma

Interposed between the corneal endothelium and epithelium, the stroma comprises approximately 90% of the total thickness of the cornea, amounting to about 500 μm in humans (Foster et al. 2004). At its circumference, the stroma interlocks with surrounding scleral connective tissue to form a rigid frame that maintains symmetric curvature for light refraction (Foster et al. 2004). Its architecture balances the competing requirements for optical transparency and sufficient tensile strength to withstand intraocular pressure (Meek and Knupp 2015).

By dry weight, the stroma is predominantly collagen, over three-fourths of which are type I and type IV fibrils (Foster et al. 2004; Hirsch et al. 2001). Despite its high protein content, the stroma is transparent due to the precise orthogonal arrangement of collagen fibrils (Farrell et al. 1973; Maurice 1957). The sparse resident keratocyte population that maintains this lamellar stroma is also specialized to have minimal effect on light transmission (Kaufman et al. 2011). Flattened between the collagenous lamellae (West-Mays and Dwivedi 2006), keratocytes contain water-soluble cytoplasmic proteins called crystallins that decrease light scatter through their cell bodies (Jester et al. 1999).

Despite a paucity of cells in the stroma, keratocytes maintain communication with neighbors through gap junctions at sites of contact between their thread-like dendritic processes (Ueda et al. 1987), forming a syncytium that rapidly activates upon detection of epithelial damage. Depending on the environmental cues, keratocytes may assume a regenerative or fibrotic phenotype, producing growth factors, cytokines, and extracellular matrix as a part of the wound healing response (West-Mays and Dwivedi 2006; Zhang et al. 2017). Dendritic cells and other bone marrow-derived monocytes also sample the stroma for signs of invasion or injury (Hamrah et al. 2003).

Bowman's layer

Unlike Descemet's membrane that underlies the corneal endothelium, Bowman's layer is not a basement membrane, but rather a 10 μm thick, acellular, collagenous division between the stroma proper and basement membrane of the corneal epithelium (Bettman 1970). It cannot be regenerated (Obata and Tsuru 2007). Essentially a randomly woven fibrous mat, Bowman's layer has multiple hypothesized functions. Some propose that it may form a rigid base for the epithelium to maximize uniformity (Kaufman et al. 2011), prevent inappropriate extracellular matrix assembly, or serve as a barrier against viral

penetration into the posterior cornea, while others suggest that it has no particular function at all and is merely a modified layer of the stroma (Bettman 1970; Foster et al. 2004; Wilson and Hong 2000). Indeed, many mammals lack Bowman's layer and manage well enough without it (Hayashi et al. 2002).

Corneal epithelium

A stratified squamous, non-keratinizing epithelium constitutes the anterior corneal surface. Five to seven cell layers deep, the corneal epithelium is characterized by consistent thickness and exceptional apical regularity. Additional smoothening of the optical surface is provided by the tear film, a complex trilaminar solution with mucinous, aqueous, and lipid components (Argüeso and Gipson 2001; Foster et al. 2004). Unlike other epithelia, the corneal epithelium is adapted to exist over avascular connective tissue (i.e., the stroma) to maximize optical transparency. As a consequence, the corneal epithelium relies on controlled exchange of nutrients and oxygen with the tear film (Beebe 2008).

Within the corneal epithelium, three cell types can be distinguished:

(1) At the apical corneal surface, three to four layers of flattened, polygonal squamous cells (squames) interface with the tear film through microplicae and microvilli to form the primary refractive surface of the eye. To maintain corneal deturgescence, a band of tight junctions (zonulae occludentes) fuses adjacent squamous cell membranes to create a high-resistance barrier to diffusion and bulk fluid flow (Ban et al. 2003). These superficial epithelial squames also produce membrane-spanning mucins that impede pathogen entrance.

(2) Wing cells reside beneath the squames in one to three layers. Named after the winglike extensions that project from their cell bodies, the lateral membranes of these mid-epithelial cells interdigitate sinuously with one another, stabilized by desmosomes and adherens junctions.

(3) A single layer of columnar basal cells forms the posteriormost layer of the corneal epithelium. Here, basal cells secrete a basement membrane to which they are anchored via hemidesmosomes that reach through the underlying Bowman's layer and into the stroma (Gipson et al. 1987). Though securely fastened to the ECM when quiescent, basal cells are highly motile transit amplifying cells (TACs) that migrate centripetally from the limbus (Wiley et al. 1991). Of the three corneal epithelial cell types, basal cells are uniquely mitotic and thus maintain the corneal epithelium by generating daughter cells through a limited set of divisions. The post-mitotic daughter cells differentiate into wing cells and terminally, into squames, migrating suprabasally to replace those shed into the tear film (Friedenwald and Buschke 1944; Hanna and O'Brien 1960; Hanna et al. 1961). Carefully balanced with the rate of desquamation (Sharma and Coles 1989), basal cell mitosis is likely regulated by signals transmitted through the extensive network of gap junctions that links neighboring cells (Williams and Watsky 2002). Precise control over vertical proliferation is critical for preserving regularity of the epithelial surface.

Limbal epithelium

The basal cells themselves are replenished by horizontal proliferation of limbal epithelial stem cells (LESCs, Thoft and Friend 1983), a unipotent stem cell pool that resides in the protective nursery of the limbal epithelium at the junction of the cornea and sclera (Cotsarelis et al. 1989). In humans with heavily pigmented eyes, the limbus may be seen at the periphery of the cornea as radial undulations or infoldings, which represent the palisades of Vogt and interpalisade rete ridges (Davanger and Evensen 1971; Wei et al. 1993). LESCs reside in the basal epithelial layer of this area, and also cluster in crypts that arise from the interpalisade rete ridges (Cotsarelis et al. 1989; Dua et al. 2005). With a closely apposed vascular network to deliver nutrients and growth factors, the limbal epithelial crypts are a specialized microenvironment containing resident melanocytes to guard against ultraviolet radiation damage (Dua et al. 2005). Though the microanatomy of this niche is well-defined, there is continued debate over specificity of putative LESCs markers, complicated by recent reports of stem cell reservoirs located in the central and peripheral cornea (Majo et al. 2008). Regardless, a structurally-intact limbus acts as a barrier to migration of bulbar conjunctival cells, which are not specialized for maintaining corneal transparency (Dua 1998).

Corneal nerves

With up to 7000 nociceptors per square millimeter, the cornea is the most densely innervated tissue in the human body (Müller et al. 2003). Polymodal nociceptor, mechanoreceptor, and cold thermal receptor-type nerve endings are distributed throughout the epithelium to maximize detection of any potentially noxious stimulus (Müller et al. 2003), enabling a rapid response of reflex tearing and blinking (Heigle and

Pflugfelder 1996) with such sensitivity that it may only require injury of a single epithelial cell to trigger corneal pain perception (Kaufman et al. 2011).

Sensory innervation is supplied by the peripheral projections of neurons located within the ophthalmic division of the trigeminal (semilunar) ganglion housed on the floor of the skull. After shedding their perineurium and myelin at the limbus, fibers carried by the nasociliary branch of the trigeminal nerve enter the anterior corneal stroma radially in thick, bundled trunks (fascicles) that branch and anastomose to form the subepithelial plexus (Müller et al. 2003; Oliveira-Soto and Efron 2001). Fibers from this plexus then travel superficially, piercing Bowman's layer and the epithelial basement membrane (Kaufman et al. 2011; Müller et al. 2003; Oliveira-Soto and Efron 2001). Here, the fibers reorient parallel to the epithelium to form a dense subbasal plexus composed of subbasal nerve leashes that whorl centrally, creating a vortex (Müller et al. 1997). The leashes contain up to 40 straight and beaded fibers that eventually ascend as individual intraepithelial fibers, terminating as free nerve endings within the epithelium or directly innervating epithelial cells (Müller et al. 1996). The cornea also receives modest autonomic innervation, with sympathetic input from the superior cervical ganglia (Marfurt, Kingsley, and Echtenkamp 1989) and parasympathetic input from the ciliary ganglia (Marfurt, Jones, and Thrasher 1998).

Most corneal nerves, both sensory and autonomic, are peptidergic, expressing a range of neurochemicals that include substance P (SP), calcitonin gene-related peptide (CGRP), pituitary adenylate cyclase-activating peptide (PACAP), vasoactive intestinal peptide (VIP), neuropeptide Y (NPY), and neurokinin A (NKA), among others (Jones and Marfurt 1998; Müller et al. 2003; Schmid et al. 2005). The effects of these peptides are equally diverse, ranging from induction of neurogenic inflammation and immune regulation to stimulation of wound healing and trophic maintenance of the corneal

epithelium (Sabatino et al. 2017). Conversely, the corneal epithelium supports development, remodeling, and survival of corneal nerves (Müller et al. 2003), demonstrating the well-documented trophic interdependence of neural and epithelial tissues in the cornea (Kaufman et al. 2011).

Vasculature

Corneal avascularity is actively maintained to preserve transparency. Despite being bathed in vascular endothelial growth factors (VEGFs), the cornea efficiently resists neovessel growth by sequestering the pro-angiogenic molecules VEGF-A, C, and D through soluble VEGF receptor-1 (sVEGFR1) and ectopic VEGF receptor-3 (VEGFR3) expression, which is supported by corneal innervation (Ambati et al. 2006; Ambati et al. 2007; Cursiefen et al. 2006; Ferrari et al. 2013). Both membrane-bound VEGFR3 and secreted sVEGFR1 act as sinks that bind VEGFs to prevent angiogenesis. Several antiangiogenic factors, including thrombospondins 1 and 2, endostatin, pigment epithelium-derived factor, and tissue inhibitor of metalloproteinases, are also expressed by the cornea to redundantly regulate avascularity (Cursiefen et al. 2004).

By contrast, the limbal connective tissue is highly vascularized, housing capillaries, arterioles, and venules, as well as large lymphatic vessels (Foster et al. 2004). Vessels arise from a pair of circumferential arterial rings (episcleral circles) fed by the anterior and long posterior ciliary arteries, and a venous plexus that connects to the concentric Schlemm's canal and drains into radial episcleral veins (Morrison and Van Buskirk 1983; Morrison et al. 1995; Woodlief 1980). Under normal circumstances, these peripheral vessels do not encroach on the cornea.

Corneal Epithelial Homeostasis

Epithelial tissues form a dynamic interface with the external environment and must often withstand constant attritive forces while maintaining homeostasis, i.e., balancing cell loss with cell replacement. This is particularly crucial in the cornea where tissue regularity is inextricably linked to its light transmission and refraction functions. With cell proliferation, differentiation, and shedding in equilibrium, the corneal epithelium exists in a dynamic state of continuous vertical turnover, renewing every 7 to 10 days while maintaining precise epithelial homeostasis through a complex regulatory network of neural, paracrine, and humoral factors (Hanna and O'Brien 1960; Hanna et al. 1961).

Contribution of limbal epithelial stem cells

In 1983, Thoft and Friend proposed the X, Y, Z hypothesis of corneal epithelial maintenance as a framework for understanding how corneal epithelial mass does not significantly fluctuate in the healthy eye. They defined the simple equation, X + Y = Z, where X represents basal epithelial cell proliferation, Y represents centripetal migration of basal cells from the periphery, and Z represents epithelial loss due to desquamation at the surface. The X, Y, Z hypothesis has since been incorporated into the LESC hypothesis, which specifies that the centripetal migration of basal cells is driven by asymmetric stem cell divisions in the limbus where TACs are generated (Dorà et al. 2015).

Accepting that LESCs are recruited for injury-induced corneal epithelial regeneration, the alternative corneal epithelial stem cell (CESC) hypothesis argues that steady-state regeneration is instead maintained by oligopotent stem cells distributed throughout the ocular surface, not by LESCs (Majo et al. 2008). Compared to the LESC hypothesis, the CESC hypothesis is less widely accepted. Many argue it is incompatible

with the bulk of existing data or based on artifactual *in vitro* findings (Dorà et al. 2015, Sun et al. 2010). Still, some human studies suggest a limited role for LESCs in corneal epithelial maintenance in the absence of injury (Dua et al. 2009). Given the abundance of conflicting data from human patients and animal models (Chang et al. 2008; Daya et al. 2005; Dua et al. 2009; Huang and Tseng 1991; Kawakita et al. 2011; Sandvig et al. 1994; Sharpe et al. 2007), a consensus on the validity of these two hypotheses is yet to be reached (Amitai-Lange et al. 2015; Dorà et al. 2015; Yoon et al. 2014).

Neuronal-epithelial interactions

Maintenance of the corneal epithelium depends on intact sensory innervation. A striking demonstration of this is neurotrophic keratopathy, a rare condition in which spontaneous corneal epithelial degeneration occurs (i.e., in the absence of direct injury) as a result of compromised innervation (Bonini et al. 2003). The manifold effects of sensory denervation on corneal epithelial architecture and cellular behavior include cellular swelling, effacement of microvilli, defective cellular proliferation and differentiation, abnormal basal lamina production, disrupted barrier function, and epithelial thinning (Alper 1975; Beuerman and Schimmelpfennig 1980; Mackie 1978; Nishida and Yanai 2009; Sigelman and Friedenwald 1954).

The broad epithelial dysfunction that occurs with denervation reflects the necessary contribution of corneal nerves to homeostasis. Aside from providing sensory innervation, corneal nerves produce epitheliotrophic factors that promote function and maintenance of the corneal epithelium (Beuerman and Schimmelpfennig 1980; Suuronen et al. 2004). The best studied of these is substance P (SP), an 11-amino acid tachykinin normally detected in human tears (Varnell et al. 1997; Yamada et al. 2002; Yamada et al. 2003). Predominantly produced and released by sensory nerves in the

cornea (Markoulli et al. 2017; Yamada et al. 2003), the neuropeptide SP sensitizes the corneal epithelium to circulating trophic factors, including insulin-like growth factor 1 (IGF-1), an endocrine hormone produced by the liver (Chikama et al. 1998; Nishida et al. 2007; Yamada et al. 2008). Loss of innervation, and thus the primary source of SP, renders the corneal epithelium unresponsive to physiologic concentrations of these agents (Nishida 2005). However, topical SP repletion, when coadministered with IGF-1, can efficiently induce resurfacing of persistent epithelial defects secondary to neurotrophic keratopathy and reestablish a stable corneal epithelium (Chikama et al. 1998; Nishida et al. 2007; Yamada et al. 2008). The unique combination of SP and IGF-1 stimulates corneal epithelial cell growth, DNA synthesis, migration, and attachment to various extracellular matrix proteins via induction of cadherin expression and activation of the integrin, FAK, and paxillin system (Araki-Sasaki et al. 2000; Nakamura et al. 1998, Nishida et al. 1996; Reid et al. 1993). Additionally, SP maintains the integrity of corneal epithelial tight junctions and promotes stratification, independent of IGF-1 (Ko et al. 2009; Ko et al. 2014). Most, if not all, of these effects require the neurokinin-1 receptor (NK1R), a high affinity SP receptor expressed by the corneal epithelium (Nakamura et al. 1997).

Stromal-epithelial interactions

Communication between corneal epithelial cells and stromal keratocytes also contributes to homeostasis. As in many tissues, stromal-epithelial interactions in the cornea are largely mediated by hepatocyte growth factor (HGF) and keratinocyte growth factor (KGF; Imanishi et al. 2000; Wilson et al. 1999). Both HGF and KGF are produced at low levels by keratocytes, with receptors most highly expressed on the epithelium (Wilson et al. 1999). Here, these paracrine growth factors regulate differentiation, proliferation, and

motility of corneal epithelial cells, acting similarly to epidermal growth factor (EGF), another paracrine molecule necessary for maintenance of the corneal epithelium (Imanishi et al. 2000; Johnson et al. 2009; Peterson et al. 2014; Wilson et al. 1999). EGF, however, is predominantly produced by the lacrimal glands, and receptors are concentrated on limbal and basal corneal epithelial cells (Johnson et al. 2009; Peterson et al. 2014). Interruption of EGF receptor signaling can lead to persistent epithelial defects in the absence of an inciting injury, as seen with use of the chemotherapeutic agent erlotinib (Johnson et al. 2009).

Corneal Wound Healing: Uncomplicated Epithelial Injury

Of the three cellular layers of the cornea, the epithelium is the most likely to be damaged due to its exposed location. However, it is also the most likely to fully regenerate, re-establishing pre-injury form and function. Based on wound closure kinetics, the course of recovery from a simple epithelial injury can be divided into two phases: an initial latent phase with no epithelial movement, and a closure phase (Crosson et al. 1986). The closure phase can be divided into the additional overlapping stages of cell migration, proliferation, differentiation, stratification, and attachment (Ljubimov and Saghizadeh 2015).

Latent phase

The latent, or lag, phase refers to the lack of appreciable wound closure for the first few hours immediately after injury (Crosson et al. 1986). During this time, damaged cells undergo apoptosis or necrosis and exfoliate into the tear film, while protein synthesis, increased glycogen utilization, and reorganization of junctional proteins occur in undamaged cells near the wound margin (Crosson et al. 1986; Estil et al. 2002; Foster et

al. 2004; Gipson et al. 1993; Khodadoust et al. 1968). Here, the basal lamina and associated hemidesmosomes are dismantled. Clusters of α6β4 integrin molecules previously associated with hemidesmosome complexes redistribute along the basal epithelial surface (Gipson et al. 1993) and associate with fibronectin, actin, and vinculin to form interim adherens junctions called focal contacts or adhesions (Gipson 1992; Murakami et al. 1992; Soong 1987). Focal contacts can be rapidly assembled and then degraded by proteases to adjust with the advancing front of migrating cells in the next phase (Teranishi et al. 2009).

Closure phase

When lag phase remodeling is complete, centripetal cell migration commences from the most proximal, viable epithelium. This marks the first stage of the closure phase. Cells at the leading edge of the wound flatten and display membrane ruffling and active filopodia formation, typical of migrating epithelia (Buck 1979; Crosson et al. 1986; Yamada et al. 1996). While hemidesmosomes were previously dismantled, desmosomes remain intact to link the spreading epithelial cells into a sliding monolayer that surges across the denuded corneal surface (Buck 1979; Kuwabara et al. 1976; Zhao et al. 2003). Focal contacts clustered at the leading edge, coupled with cytoskeletal contractile mechanisms (i.e., actin stress fibers), enable closure of a simple epithelial abrasion at a rate of approximately 0.1 mm/hour (Anderson 1977; Matsuda et al. 1985; Soong 1987). Polymerized over the denuded corneal surface, fibronectin serves as a provisional ECM to facilitate this rapid cell migration and adhesion (Fujikawa et al. 1981; Murakami et al. 1992; Nishida et al. 1982). Because initial wound closure is independent of cell proliferation, mitotic activity does not increase above baseline during this stage (Anderson 1977; Hanna 1966; Kuwabara et al. 1976).

Depending on the extent of epithelial injury, cell migration continues for 12 to 15 hours or more with a directional persistence towards the wound center (Foster et al. 2004; Matsuda et al. 1985; Zhao et al. 2003). Tight junctions reassemble behind the wound margin, restoring barrier properties (McCartney and Cantu-Crouch 1992), while the basement membrane is remodeled underneath migrating epithelial cells (Suzuki et al. 2000). Once the defect is repopulated by epithelial cells, migration ceases (Blanco-Mezquita et al. 2011; Foster et al. 2004). Contact inhibition also induces a change in cellular morphology: flattened migrating cells reassume the typical cuboidal configuration of basal cells (Foster et al. 2004). This marks a transition to the overlapping stages of proliferation, differentiation, and stratification in corneal wound healing.

Basal corneal and limbal epithelial cells outside the wound synchronously enter the cell cycle (Chung et al. 1999; Park et al. 2006), resulting in a proliferative peak approximately 24 hours after injury (Cotsarelis et al. 1989). Similar to the homeostatic process that supports corneal epithelial maintenance, injury-induced regeneration recruits LESCs to generate TACs, which migrate centrally, progress through a limited set of divisions, and then terminally differentiate into wing and squamous cells that repopulate and restratify the epithelium (Hanna 1966; Park et al. 2006). In the context of injury, however, TACs have increased proliferative potential and a shortened cell cycle, compared to TACs involved in steady-state corneal maintenance. This injury-induced phenotype serves to expedite resurfacing of the corneal epithelium (Lehrer et al. 1998; Park et al. 2006). In contrast, basal epithelial cells that migrated into the wound as a sliding sheet do not appear to synthesize new DNA, suggesting that migration and proliferation are compartmentalized (Chung et al. 1999).

Finally, in the case of basement membrane-sparing injury, hemidesmosomes rapidly reassemble over preexisting anchoring fibrils following restratification (Gipson

1992; Khodadoust et al. 1968). If the basement membrane sustains damage, however, the corneal wound healing process is appreciably lengthened, and hemidesmosomes may not reform for up to a year, depending on the extent of associated stromal injury (Gipson et al. 1989; Kenyon et al. 1977; Hirst et al. 1982).

Corneal Wound Healing: Severe Injury and Its Complications

In basement membrane-sparing injury, corneal regeneration progresses rapidly and completely in a well-defined sequence of events, but deeper injury complicates the healing process and can prevent complete functional restoration. Though the cornea may initially undergo reepithelialization, severe injury often results in vision-compromising sequelae, including recurrent or persistent epithelial defects, stromal opacity, scarring, and neovascularization (Wagoner 1997). Understanding the pathophysiology of these unfavorable outcomes is critical for development of effective treatment strategies and is therefore the focus of this work, and the work of many others.

Epithelial basement membrane injury

Outcomes after corneal injury are strongly contingent on the epithelial basement membrane. Repair of any basement membrane damage is delayed until 5 to 7 days after injury and occurs in short, discontinuous segments (Kenyon et al. 1977). Following extensive injury, basement membrane synthesis may take months to complete, and without a strong adhesion framework in place, the corneal epithelium is prone to surface irregularities, sloughing, recurrent erosions (Foster et al. 2004; Gipson et al. 1989, Kenyon et al. 1977; Kenyon 1979; Khodadoust et al. 1968). In addition, the basement membrane normally limits access of cytokines and epithelium-derived growth factors to the stroma. Defects in this barrier allow transforming growth factor-beta (TGF-β) to

promote myofibroblast development and survival, which, when protracted, leads to pathologic stromal reactions (Netto et al. 2006; Wilson 2012).

Stromal injury

Cytokines and growth factors released by damaged corneal epithelium modulate the stromal response to injury. Interleukin-1 (IL-1) and tumor necrosis factor alpha (TNF-α) trigger an acute apoptotic response in stromal keratocytes proximal to the wound (Wilson et al. 1996; Wilson et al. 1997; Wilson and Kim 1998; Wilson et al. 2007), while TGF-β stimulates surviving keratocytes to transition to myofibroblasts (Netto et al. 2006; Wilson 2012). Myofibroblasts arise mainly from keratocytes but are also derived from bone marrow-derived cells that gain access to the stroma following basement membrane damage (Barbosa et al. 2010; Stramer et al. 2003; Wilson et al. 2004). Regardless of origin, myofibroblasts are specialized for fibrotic repair, and the transition to this phenotype initiates stromal wound healing (Fini 1999; Jester et al. 2005).

Sharing features with both fibroblasts and smooth muscle cells, myofibroblasts contract stromal wounds, secrete copious amounts of ECM, and generate adhesion structures within the surrounding substrate (Fini and Stramer 2005; Mohan et al. 2003, Wilson 2012). Myofibroblast-driven repair may be beneficial when limited, since the opaque fibrotic tissue that seals a penetrating corneal wound can be slowly remodeled through enzyme-driven turnover to restore stromal transparency (Jester et al. 1999). However, prolonged stimulation of myofibroblasts prevents stromal remodeling and leads to hypercellularity, excessive contracture, and scarring (Fini and Stramer 2005). To modulate the myofibroblast reponse, stromal keratocytes undergo a second wave of apoptosis (Wilson et al. 1996; Wilson et al. 1997; Wilson et al. 2007). Though this culls available fibrotic progenitors in the wounded region, delayed or abnormal regeneration of

the epithelial basement membrane inevitably leads to stromal haze, a type of corneal opacity associated with unrestrained myofibroblast proliferation and activity (Torricelli et al. 2013).

Endothelial injury

Endothelial defects are rapidly resurfaced through centripetal migration and enlargement of surrounding, uninjured cells; however, the human corneal endothelium is arrested in a non-replicative state, which limits *in vivo* proliferation even in response to injury (Bourne et al. 1997; Joyce 2003; Konomi et al. 2005; Matsuda et al. 1985). To restore and maintain stromal deturgescence after injury, endothelial cell density must remain above a critical level, typically at least 500 cells/mm^2 (Claerhout et al. 2008; Kim et al. 2008). Temporary stromal edema may occur after injury as physiologic recovery lags behind histologic recovery by four to five days (Khodadoust and Green 1976), but if the endothelial cell density drops below threshold, barrier function falters and stromal edema cannot be reversed by the remaining cells (Claerhout et al. 2008; Kim et al. 2008, Khodadoust and Green 1976; Yee et al. 1985). Fortunately, endothelial transplantation with or without a Descemet's membrane scaffold can successfully restore stromal deturgescence and corneal clarity (Ljubimov and Saghizadeh 2015).

Limbal injury

Ocular surface injury that extends into or beyond the limbus endangers LESCs. Damage to this stem cell population may result in complete or partial limbal stem cell deficiency (LSCD), and destruction of the limbal epithelium additionally jeopardizes the physical barrier it maintains between corneal and conjunctival epithelia (Chen and Tseng 1990; Dua 1998). When the corneal epithelium cannot regenerate from the limbus, bulbar

conjunctival cells invade the corneal surface as a last recourse for closing the epithelial defect (Chen and Tseng 1991; Dua 1998; Friend and Thoft 1978; Shapiro et al. 1981).

Though this process of conjunctivalization closes the wound, overgrowth of conjunctival epithelium onto the cornea results in an unstable mucosal epithelium that is not specialized for maintaining transparency (Friend and Thoft 1978; Shapiro et al. 1981). As a result, corneal conjunctivalization predisposes the optical surface to chronic inflammation, tear film irregularities, recurrent erosions, sterile ulceration, neovascularization, and scarring, all of which lead to compromised visual acuity and extended clinical morbidity (Bakhtiari and Djalilian 2010; Chen and Tseng 1991; Huang and Tseng 1991; Kenyon and Tseng 1989). Furthermore, any remaining corneal epithelial cells at the margins of persistent defects often appear and behave abnormally, with elevated borders and arrest of migration, mitosis, and basement membrane synthesis (Hirst et al. 1981). Reconstruction of the conjunctivalized ocular surface may be achieved through surgical means, though outcomes are sensitive to tear film stability, intraocular pressure, and inflammation (Liang et al. 2009; Tuft and Shortt 2009).

Corneal nerve injury

Corneal wounds, whether superficial or deep, result in concomitant corneal nerve injury, given the presence of bundles, branches, and terminals throughout the stroma and epithelium. In response to damage, severed axons of subepithelial corneal nerves rapidly seal their terminal stump to form a swelling from which fine branches, or sprouts, arise (Beuerman and Rózsa 1984; Beuerman and Schimmelpfennig 1980; de Leeuw and Chan 1989; Rózsa et al. 1983). The sprouts then penetrate into the denervated tissue (Beuerman and Schimmelpfennig 1980), though only a subset of regenerated fibers typically re-establish innervation (Chan et al. 1990; Wolter 1966). Recovery is

often partial, and regenerated axons rarely restore the pre-injury pattern of corneal innervation, instead assuming a more disorderly distribution (Chan et al. 1990; Lee et al. 2002; Namavari et al. 2011; Rózsa et al. 1983; Wolter 1966). Hyper-regenerated neurites, abnormal morphologies of tangled aborted sprouts and end bulbs, and microneuromas may coexist with successfully regenerated fibers, or dominate the reinnervated tissue, particularly in the presence of extensive scar tissue (Chan et al. 1990; Lee et al. 2002; Rózsa et al. 1983; Wolter 1966). Distorted corneal nerve architecture in both the stroma and epithelium may persist long term and correlate with functional deficits (Chan-Ling et al. 1987).

Depending on the extent and location of injury along the nerve trajectory (i.e., stromal branches versus epithelial terminals), sensory deficits in the denervated region may persist for weeks to months (Gallar et al. 2004; Lee et al. 2002), though the temporal pattern of regeneration is highly variable (Belmonte et al. 2004). Conversely, drastic injury-induced changes in expression, distribution, and post-translational modification of ion channels can lead to aberrant ectopic activity, particularly in microneuromas (Belmonte et al. 2015). These microneuromas may become hypersensitive to light and air movement, evoking spontaneous pain or pain in response to benign stimuli, such as a person’s own tears (Belmonte et al. 2004; Belmonte et al. 2015). This triad of hyperalgesia, allodynia, and spontaneous pain characterizes corneal neuropathic pain, a potentially debilitating and often intractable condition caused by corneal injury (Belmonte et al. 2004; Goyal and Hamrah 2016).

Because the corneal epithelium produces and releases neuropeptides, neurotrophins, and growth factors that promote survival and maturation of nerve fibers (Chan and Haschke 1981; Emoto and Beuerman 1987; You et al. 2000), extensive damage to this region can result in deficient neurotrophic support and consequently poor

corneal nerve regeneration (Chan et al. 1990). While Schwann cells support repair and regrowth of stromal and subepithelial nerves, intraepithelial nerves (IENs) lack this beneficial association and instead rely on corneal epithelial cells as surrogate glia, which leaves IENs in a vulnerable position post-injury (Chan et al. 1990; Stepp et al. 2016). In a reciprocal manner, corneal nerves produce epitheliotrophic factors that promote physiological renewal as well as wound healing, and loss of this support leads to sluggish epithelial repair (Beuerman and Schimmelpfennig 1980; Lambiase et al. 1998; Mastropasqua et al. 2016). Due to the cooperative and reciprocal nature of corneal nerve-epithelial interactions, damage to one component endangers the other, jeopardizing regeneration of both. This cycle can ultimately lead to delayed wound healing and increased susceptibility to recurrent epithelial breakdown (Alper 1975; Beuerman and Schimmelpfennig 1980; Bonini et al. 2003; Ferrari et al. 2011; Mackie 1978; Sigelman and Friedenwald 1954).

Neprilysin

Due to its ubiquity and substrate promiscuity, neprilysin (NEP, EC 3.4.24.11) has appeared under a number of guises since its initial discovery and characterization as a “neutral metallo-endopeptidase” in the renal brush border where it hydrolyzes insulin B-chain (George and Kenny 1973; Kerr and Kenny 1974a; Kerr and Kenny 1974b). At the time, NEP was the first recognized mammalian example of a zinc-dependent endopeptidase, bearing structural and functional similarity to the bacterial enzyme thermolysin (Devault et al. 1987). Soon thereafter, the renal enzyme was exposed as being identical to the synaptic enzyme enkephalinase (Malfroy et al. 1978; Schwartz et al. 1980) and to the common acute lymphoblastic leukemia antigen (CALLA or CD10; Brown et al. 1975; Greaves et al. 1983).

Table 1. Neprilysin substrates.

Peptide	Main function
Adrenocorticotrophic hormone	Stimulates adrenal secretion of glucocorticoids
Adrenomedullin	Vasodilation
Amyloid β peptide	Implicated in the pathogenesis of Alzheimer disease
Angiotensin I	Precursor to angiotensin 1-7 and angiotensin II
Angiotensin II	Vasoconstriction and vasodilation (angiotensin receptor subtype-dependent)
Angiotensin 1-7	Vasodilation, natriuresis, diuresis; inhibition of cardiac hypertrophy and fibrosis
Atrial, B-type, and C-type natriuretic peptides	Vasodilation, natriuresis, diuresis; inhibition of renin-angiotensin system, cardiac hypertrophy, and fibrosis
Bombesin-like peptides	Stimulate gastrin and cholecystokinin secretion, mitogenesis
Bradykinin	Vasodilation; increased endothelial permeability, pain and inflammation
Calcitonin gene-related peptide	Vasodilation, pain and inflammation
Chemotactic peptide (FMLP peptide)	Neutrophil chemotaxin
Cholecystokinin	Stimulates gallbladder contraction, pancreatic secretion, intestinal motility, and satiety
Dynorphin	Analgesia
β-Endorphin	Analgesia
Endothelins	Vasoconstriction, mitogenesis
Enkephalins	Analgesia
Fibroblast growth factor-2	Angiogenesis

Table 1 – continued. Neprilysin substrates.

Peptide	Main function
Galanin	Inhibits neurotransmitter release
Gastrin-releasing peptide	Stimulates gastrin, somatostatin, cholecystokinin, and gastric acid secretion; mitogenesis
Glucagon	Stimulates hepatic glucose release and ketone production
Gonadotropin-releasing hormone	Stimulates pituitary secretion of follicle-stimulating hormone and luteinizing hormone
Interleukin-1β	Lymphocyte mitogenesis, inflammation
Insulin B-chain	With the insulin A-chain, comprises insulin
α-Melanocyte-stimulating hormone	Stimulates melanogenesis; cardio- and neuroprotective, anti-inflammatory
Neurokinin A	Vasodilation, bronchoconstriction; increased endothelial permeability, pain and inflammation
Neurotensin	Neurotransmission and neuromodulation
Oxytocin	Stimulates uterine contraction and milk ejection
Peptide YY	Appetite reduction
Secretin	Inhibits gastric acid production and emptying; stimulates pancreatic exocrine secretions
Substance P	Vasodilation, bronchoconstriction; increased endothelial permeability, pain and inflammation
Vasoactive intestinal peptide	Smooth muscle relaxation in the gastrointestinal and respiratory systems

Modified from Campbell, 2016; Bayes-Genis et al. 2016; and Erdos and Skidgel, 1989.

Reports of NEP expression in a smattering of tissues quickly followed, with an equally sizable list of *in vitro* and *in vivo* substrates (Table 1) suggesting a role for the endopeptidase in pain perception, blood pressure regulation, metastasis, amyloid accumulation, and inflammation in the pulmonary and gastrointestinal systems (Hashimoto et al. 2010; Horiguchi et al. 2008; Iwata et al. 2000; Johnson et al. 1985; Lu et al. 1995; Malfroy et al. 1978; Shipp et al. 1991; Skryzdło-Radomańska et al. 1994; Vanneste et al. 1988). Most recently, NEP has enjoyed a renaissance in the field of cardiovascular medicine, where it has gained considerable clinical attention as a novel target for antihypertensive drug development (Lu et al. 1997; McMurray et al. 2014).

Gene and protein structure

NEP is a 749-amino acid (aa) protein encoded by 24 exons within an 80 kilobase gene on human chromosome 3 (3q21-27; D'Adamio et al. 1989). A single exon (exon 3) encodes the short amino-terminal (N-terminal) cytoplasmic and membrane domains of the NEP protein, while exons 4 to 23 encode the bulk of its extracellular domain, including the pentapeptide sequence His-Glu-Ile-Thr-His associated with the zinc-bound catalytic site (exon 19). The remaining carboxy-terminal (C-terminal) residues are encoded by the final exon 24 (D'Adamio et al. 1989; Devault et al. 1987).

As outlined above, the 90 - 110 kDa NEP protein is organized into three domains: an N-terminal cytoplasmic domain of 27 aa; a hydrophobic, transmembrane helical region of 22 aa; and a large, hydrophilic extracellular domain of 700 aa, which includes its spherical catalytic cleft containing the canonical HExxH zinc motif of metallopeptidases (Devault et al. 1987; Hooper 1994). The two zinc-coordinating histamine residues within the pentapeptide motif are highly conserved, as well as a glutamate contained within another consensus sequence (ExxA/GD) that serves as the

third zinc ligand (Devault et al. 1987). As a type II integral membrane protein, NEP is anchored to the lipid bilayer through a single transmembrane pass, with an intracellularly-oriented N-terminus and an extracellularly-oriented C-terminus (Devault et al. 1987). Intrachain disulfide bridges maintain its structure and activity (Malfroy et al. 1987). On the cell membrane, NEP normally exists as a non-covalently associated homodimer (Hoang et al. 1997; Shimada et al. 1996). However, there is mounting evidence for a soluble human NEP, based on activity detected in plasma, cerebrospinal fluid (CSF), and urine (Johnson et al. 1985; Spillantini et al. 1990; Yandle et al. 1992), though the mechanism of NEP solubilization from its predominant membrane-bound form is unknown.

Mechanism of action and substrate specificity

Originally assumed to be a peptidyl dipeptidase similar in mechanism of action to angiotensin-converting enzyme (ACE; Schwartz et al. 1981), NEP was later determined to function as an endopeptidase, preferentially hydrolyzing oligopeptides by cleaving the amino side of internal hydrophobic amino acids (Matsas et al. 1984). Aside from the requisite internal hydrophobic residue for cleavage, NEP is otherwise fairly non-discriminating among peptide substrates up to about 3000 daltons (see Table 1; Erdös and Skidgel 1989; Turner et al. 2001). However, NEP appears to cleave a few small proteins, including the 17 kDa interleukin-1β (Pierart et al. 1988) and the 18 kDa fibroblast growth factor-2 (FGF-2; Goodman et al. 2006), indicating that this putative size restriction may be circumvented if the substrate contains sterically permissive tertiary structures. With its lax substrate selectivity, the specific function of NEP is instead dictated by its localization and the particular milieu of signalling peptides present at each

tissue site (Fulcher et al. 1982; Matsas et al. 1983). This, of course, broadens the range of its potential physiological roles to an almost bewildering degree.

Distribution and physiological functions

With its catalytic site oriented outwards, NEP is well-positioned to cleave signaling peptides at the cell surface, in lumina of tubules or vessels, or at synapses of the tissues to which it localizes. The renal brush border, specifically of the proximal tubule, was the first recognized location of membrane-bound NEP, where it cleaves plasma-derived peptides following glomerular filtration (Kerr and Kenny 1974b; Schulz et al. 1988). Studies in rodents, pigs, and human tissues have since identified NEP in a diversity of locations, including the thyroid and adrenal glands (Ronco et al. 1988), gastrointestinal brush border (Bunnett et al. 1993; Skryzdło-Radomańska et al. 1994), synovial joints (Appelboom et al. 1991; Mapp et al. 1992), and keratinocytes (Olerud et al. 1999). The enzyme is also found throughout the male genital tract and in seminal fluid, where it may contribute to sperm motility (Bosler et al. 2014; Erdös et al. 1985; Ronco et al. 1988), and throughout the respiratory system in large conducting airways and associated smooth muscle, nerves, glands, and blood vessels, down to the epithelium of alveoli, where it modulates the diverse activities of inflammatory peptides like the tachykinins (Borson 1991; Johnson et al. 1985; Ronco et al. 1988). On the membranes of circulating granulocytes, NEP likely cleaves the chemotactic peptide N-formylmethionyl-leucyl-phenylalanine (FMLP) to temper neutrophil chemotaxis (Connelly et al. 1985; Painter et al. 1988; Tran-Paterson et al. 1990).

A major and well-studied location of NEP is the central nervous system (CNS). Here, it is considered the cholinesterase of peptidergic synapses (Turner et al. 2001), expressed alongside opioid receptors in centers of pain control (Malfroy et al. 1978;

Schwartz et al. 1980; Waksman et al. 1987) and presynaptically in the globus pallidus and substantia nigra (Matsas et al. 1985; Waksman et al. 1987). Expression of NEP in these CNS regions and others is inversely correlated with β-amyloid deposition (Fukami et al. 2002), which can be degraded by NEP prior to plaque formation (Howell et al. 1995; Yasojima et al. 2001). Among related enzymes, NEP is also uniquely and abundantly found on epithelial surfaces in contact with CSF such as the choroid plexus, pia, and ependyma (Erdös and Skidgel 1989; Matsas et al. 1986). Outside the CNS, NEP is detected in a minority of myelin-forming Schwann cells, but in a majority on non-myelin-forming Schwann cells (Kenny and Bourne 1991; Kioussi and Matsas 1991; Kioussi et al. 1992). Interestingly, axonal injury briefly induces NEP expression in myelin-forming Schwann cells, suggesting a role for the enzyme in axon-myelin maintenance and regeneration (Kioussi et al. 1995).

Clinical interest in NEP has been revived over the past two decades in the field of cardiovascular medicine. Expressed in cardiac fibroblasts, cardiomyocytes, and venous and arterial endothelial cells (Kokkonen et al. 1999; Llorens-Cortes et al. 1992), NEP inactivates atrial natriuretic peptide (ANP), a hormone released by cardiomyocytes in response to increased effective circulating blood volume (Vanneste et al. 1988). In addition, NEP metabolizes bradykinin and angiotensin I and II, overlapping in function with angiotensin-converting enzyme (ACE; Campbell et al. 1998; Campbell 2001). The potential for modulating these systems as a therapeutic strategy for cardiovascular disease drove the development of numerous NEP inhibitors, though with limited clinical success (Campbell et al. 1998; Favrat et al. 1995; Kostis et al. 2004; O'Connell et al. 1992) until the landmark trial of LCZ696 (sacubitril/valsartan), a dual angiotensin receptor-neprilysin inhibitor. In the PARADIGM-HF clinical trial, LCZ696 proved superior to the standard of care in reducing the risks of death and hospitalization for heart failure

(McMurray et al. 2014). The Food and Drug Administration has since approved LCZ696, which is now sold under the brand name Entresto.

Unlike in the cardiovascular system, the expression and function of NEP in the eye has received very little attention, aside from a handful of studies on retinal amyloid accumulation (He et al. 2014; Parthasarathy et al. 2015) and on the prevention of corneal diabetic neuropathy with NEP inhibition (Davidson et al. 2012a; Yorek et al. 2016). A single histological study has identified NEP in basal epithelial cells of normal human corneas and throughout the corneal epithelium in those with keratoconus, a progressive disease in which the cornea thins and protrudes (Hasby and Saad 2013). However, the function of NEP in the cornea is unknown.

Thesis Overview

Clinical context and motivation

Second only to cataracts as the most common cause of visual impairment worldwide (Négrel and Thylefors 1998), corneal injury accounts for an estimated 2.4 million emergency department visits in the United States annually (Haring et al. 2015). With an array of etiologies and a complicated epidemiology, corneal injury is an underreported, significant cause of visual impairment that can result in chronic complications and life-long disability (Négrel and Thylefors 1998; Whitcher et al. 2001). This is particularly true of chemical corneal injuries, which constitute a small but significant fraction of ocular trauma due to the rapidity and severity of damage that confer a high risk of permanent vision loss (Wagoner 1997). Notably, the development of chemical industries in industrialized nations has led to increased incidence of chemical corneal injury over the past few decades (Négrel and Thylefors 1998). Furthermore, recent epidemiological data indicate that children aged 1 to 2 years represent the single highest risk group for ocular

chemical injuries in the United States, a previously unrecognized and disturbing statistic (Haring et al. 2016).

Chemical corneal injuries, whether due to acid or alkali exposure, are ophthalmologic emergencies (Kuckelkorn et al. 1994; Rozenbaum et al. 1991). Following copious irrigation of the ocular surface, the main objectives during acute phase treatment include control of inflammation, prevention of further epithelial and stromal breakdown, and promotion of reepithelialization (Baradaran-Rafii et al. 2017; Brodovsky et al. 2000; Bunker et al. 2014). If medical therapy alone cannot restore corneal structure and function after injury, ocular surface reconstruction may be achieved through surgical means. However, medical management of the chemically-injured cornea remains a major determinant of surgical outcome, particularly through the first week after injury (Kuckelkorn et al. 2002; Tuft and Shortt 2009). This time period constitutes a “window of opportunity” (Tuft and Shortt 2009) during which treatment can limit potentially blinding sequelae and optimize the ocular surface for surgical reconstruction. Still, with our current medical and surgical treatment modalities, prognosis after chemical corneal injury remains guarded, and those with high-grade injuries are prone to failure despite aggressive management (Burcu et al. 2014; Sharma et al. 2012). From a clinical standpoint, parsing the physiology of corneal wound healing may generate the development of novel therapeutic strategies to restore corneal structure and function after injury.

Purpose and structure of this study

Broadly, the purpose of this work is to increase our current understanding of corneal wound healing mechanisms that could be targeted to accelerate recovery and improve outcomes after injury. The enzyme neprilysin serves a protective role in a variety of

systemic inflammatory conditions (Day et al. 2005; Hashimoto et al. 2010; Lu et al. 1995; Lu et al. 1997; Shipp et al. 1991) but is conversely linked to impaired wound healing and peripheral neuropathy in diabetes (Antezana et al. 2002; Davidson et al. 2012a; Davidson et al. 2012b; Spenny et al. 2002; Yorek et al. 2016). While NEP expression has been detected in the human cornea (Hasby and Saad 2013), its physiological role in this tissue is unknown, despite being an amenable therapeutic target. The research presented herein aims to address this gap in knowledge with the following questions:

1. Does NEP contribute to homeostasis in the uninjured cornea?
2. Does NEP participate in acute phase wound healing in the chemically-injured cornea?

Furthermore, we expanded our investigation to address a third question of more immediate clinical relevance:

3. Does the NEP inhibitor thiorphan accelerate corneal wound healing after chemical injury?

Chapter 2 of this dissertation deals with the question of NEP in corneal homeostasis; Chapter 3 considers the effect of NEP on corneal wound healing and its candidacy for therapeutic inhibition. In Chapter 4, implications of our findings and future directions are addressed.

CHAPTER 2: CONSTITUTIVE LOSS OF NEP ACTIVITY DOES NOT DISRUPT HOMEOSTASIS IN THE UNINJURED CORNEA

Background and Rationale

Epithelial tissues form a dynamic interface with the external environment and must often withstand constant attritive forces while maintaining a precise balance between cell loss and replacement to preserve homeostasis. This is particularly crucial in the cornea where innate immune defenses, light transmission, and light refraction depend on an intact, uniform epithelium. While physical injury is the most common cause of corneal epithelial disruption (Négrel and Thylefors 1998), nontraumatic alterations in corneal homeostasis develop consequent to common systemic diseases, such as diabetes (Schultz et al. 1981), and as side effects of medications, including the chemotherapeutic agents erlotinib (Johnson et al. 2009) and cetuximab (Foerster et al. 2008).

With cell proliferation, differentiation, and exfoliation in equilibrium, the corneal epithelium exists in a dynamic state of continuous vertical turnover while maintaining a constant mass (Hanna et al. 1961; Hanna and O'Brien 1960; Sharma and Coles 1989). To describe this phenomenon, Thoft and Friend (1983) proposed the simple equation, X + Y = Z, where X represents epithelial cell proliferation, Y represents centripetal migration of cells from the periphery, and Z represents epithelial loss due to desquamation at the corneal surface. Though there is continued discussion regarding the origin of the centripetally-migrating cells (Majo et al. 2008; Sherwin and McGhee 2010), the basic tenant of their X, Y, Z hypothesis of corneal epithelial maintenance remains valid: perturbation of one or more of the three variables results in loss of homeostasis. The reality is more complicated than a three-variable equation, however. A complex regulatory network of neural, paracrine, and humoral factors influences the rate

of corneal epithelial proliferation, differentiation, and migration to match desquamation (Hanna et al. 1961; Hanna and O'Brien 1960). Understanding the mechanisms of this control system and its associated molecular signals represents a major challenge in the field, and though an array of growth factors, cytokines, hormones, and epitheliotrophic neurochemicals have been implicated in the regulation of corneal homeostasis (Beuerman and Schimmelpfennig 1980; Imanishi et al. 2000; Reins et al. 2017; Wilson et al. 1999), much remains unknown.

Accumulating evidence suggests that these neuropeptides perform homeostatic functions in the cornea that contribute to tissue maintenance and steady-state renewal (Müller et al. 2003; Sabatino et al. 2017). Blinking appears sufficient to trigger baseline release of neuropeptides from corneal nerves into the tear film, which is likely supplemented by additional neuropeptide release from lacrimal and accessory glands (Müller et al. 2003; Yamada et al. 2003). While multiple combinations of neuropeptide expression profiles are possible in both sensory and autonomic corneal fibers, the trophic effects of substance P (SP), calcitonin gene-related peptide (CGRP), vasoactive intestinal peptide (VIP), and neuropeptide Y (NPY) in the cornea are currently the best defined (Sabatino et al. 2017). Expressed by approximately 40% of sensory corneal nerves in the mouse (LaVail et al. 1993), SP and CGRP often colocalize to the same fibers (Müller et al. 2003), while autonomic nerves are fewer in number, restricted to the corneal stroma, and express VIP if parasympathetic or NPY if sympathetic in origin (Jones and Marfurt 1998).

The necessity of these neurochemicals in maintenance of corneal homeostasis is exemplified by the strikingly abnormal corneal phenotype of mice lacking functional neurokinin-1 receptors (NK1R). Expressed by corneal epithelial cells and keratocytes, NK1R is the highest affinity SP receptor (Bignami et al. 2016; Słoniecka et al. 2015).

Mice without NK1R exhibit excessive desquamation of apical corneal epithelial cells (CECs) with increased CEC proliferation and density, but decreased CEC size. Corneal nerve density, basal tear volume, and corneal epithelial dendritic cell numbers are also decreased (Gaddipati et al. 2016), reflecting the pleiotropic effects of SP on corneal homeostasis.

The widely distributed enzyme neprilysin (NEP) modulates neurogenic inflammation by terminating the action of various signaling peptides throughout the body. Among its many substrates, NEP has the highest affinity for SP but also cleaves VIP, NPY, and CGRP (Erdös and Skidgel 1989; Goetzl et al. 1989; Katayama et al. 1991; Matsas et al. 1984; Medeiros and Turner 1996; Turner et al. 1985). Given the involvement of these neuropeptides in corneal maintenance and steady-state renewal (Müller et al. 2003; Sabatino et al. 2017) and their susceptibility to cleavage by NEP, we wondered whether modulation of NEP activity might alter ocular surface homeostasis.

In this chapter, we examine the contribution of NEP to homeostatic maintenance of the uninjured cornea using mice that lack the functional enzyme, abbreviated throughout as $NEP^{-/-}$ (Lu et al. 1995). Functional expression of NEP is first established in the WT mouse cornea, and $NEP^{-/-}$ corneal morphology is then characterized with multiple *in vivo* imaging and histologic techniques, suggesting a minimal role for NEP in the cornea at steady-state.

Materials and Methods

Animals

Eight to twelve week old male mice were used for all experiments. Breeding pairs of mice with a targeted disruption of the membrane metallo-endopeptidase gene (B6.129S4-*Mme*^{tm1Cge}) were provided by Drs. Lu and Gerard (Lu et al. 1995) and bred to

establish colonies at the Iowa City Department of Veterans Affairs and University of Iowa (Iowa City, IA) in certified animal care facilities. Offspring were backcrossed to C57BL/6J mice for more than nine generations. Control C57BL/6J mice (The Jackson Laboratory, Bar Harbor, ME) were also housed at these locations. Standard diet (Harlan Teklad, #7001, Madison, WI, USA) and water were provided *ad libitum* at both facilities. Mice were handled in compliance with the ARVO Statement for the Use of Animals in Ophthalmic and Vision Research, and protocols were approved by the Institutional Animal Care and Use Committees at the Iowa City Department of Veterans Affairs and University of Iowa.

Immunoblot analysis of corneas

Freshly enucleated eyes were trimmed at the sclerocorneal limbus. Corneas from each mouse were pooled and homogenized (VWR 200 Homogenizer, Radnor, PA, USA) in 100 µL cold RIPA buffer containing protease/phosphatase inhibitors (Halt Cocktail; Thermo Scientific Pierce Biotechnology, Rockford, IL, USA). Total protein in each sample was determined by BCA assay according to manufacturer's instructions (Thermo Scientific). Corneal lysates containing equal amounts of protein (15 µg) were separated on a 10% Mini-PROTEAN TGX precast polyacrylamide gel (BioRad, Hercules, CA, USA) and transferred to a nitrocellulose membrane with the BioRad Trans-Blot Turbo Transfer system.

For detection of NEP and the loading control glyceraldehyde 3-phosphate dehydrogenase (GAPDH), membranes were cut at 50 kDa and blocked in 5% skim milk in TBST buffer at room temperature (RT for 1.5 h. The upper half of the membrane (> 50 kDa) was incubated in goat anti-CD10 (NEP; PA5-47075; Invitrogen) at 1:100, and the lower half (< 50 kDa) was incubated in mouse anti-GAPDH (MAB374; EMD Millipore,

Burlington, MA, USA) at 1:1000, both overnight at 4°C. After washing in TBST, membranes were incubated with HRP-conjugated secondary antibodies (Abcam, Cambridge, UK) at 1:5000 for 1 h at RT and developed with SuperSignal West Femto Maximum Sensitivity Substrate (Thermo Scientific). Chemiluminescence was detected using the BioSpectrum 810 imaging system with a CCD camera (Ultra-Violet Products, Upland, CA, USA).

For detection of NK1R and the loading control GAPDH, membranes were cut at 40 kDa and blocked in 5% skim milk in TBST buffer at RT for 1 h. The upper half of the membrane (> 40 kDa) was incubated in mouse anti-NK1R (ab183713; Abcam) at 1:1000, and the lower half (< 40 kDa) was incubated in mouse anti-GAPDH at 1:1000, both overnight at 4°C. After washing in TBST, membranes were incubated with HRP-conjugated secondary antibodies (Abcam) at 1:5000 for 1 h at RT. Membranes were developed and imaged as above.

NEP immunofluorescence and microscopy

For immunofluorescent localization of NEP, freshly enucleated eyes were fixed whole in 4% paraformaldehyde for 30 min at RT prior to routine dehydration and paraffin-embedding. Eyes were sectioned sagittally at 5 µm intervals, mounted on Fisherbrand Superfrost Plus slides, deparaffinized, and rehydrated. For antigen retrieval, sections were placed in a IHC-Tek Epitope Retrieval Steamer (IHC World, Ellicott City, MD, USA) for 45 min in Citra Plus Antigen Retrieval Solution (BioGenex, Fremont, CA, USA). Sections were then incubated in blocking buffer (5% BSA in 0.1% Triton X-PBS) for 2 h at RT. Goat anti-CD10 (NEP; PA5-47075; Invitrogen) was applied to tissue mounted on slides with CoverWell Incubation Chamber Gaskets (Thermo Scientific) at 1:20 in blocking buffer overnight at 4°C. Negative controls were incubated in buffer only. After

washing in 0.1% Tween, sections were incubated with an Alexa Fluor 647-conjugated secondary antibody (Abcam) at 1:500 for 2 h at RT. Finally, slides were washed and coverslipped with ProLong Diamond Antifade Mountant with 4',6-diamidino-2-phenylindole (DAPI) to label nuclei (Thermo Scientific). Slides were imaged on a Zeiss Axio Imager 2 at 40X with identical exposure settings for all sections.

NEP enzyme activity

Corneas from each mouse were pooled, frozen in liquid nitrogen, and transferred to -80°C storage. Frozen samples were homogenized in 100 µL of 0.5% NP-40 lysis buffer in two 15 s bursts with 30 s incubations on ice between bursts. Aprotinin (5 µg/mL; Thermo Scientific) and phenylmethylsulfonyl fluoride (PMSF; 200 µM; Thermo Scientific) were added to the buffer to prevent protein degradation. Samples were centrifuged at 10,000 g for 5 min at 4°C, and pellets were discarded. Total protein in each supernatant was determined by BCA assay according to manufacturer's instructions (Thermo Scientific).

NEP activity was determined using the SensoLyte 520 Neprilysin Activity Assay Kit (AnaSpec, Fremont, CA, USA). Samples were diluted in 1x assay buffer to 15 µg protein/50 µL/well and loaded in triplicate in 96-well plates. Positive, negative, and substrate controls were run according to manufacturer's protocol. Plates were incubated and read at 24°C. Endpoint fluorescence was recorded on a SpectraMax M2 microplate reader (Molecular Devices, Sunnyvale, CA, USA) with excitation at 490 nm and emission at 520 nm, per manufacturer's protocol. The assay was performed twice on different sets of tissue samples. Background-subtracted data are presented from a single assay.

Corneal nerve and vessel immunofluorescence and microscopy

For corneal whole mount CD31 and TUJ1 immunostaining, enucleated eyes were fixed in Zamboni's (Newcomer Supply, Middleton, WI, USA) for 30 min at RT. Corneas were dissected at the sclerocorneal limbus, incubated in blocking buffer (2% BSA, 2% normal donkey serum, 0.2% Triton-X) for 2 h at RT, and then incubated in antibodies against endothelial adhesion marker CD31 and pan-neuronal marker βIII tubulin/TUJ1 (rabbit anti-CD31 at 1:200, Abcam; mouse anti-TUJ1 at 1:1000, Biolegend, San Diego, CA, USA) overnight at 4°C. After washing in 0.1% Tween, corneas were incubated with Alexa Fluor 488- and 647-conjugated anti-rabbit and anti-mouse secondary antibodies (Abcam), respectively, at 1:500 for 2 h at RT. Corneas were washed in 0.1% Tween and mounted on glass slides as above.

Tiled images were taken on an Olympus BX-61 motorized microscope (Waltham, MA, USA) at 10X with identical exposure settings for all corneas, and stitched using Olympus cellSens software. The area of positive CD31 staining was measured in ImageJ software (NIH) using thresholding and region of interest functions. Subbasal nerve leashes were counted manually in ImageJ using the cell counter plugin (Kurt De Vos, University of Sheffield, 2001).

Corneal epithelial cellularity

Paraffin-embedded 5 µm sections prepared for NEP immunostaining were used to determine corneal epithelial cellularity based on DAPI-stained nuclei. Central corneal fields were randomly selected and imaged on a Zeiss Axio Imager 2 at 40X. Corneal epithelial cell nuclei were counted manually in ImageJ using the cell counter plugin. Counts were normalized to the length of corneal epithelium sampled in millimeters.

Nuclei were not normalized to area or volume of corneal epithelium due to variability of layer thickness from tissue processing.

Ocular examination and imaging

The ocular surfaces of conscious mice were examined under a slit lamp microscope (SL-D7; Topcon, Tokyo, Japan) by an investigator blinded to genotype. Images were taken with a digital camera (D800; Nikon, Tokyo, Japan).

Optical coherence tomography

Mice were anesthetized with intraperitoneal (*i.p.*) ketamine/xylazine (100 mg ketamine + 10 mg xylazine/kg body weight) for bilateral measurement of central corneal thickness (CCT) with spectral domain optical coherence tomography (SD-OCT; Bioptigen, Durham, SC, USA). Scans of the anterior segment were obtained with a 12 mm telecentric bore centered over the pupil, with the following parameters: 2.0 mm radial volume scans, 1000 A scans/B scan, 100 B scans/volume, 1 frame/B scan, 1 volume. CCT, epithelial thickness, and stromal thickness were measured with vertical-locked B scan calipers in the Bioptigen InVivoVue Clinic software. Mice were omitted from analysis if variation in CCT between left and right eyes exceeded 5 µm.

Substance P immunoassay in the cornea

Corneas from each mouse were pooled and homogenized (VWR 200 Homogenizer) in 100 µL cold RIPA buffer containing protease/phosphatase inhibitors (Halt Cocktail; Thermo Scientific). Total protein in each sample was determined by BCA assay according to manufacturer's instructions (Thermo Scientific).

To quantify corneal SP, each sample was diluted to a concentration of 0.5 µg/µL in 1x ELISA buffer provided in the Cayman Chemical Substance P ELISA Kit (Ann Arbor, MI, USA), then plated in the pre-coated 96 well plate at 1:100 in triplicate. Blank, non-specific binding, maximum binding, and total activity wells were included as controls, and an eight-point standard curve was plated in duplicate per manufacturer's instructions. Plates were incubated overnight at 4°C in antiserum and acetylcholinesterase tracer, then washed and developed in Ellman's reagent for 2 h at RT in the dark. Absorbance was measured at 420 nm on a SpectraMax M2 microplate reader. Data were background-subtracted and presented as pg SP per µg total protein.

Statistics

Results are presented as mean ± SEM. Student's unpaired *t* test was used to compare CCT, corneal epithelial thickness, stromal thickness, positive CD31 immunostaining, subbasal nerve leash count, corneal epithelial cellularity, and NK1R band density between groups. All statistical analyses were performed in Graphpad Prism 7 (San Diego, CA, USA). Throughout, $P \leq 0.05$ was considered statistically significant.

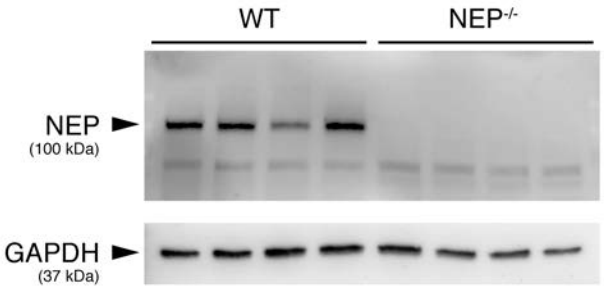

Figure 1. Expression of NEP protein in mouse cornea. Immunoblot of NEP (100 kDa) in whole cornea lysates from WT and NEP$^{-/-}$ mice with glyceraldehyde 3-phosphate dehydrogenase (GAPDH, 37 kDa) run as a loading control. Membrane was cut at 50 kDa**.**

Results

NEP is functionally expressed in the mouse cornea

Immunoblot analysis of whole cornea lysates with anti-NEP antibody revealed the expected 100 kDa band in WT but not $NEP^{-/-}$ tissue (Fig. 1). To determine whether truncated forms of NEP are expressed in $NEP^{-/-}$ tissue, we performed an immunoblot analysis of whole corneal lysates with the same NEP antibody but did not include a loading control in order to visualize lower molecular weight bands. The full-length, overexposed blot did not reveal obvious differences in < 100 kDa banding between WT and $NEP^{-/-}$ corneal samples (Fig. 2).

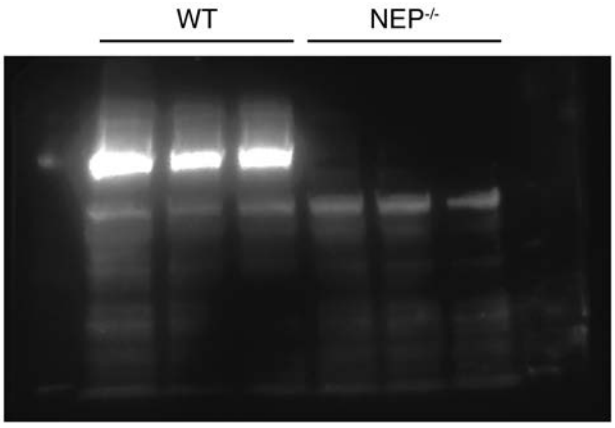

Figure 2. Full length immunoblot for NEP protein in mouse cornea. Immunoblot of NEP in whole cornea lysates from WT and $NEP^{-/-}$ mice (n = 3). Blot was overexposed to allow visualization of additional bands.

With the same primary antibody, we then examined the cellular distribution of NEP with immunohistochemistry (Fig. 3). In the WT cornea, NEP was localized prominently in the apical epithelial layer and stromal keratocytes, with occasional signal in the cytoplasm of basal epithelial cells. Unexpectedly, $NEP^{-/-}$ corneal sections also showed NEP staining but in a different distribution, with signal localizing to the basal epithelium in a perinuclear distribution. No signal was detected in the no primary

antibody controls. Notably, similar staining in NEP$^{-/-}$ tissue was observed using other monoclonal and polyclonal NEP antibodies, visualized with Anti-Rabbit ImmPRESS Anti-Rabbit IgG (Peroxidase) Polymer Detection and ImmPACT NovaRED Kits (VectorLabs, Burlingame, CA, USA), though the signal in WT tissue was less intense with this technique (data not shown).

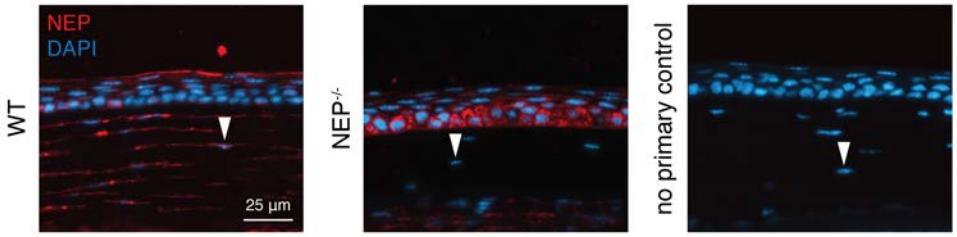

Figure 3. Localization of NEP in the mouse cornea. Representative immunofluorescence images labeled for NEP (red) and DAPI (blue) in WT corneal sections (n = 3), compared to NEP$^{-/-}$ (n = 3) and no primary control (n = 2) sections. NEP localizes to superficial epithelial cells and stromal keratocytes (arrowheads) in WT sections. Original magnification, 40X; scale bar, 25 µm.

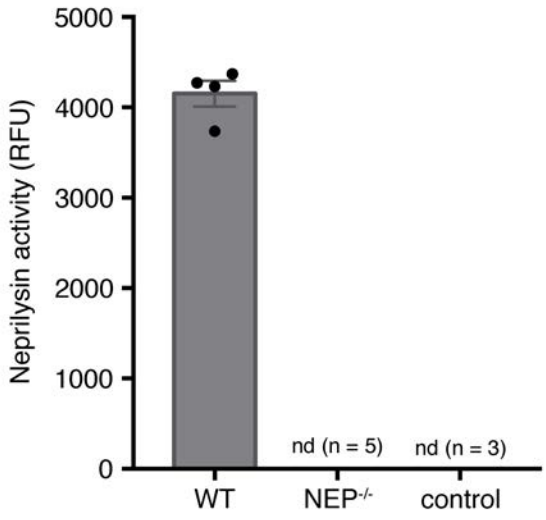

Figure 4. NEP enzyme activity in mouse cornea. NEP activity in whole cornea lysates from WT and NEP$^{-/-}$ mice, determined with a FRET-based assay (lower limit of detection, 0.78 ng/mL of active NEP). NEP activity in NEP$^{-/-}$ cornea lysates and negative control wells were not detectable (nd).

To establish whether these signals represented functional NEP protein, we assayed for NEP activity in whole cornea lysates (Fig. 4). Activity in WT samples was readily detected at levels above that in $NEP^{-/-}$ samples and negative control wells, which were not detectable. This suggests that the NEP signal seen on histology in $NEP^{-/-}$ tissue represents either non-specific staining or an inactive, truncated form of the NEP protein that could not be discerned on immunoblots.

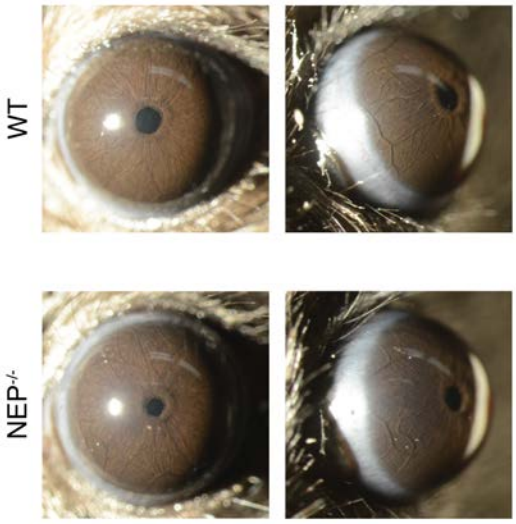

Figure 5. Constitutive genetic disruption of NEP activity does not affect morphological development of the ocular surface. Broad beam slit lamp images of WT and $NEP^{-/-}$ eyes showing corneal and limbal regions (n = 3 mice/group). Ocular surfaces of WT and $NEP^{-/-}$ mice are grossly indistinguishable.

NEP deficiency is associated with normal ocular surface and corneal thickness

To assess the effect of constitutive NEP disruption on corneal morphology, we used two *in vivo* imaging techniques: slit lamp biomicroscopy, which uses an adjustable beam of incandescent light to image the eye from various angles; and anterior segment optical coherence tomography (OCT), which uses long wavelength light to non-invasively capture micrometer-resolution images of the eye. Non-invasive *in vivo* imaging allows examination of corneal morphology in the absence of artifacts that are typically

introduced during tissue processing for histology. No epithelial defects, cataracts, corneal opacities, or corneal neovascularization were observed on slit lamp examination of awake, unmanipulated WT or NEP$^{-/-}$ mice (Fig. 5).

Central corneal thickness (CCT), epithelial thickness, and stromal thickness were then quantified using OCT. Representative OCT images are shown in Fig. 6a. No significant differences were detected in CCT or epithelial thickness between groups, though there was a trend for increased stromal thickness in NEP$^{-/-}$ corneas compared to WT controls (Fig. 6b, $P = 0.0534$). In concordance with OCT data, corneal epithelial cellularity did not significantly differ between WT (Fig. 7a) and NEP$^{-/-}$ mice (Fig. 7b), based on nuclei count in DAPI-labeled corneal sections (Fig. 7c, $P = 0.8506$).

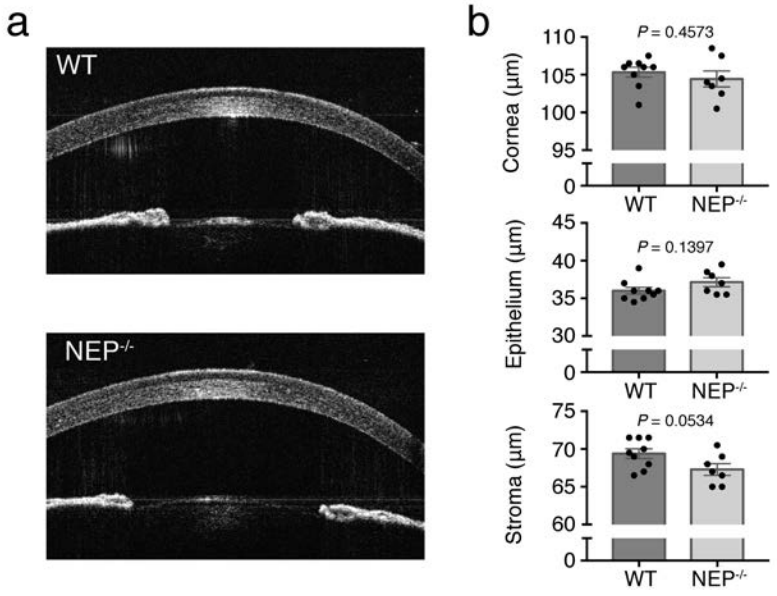

Figure 6. *In vivo* measurement of central corneal thickness in WT and NEP$^{-/-}$ mice.
(**a**) Representative images of WT and NEP$^{-/-}$ corneas obtained with anterior segment optical coherence tomography (OCT). (**b**) Quantification of central corneal thickness and thickness of epithelial and stromal layers (n = 7 - 9 mice/group; mean ± SEM; two-tailed *t*-test).

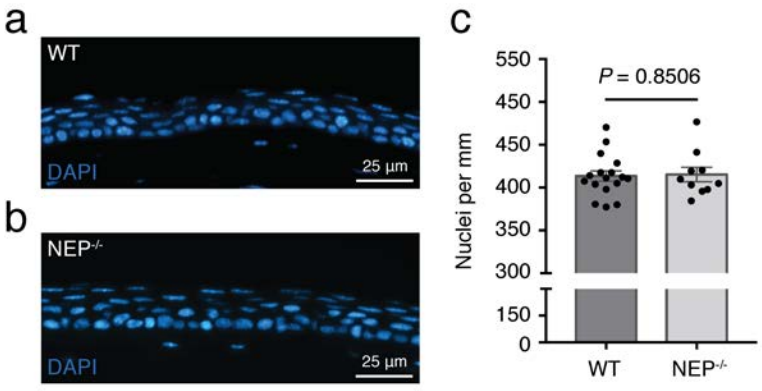

Figure 7. NEP deficiency does not alter corneal epithelial cellularity. Representative images of WT (**a**) and NEP$^{-/-}$ (**b**) corneas labeled with DAPI to visualize epithelial nuclei. (**c**) Quantification of corneal epithelial cell nuclei, normalized to the length of central corneal epithelium sampled in millimeters (n = 10 - 17 fields/group; n = 3 mice/group; mean ± SEM; two-tailed *t*-test). Original magnification, 40X; scale bar, 25 µm.

NEP$^{-/-}$ mice have increased corneal innervation and normal pericorneal vasculature

To further assess the pericorneal vasculature, we immunolabeled whole mount corneas for the endothelial marker CD31 to visualize blood vessels. As expected, the pericorneal plexus was appropriately confined to the limbal area and did not encroach onto the peripheral cornea in either WT or NEP$^{-/-}$ mice (Fig. 8a, b). Quantification of CD31 staining confirmed that there was no significant difference in the total area of vasculature between groups (Fig. 8c, $P = 0.786$).

In the same corneas, we also immunolabeled for βIII tubulin (TUJ1) to visualize corneal innervation at the level of the subbasal nerve plexus (Fig. 9a, b), which is composed of radially-oriented unmyelinated fibers that run beneath the basal epithelium and terminate between superficial epithelial cells as intraepithelial nerves (Müller et al. 2003). Notably, NEP$^{-/-}$ corneas had 33.47 ± 8.11% more subbasal nerve leashes than WT corneas (Fig. 9c, $P = 0.0103$).

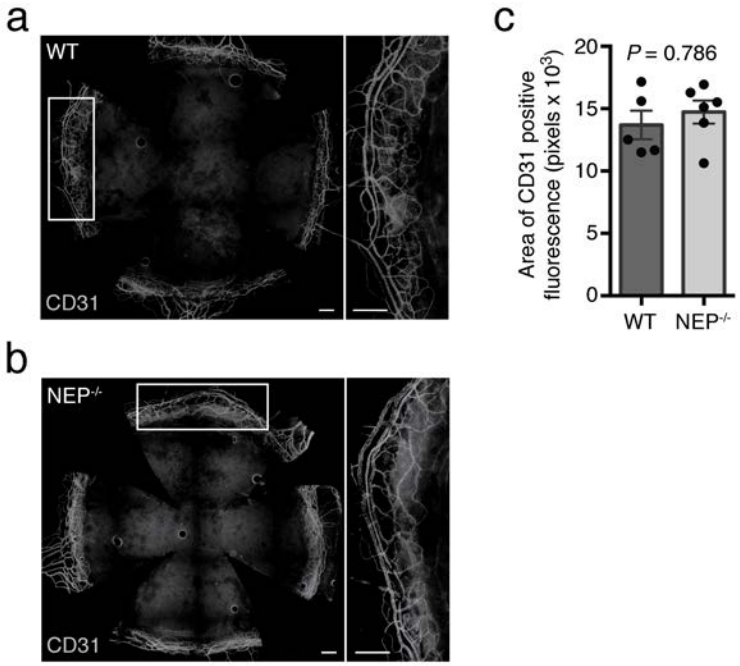

Figure 8. NEP deficiency does not alter limbal vasculature. Representative corneal flat mounts from a WT (**a**) and NEP$^{-/-}$ (**b**) mouse immunostained with the vascular marker CD31. Higher magnification images of boxed areas in (**a**) and (**b**) are shown to the right of each image, respectively. Original magnification, 10X; scale bar, 250 µm. (**c**) Area of positive CD31 immunofluorescence (n = 5 - 6 mice/group, mean ± SEM; two-tailed *t*-test).

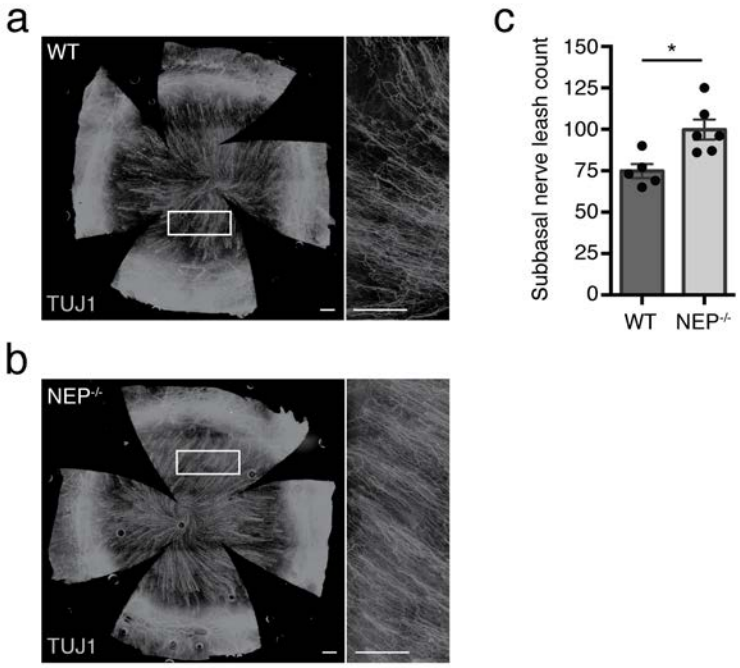

Figure 9. NEP$^{-/-}$ mice have increased corneal innervation at the level of the subbasal plexus. Representative corneal flat mounts from a WT (**a**) and NEP$^{-/-}$ (**b**) mouse immunostained with the pan-neuronal marker βIII tubulin (TUJ1). Higher magnification images of boxed areas in (**a**) and (**b**) are shown to the right of each image, respectively. Original magnification, 10X; scale bar, 250 µm. (**c**) Subbasal nerve leash counts (n = 5 - 6 mice/group, mean ± SEM; **P* = 0.0103; two-tailed *t*-test).

NEP deficiency does not alter SP or NK1R expression in the cornea

An excess of SP can result in pathologic inflammation and corneal neovascularization, while insufficient levels lead to persistent corneal epithelial defects (Bignami et al. 2016; Gaddipati et al. 2016; Nishida and Yanai 2009; Twardy et al. 2011). Since we did not observe pathologic changes at either end of this spectrum in NEP$^{-/-}$ animals, we predicted that the corneal SP-NK1R signaling axis would not differ between WT and NEP$^{-/-}$ mice, despite SP being the highest affinity substrate of NEP (Turner et al. 1985). As expected, SP levels and NK1R protein expression in the cornea did not significantly differ between WT and NEP$^{-/-}$ mice (Fig. 10, $P = 0.9125$; Fig. 11, $P = 0.8112$). These data indicate that loss of NEP function does not affect SP or its receptor expression in the cornea at baseline.

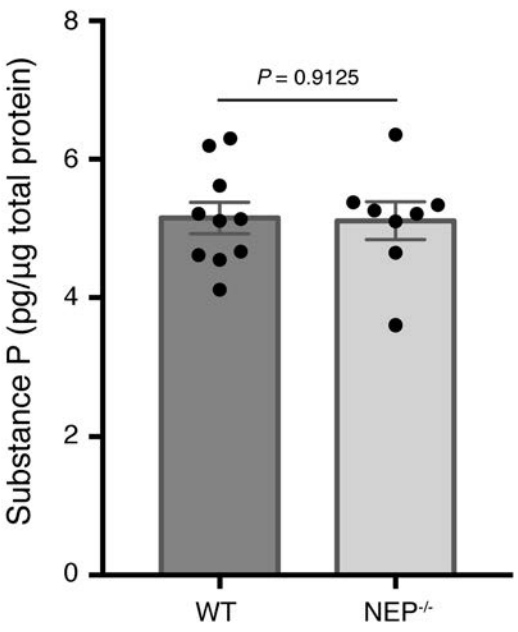

Figure 10. NEP deficiency does not alter substance P levels in the cornea. Substance P-like immunoreactivity determined by enzyme immunoassay in whole cornea lysates from WT and NEP$^{-/-}$ mice. Data presented as pg SP per µg total protein assayed (n = 8 - 10 mice/group, mean ± SEM; two-tailed *t*-test).

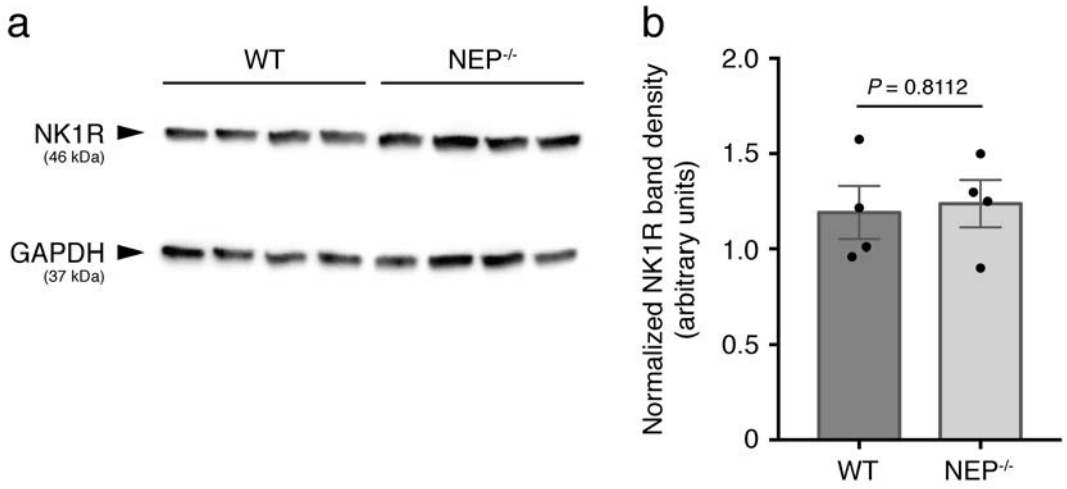

Figure 11. NEP deficiency does not alter neurokinin-1 receptor expression in the cornea. (**a**) Immunoblot of neurokinin-1 receptor (NK1R; 46 kDa) in whole cornea lysates from WT and NEP$^{-/-}$ mice with glyceraldehyde 3-phosphate dehydrogenase (GAPDH, 37 kDa) run as a loading control on the same gel. Membrane was cut at approximately 40 kDa. (**b**) Densitometric analysis of NK1R bands normalized to GAPDH (n = 4 mice/group, mean ± SEM; two-tailed *t*-test).

Discussion

Overview of findings

In this chapter, we report functional expression of NEP in the mouse cornea. Previously, a single study described NEP expression in the human cornea, but its physiological function was not investigated (Hasby and Saad 2013). Our examination of the adult mouse cornea with *in vivo* imaging and histology has now revealed that gross corneal morphology, epithelial and stromal thickness, epithelial cellularity, and perilimbal vasculature are all unaltered by NEP deficiency. Furthermore, loss of NEP activity does not appear to disrupt the SP-NK1R signaling system at baseline. However, we did observe increased corneal innervation in NEP$^{-/-}$ mice, based on subbasal nerve leash number.

Functional expression of NEP in the cornea

In this study, we generated multiple lines of evidence that document expression of NEP in the uninjured mouse cornea: first, NEP protein in whole corneal lysates was detected by immunoblot; second, cellular localization of NEP in the cornea was determined by immunohistochemistry; lastly, an enzymatic assay established the presence of NEP activity while verifying the lack of functional NEP protein in $NEP^{-/-}$ corneas. NEP is expressed in an assortment of epithelial tissues, including the epidermis (Olerud et al. 1999), gastrointestinal brush border (Skryzdło-Radomańska et al. 1994), pulmonary epithelium (Johnson et al. 1985), nasal mucosa (Ohkubo et al. 1994), and renal brush border where the enzyme was first isolated (George and Kenny 1973). It is therefore unsurprising that NEP is also expressed in the corneal epithelium, particularly given its high density of peptidergic innervation (Müller et al. 2003).

In support of our results, a previous study detected NEP in the human cornea with immunohistochemical methods (Hasby and Saad 2013). The authors reported occasional perinuclear staining in the basal corneal epithelium similar to that described here, though we also detected NEP in the apical epithelial layer and stromal keratocytes. With the superficial cornea bathed in tears containing growth factors, cytokines, and neuropeptides (Kaufman et al. 2011; Yamada et al. 2002), NEP expression at this interface positions the enzyme to modulate signals exchanged between the tear film and corneal epithelium.

Given that NEP is a membrane-bound protein, an explanation for its perinuclear localization in basal epithelial cells is not as readily apparent, though this expression pattern has been previously described in nasal mucosa (Ohkubo et al. 1994), epidermis (Olerud et al. 1999), and pulmonary epithelium (Nadel and Borson 1991). In a study on NEP expression in human epidermis, Olerud *et al* (1999) proposed that NEP

predominantly clusters in cells that express neuropeptide receptors to facilitate competition between receptors and degradative enzymes for neuropeptides (Olerud et al. 1999). If this is the case, it then would follow that clusters of basal corneal epithelial cells highly express such receptors. To the best of our knowledge, however, the differential expression of neuropeptide receptors in corneal epithelial cell types has not been studied. Still, this would not explain the perinuclear location of NEP in the basal corneal epithelium of both WT and $NEP^{-/-}$ mice. A potential explanation may reside in the post-translational modification of NEP. As a glycosylated protein processed in the endoplasmic reticulum (ER) and Golgi apparatus (Stewart and Kenny 1984), NEP may be temporarily concentrated in these perinuclear organelles and therefore readily labeled.

A similar explanation may account for the unexpected staining observed in $NEP^{-/-}$ mice. Conceivably, a truncated NEP protein may be produced as a result of the exonic cassette inserted to generate the $NEP^{-/-}$ mouse line. Exon 13 of the murine NEP locus, which encodes a portion of the extracellular domain, was replaced with a neomycin resistance cassette through homologous recombination. Subsequent Northern analysis did not detect NEP mRNA when probed with cDNA spanning exons 14-20 (Lu et al. 1995); however, no studies were conducted to evaluate potential translation of truncated NEP protein. In this study, the polyclonal antibody used for immunoblotting and immunohistochemistry recognizes mouse NEP residues 52 - 750, which comprise its entire extracellular domain. The antibody may therefore retain the ability to bind a truncated NEP protein, accounting for the immunofluorescent signal in $NEP^{-/-}$ corneas, while retention of truncated NEP in the ER or Golgi would explain the perinuclear localization observed. Indeed, intracellular trapping of NEP is known to occur with partially glycosylated forms of the enzyme, likely due to misfolding (Lafrance et al. 1994).

Alternatively, the antibody may recognize portions of the related endopeptidase, NEP2, a soluble enzyme sharing 42.7% sequence identity with NEP in its N-terminal region (amino acids 1 - 510 of NEP2; Ikeda et al. 1999). During processing, NEP2 is temporarily membrane-bound in the ER and a portion of the Golgi (Ikeda et al. 1999) but requires post-translational modification and transportation out of the ER to become active (Rose et al. 2002). Other glycoforms of NEP2 may be retained in the ER permanently (Ikeda et al. 1999; Whyteside and Turner 2008). Expression of NEP2 in the cornea is unknown but could account for perinuclear immunostaining in both WT and $NEP^{-/-}$ corneas. Critically, the NEP enzyme activity assay confirmed loss of activity in the $NEP^{-/-}$ corneas, despite detection of putative NEP or NEP2 protein by immunostaining.

NEP deficiency does not alter development or homeostatic maintenance of the cornea

To maintain corneal homeostasis, a complex regulatory network of neural, paracrine, and humoral factors modulates corneal epithelial cell production to match the rate of desquamation (Hanna et al. 1961; Hanna and O'Brien 1960). Neuropeptides of both neural and paracrine origin are among the factors that contribute to homeostatic maintenance, yet constitutive loss of the neuropeptide-metabolizing activity of NEP does not appear to cause significant imbalance in the system: WT and $NEP^{-/-}$ corneas are morphologically indistinguishable at the gross anatomic and cellular levels, suggesting that NEP is not essential for development or homeostatic maintenance of the cornea. Alternatively, activation of compensatory responses in $NEP^{-/-}$ mice may serve to buffer against any deleterious effects of constitutive NEP inactivation, effectively masking any resultant phenotype. An inducible cornea-specific knockout or antisense-knockdown approach would be necessary to probe the possible role of compensation, since these

techniques are less likely to induce counteracting genetic mechanisms (El-Brolosy and Stainier 2017; Rossi et al. 2015).

NEP deficiency alters corneal innervation

Phenotypic characterization of $NEP^{-/-}$ corneas revealed an increased number of nerve leashes in the subbasal plexus, a whorl of bundled fibers with terminations that innervate the epithelium (Müller et al. 1996). The physiological significance of this increased innervation cannot be surmised without additional investigation, given that subbasal nerve density does not necessarily correlate with intraepithelial nerve density or corneal sensitivity (Davidson et al. 2012a). However, our findings agree with a recent study on the effect of NEP on diabetic neuropathy, in which Yorek *et al.* reported a trend of increased corneal nerve density in nondiabetic $NEP^{-/-}$ mice compared to WT controls. The authors ascribe this to the accompanying increase in CGRP-positive fibers observed in $NEP^{-/-}$ corneas, proposing that CGRP could promote corneal nerve generation (Yorek et al. 2016).

Other studies have suggested that NEP regulates peripheral nerve development through different mechanisms. Expressed on the plasma membranes of both myelin-forming and non-myelin-forming Schwann cells in prenatal and early postnatal development (Kioussi and Matsas 1991), NEP levels decline in myelin-forming Schwann cells as myelination concludes in adulthood, paralleling the developmental profile of other axonally-controlled antigens (Kioussi et al. 1992). Though the substrate(s) for NEP on Schwann cell membranes are unknown, interleukin-1 (IL-1) has been suggested as a potential candidate. Macrophages closely associate with peripheral nerves in neonatal life (Stoll and Müller 1986) and function as a source of IL-1 to stimulate nerve growth factor (NGF) production by Schwann cells (Lindholm et al. 1987). NEP may therefore

compete with IL-1 receptors on Schwann cell membranes to modulate NGF production. Loss of NEP activity would then increase NGF production and perhaps account for increased corneal innervation in $NEP^{-/-}$ mice.

NEP deficiency does not alter SP-NK1R signaling in the cornea

Predominantly secreted by neurons and inflammatory cells, substance P (SP) is an ubiquitous, injury-inducible mitogenic neuropeptide found in tear fluid, corneal nerves, and corneal epithelial cells (Reid et al. 1993; Tervo et al. 1982; Watanabe et al. 2002; Yamada et al. 2002). As with other signaling molecules, rates of synthesis, release, and degradation regulate the active pool of SP available for receptor binding and signal transduction, and perturbation of this balance can result in corneal pathology.

Despite SP being the highest-affinity substrate of NEP (Turner et al. 1985), we did not observe baseline pathologic changes in $NEP^{-/-}$ mice, nor did we detect a difference in corneal SP levels or neurokinin-1 receptor expression. This suggests that NEP is not a major regulator of SP in the cornea under homeostatic conditions. Alternatively, other degradative mechanisms may be upregulated to compensate for the loss of NEP activity, ultimately correcting any potential imbalance. Indeed, SP can be cleaved by dipeptidyl peptidase IV, deamidase, and angiotensin-converting enzyme, plus undergo non-enzymatic degradation and oxidation in the extracellular space (Jackman et al. 1990; Michael-Titus et al. 2002; Rissler 1995).

Importantly, interpretation of these findings is limited by the methods used to quantify SP levels in the cornea. Extracellular SP is rapidly degraded *in vivo*, with its metabolites exhibiting significant differences in rate of clearance (Michael-Titus et al. 2002). Furthermore, SP metabolites exhibit a range of biological actions, from the beneficial promotion of corneal epithelial migration (Nakamura et al. 1999) to the

detrimental induction of allergic inflammation (Iwamoto et al. 1991). While the ELISA-based kit used in this study detects the full-length SP undecapeptide, only a limited number of possible SP fragments are detectable, and at significantly different efficacies: SP (2-11) and SP (4-11) have approximately equal reactivity as SP (1-11); SP (7-11) is fractionally reactive; and SP (1-4) and SP (8-11) are negligibly reactive. Importantly, SP (7-11) and SP (8-11) are NEP cleavage products, as are SP (1-6), (1-7), (1-9), and (10-11), which are not detected by the kit (Byrd et al. 2008; Matsas et al. 1984). Though the sum of SP (1-11), (2-11), and (4-11) levels did not differ between $NEP^{-/-}$ and WT mice in this study, we cannot conclude that other SP metabolites are unaltered by NEP deficiency. In humans, SP and SP metabolites have been quantified in tear fluid samples by high-performance liquid chromatography (Yamada et al. 2002). A similar approach, coupled with mass spectrometry, would be needed for detailed quantitative analysis of SP in the mouse cornea.

Conclusions

Collectively, our findings demonstrate that NEP, while functionally expressed in the uninjured cornea, is not required for normal development and homeostatic maintenance of the cornea, with the caveat that NEP activity was constitutively and globally disrupted in this study. However, NEP may be involved in regulating development and/or maintenance of corneal nerves. As a cell surface peptidase readily detected in the corneal epithelium, NEP is well-positioned to modulate peptidergic and neuroimmune crosstalk between corneal epithelial cells, immune cells, and intraepithelial nerve fibers, perhaps accounting for the increased subbasal nerve density observed in $NEP^{-/-}$ mice.

CHAPTER 3: CONSTITUTIVE LOSS OR PHARMACOLOGICAL INHIBITION OF NEP ACCELERATES CORNEAL EPITHELIAL WOUND HEALING

Background and Rationale

Recovery from corneal injury begins with the acute phase of wound healing, during which reepithelialization is undertaken through a multistep process involving cell migration, proliferation, differentiation, stratification, and attachment (Ljubimov and Saghizadeh 2015). This complex cascade is promoted by release of neuropeptides from a dense network of corneal nerves that arise from the trigeminal ganglia, in conjunction with growth factors and cytokines released locally by resident cells and systemically by distant organs (Garcia-Hirschfeld et al. 1994; Imanishi et al. 2000; Reid et al. 1993). The resulting inflammatory reaction supports corneal nerve and epithelial regrowth after injury (Li et al. 2011; Namavari et al. 2012; Zhang et al. 2016) but when dysregulated, can lead to corneal ulceration, neovascularization, and opacification (Bignami et al. 2016; Wagoner 1997).

If endogenous repair mechanisms fail to restore corneal transparency, reconstruction of the ocular surface after severe injury is often attempted through surgical means. Though recent advances in corneal stem cell transplantation can potentially restore a stable corneal epithelium without risk of rejection (Atallah et al. 2016; Dua et al. 2016; Pellegrini et al. 1997; Rama et al. 2010), surgical outcomes are sensitive to tear film stability, intraocular pressure, infection, and inflammation (Liang et al. 2009; Tuft and Shortt 2009). As a consequence, early medical interventions serve an essential role in the management of corneal injury and can ultimately be major determinants of surgical outcomes (Wagoner 1997). However, for severe corneal injuries, visual prognosis often remains guarded despite currently available medical and

surgical techniques (Kuckelkorn et al. 1994; Sharma et al. 2012), emphasizing an unmet need for improved therapeutic strategies. From a clinical standpoint, parsing the physiology of corneal wound healing may generate novel approaches to managing the injured ocular surface.

In the previous chapter, we established functional expression of neprilysin (NEP) in the mouse cornea and showed that constitutive disruption of its enzymatic activity does not affect normal corneal development or homeostasis. However, numerous studies have documented that this ubiquitous and promiscuous enzyme has *in vivo* and *in vitro* effects on apoptosis, peripheral axonal regeneration, epithelial wound healing, and modulation of inflammation in other tissues (Antezana et al. 2002; Bahadir et al. 2009; Day et al. 2005; Hasby and Saad 2013; Kioussi et al. 1995; Lu et al. 1995; Shipp et al. 1991; Spenny et al. 2002; Olerud et al. 1999). In this chapter, we therefore investigate the role of NEP in the injured cornea using genetic and pharmacological *in vivo* approaches, providing preclinical evidence that NEP inhibition significantly accelerates corneal epithelial wound healing.

Materials and Methods

Animals

Eight to twelve week old male mice were used for all experiments. Breeding pairs of mice with a targeted disruption of the membrane metallo-endopeptidase gene (B6.129S4-*Mme*^{tm1Cge}) were provided by Drs. Lu and Gerard (Lu et al. 1995) and bred to establish colonies at the Iowa City Department of Veterans Affairs and University of Iowa (Iowa City, IA) in certified animal care facilities. Offspring were backcrossed to C57BL/6J mice for more than nine generations. Control C57BL/6J mice (The Jackson Laboratory, Bar Harbor, ME) were also housed at these locations. Standard diet (Harlan Teklad,

#7001, Madison, WI, USA) and water were provided *ad libitum* at both facilities. Mice were handled in compliance with the ARVO Statement for the Use of Animals in Ophthalmic and Vision Research, and protocols were approved by the Institutional Animal Care and Use Committees at the Iowa City Department of Veterans Affairs and University of Iowa.

Alkali burn model of corneal injury

Prior to wounding, mice were anesthetized with intraperitoneal (*i.p.*) ketamine/xylazine and received topical 0.5% proparacaine (Bausch + Lomb, Rochester, NY, USA) for corneal analgesia. A single 5 µL drop of 0.5 M NaOH was applied unilaterally to the ocular surface for 30 s, followed by immediate irrigation with 5 mL isotonic saline. A unilateral, saline instillation served as a sham injury. Ocular surfaces were coated with a 2.5% methylcellulose ophthalmic lubricant (Goniovisc, HUB Pharmaceuticals, Rancho Cucamonga, CA, USA) to prevent drying and reduce infection risk after injury. After injury, animals were monitored until ambulatory. Subcutaneous meloxicam (2 mg/kg; Newbrook, Newry, Northern Ireland) was provided up to 48 h after injury for pain control. All animals were euthanized by rapid decapitation under isoflurane anesthesia 7 d after injury.

Analysis of wound closure

Corneal wounds were visualized with 0.1% rose bengal (Sigma-Aldrich, St. Louis, MO, USA) under a slit lamp microscope (Zeiss) equipped with a digital camera (Olympus DP21). Duplicate images were acquired of the ocular surface at 1, 3, and 7 d post-injury under ketamine-xylazine anesthesia. During each anesthetic event, eyes were protected

with a sterile, water-soluble ophthalmic lubricant (Optixcare; CLC Medica, Waterdown, Ontario, Canada) to prevent drying of the ocular surface before and after imaging.

Quantitative analyses of corneal rose bengal staining were performed using a custom-written color deconvolution algorithm in Aperio Spectrum software (Leica Biosystems, Buffalo Grove, IL, USA). Regions of reflected light were omitted from the analyzed area. Total percent staining within a user-defined area (here, the cornea) was averaged for each pair of images. Data are representative of more than three independent experiments.

NEP enzyme activity following thiorphan administration

To determine optimal route of thiorphan administration and efficacy in the cornea, uninjured WT mice were administered a single dose of topical or *i.p.* thiorphan ((DL-3-mercapto-2-benzylpropanoyl)-glycine; N1195; Bachem, Bubendorf, Switzerland). Mice receiving a topical preparation were administered 10 µL of 0.1 mg/mL or 0.5 mg/mL thiorphan or vehicle (saline), applied directly to the ocular surface with a pipette.

Mice receiving an *i.p.* injection were administered 15 mg/kg thiorphan or vehicle (5% ethanol in saline) with a 28 gauge U-100 insulin syringe (Becton-Dickinson, Franklin Lake, NJ, USA). Mice were decapitated under deep isoflurane anesthesia 30 min after topical thiorphan, or 1 or 6 hours after *i.p.* thiorphan for collection of bilateral trigeminal ganglia and corneas. Tissue was frozen in liquid nitrogen and stored at -80°C.

Frozen corneas were homogenized in 100 µL of 0.5% NP-40 lysis buffer in two 15 s bursts with 30 s on ice between bursts. Frozen trigeminal ganglia were homogenized in 200 µL of buffer for 10 s. Aprotinin (5 µg/mL; Thermo Scientific) and phenylmethylsulfonyl fluoride (200 µM; Thermo Scientific) were added to the buffer to prevent protein degradation. Samples were centrifuged at 10,000 g for 5 min at 4°C, and

pellets were discarded. Total protein in each supernatant was determined by BCA assay according to manufacturer's instructions (Thermo Scientific).

NEP activity was determined using the SensoLyte 520 Neprilysin Activity Assay Kit (AnaSpec). Samples were diluted in 1x assay buffer to 10 µg protein/50 µL/well and loaded in triplicate in 96-well plates. Positive, negative, and substrate controls were run according to manufacturer's protocol. Plates were incubated and read at 24°C. Endpoint fluorescence was recorded on a SpectraMax M2 microplate reader (Molecular Devices) with excitation at 490 nm and emission at 520 nm, per manufacturer's protocol.

Thiorphan preparation and administration

Stock solutions of 30 mg/mL thiorphan were prepared in 100% ethanol and stored at -20°C. Working solutions of 1.5 mg/mL were prepared daily by dilution in isotonic saline. Saline containing 5% ethanol served as a vehicle control. Intraperitoneal 5 mg/kg or 15 mg/kg thiorphan, or vehicle was administered to mice within 1 h after corneal injury. Administration was continued daily in each group until euthanasia on day 7 after injury. Ocular surface imaging and analysis of wound closure was performed as above. Data are representative of two independent experiments.

Immunoblot analysis of WT corneas after alkali injury

Anesthetized WT mice were unilaterally injured with a 5 µL drop of 0.5 M NaOH on the left ocular surface for 30 s. Saline served as a sham injury. Subcutaneous meloxicam (2 mg/kg) was administered in sham and injured groups immediately after injury and 24 h after injury. Mice received *i.p.* 15 mg/kg thiorphan or vehicle (5% ethanol in saline) within 1 h after corneal injury and each day thereafter until euthanasia at the end of one week.

In order to avoid any effects of manipulation on the ocular surface, mice used for immunoblot analysis were not imaged.

Freshly enucleated eyes were trimmed at the sclerocorneal limbus. The left cornea from each mouse was homogenized (VWR 200 Homogenizer) in 100 µL of cold RIPA buffer containing protease/phosphatase inhibitors. Three gels were required to represent all experimental groups. Corneal lysates containing equal amounts of protein (9.5 µg), determined by BCA assay, were randomized among the three 7.5% Mini-PROTEAN TGX precast polyacrylamide gels (BioRad), separated by electrophoresis, and transferred to nitrocellulose membranes with the BioRad Trans-Blot Turbo Transfer system. An equal concentration of intermembrane (IM) reference sample (pooled TKE2 lysate) was run on each gel in the same location. Membranes were cut at 50 and 150 kDa and blocked in 5% skim milk in TBST buffer at RT for 1 h. The upper third of each membrane (> 150 kDa) was immunoblotted in rabbit anti-CD45 (ab208022; Abcam) at 1:1000, the middle third (50 - 150 kDa) in rabbit anti-CD31 (ab28364; Abcam) at 1:250, and the bottom third (< 50 kDa) in mouse anti-alpha smooth muscle actin (SMA; ab7817; Abcam) at 1:500 overnight at 4°C. The IM reference lane was incubated in rabbit anti-neurokinin-1 receptor (NK1R; ab183713; Abcam) at 1:1000. After washing in TBST, all membranes were incubated with HRP-conjugated secondary antibodies (Abcam) at 1:5000 for 1 h at RT and developed with SuperSignal West Femto Maximum Sensitivity Substrate. Chemiluminescence was detected using a BioRad ChemiDoc XRS+ system with Image Lab software.

Following chemiluminescent detection, membranes were stained for total protein using amido black according to a published protocol (Goldman et al. 2016). In brief, membranes were washed in dH2O and submerged in 0.01% (w/v) amido black 10B (Abcam) in 10% acetic acid for 1 min. Membranes were then destained in 5% acetic

acid, washed in dH2O, and dried at RT. Dried membranes were imaged using the Epi-White illumination setting with identical exposure times on the ChemiDoc XRS+ system.

For relative quantification, the integrated optical density value (defined as the sum of each background-subtracted pixel value) was determined for equal-sized boxes drawn around bands for each antibody in Image Studio Lite software (LI-COR Biosciences, Lincoln, NE, USA). Median background was calculated from perimeter values around each band of interest. As a loading control, the total amido black signal was determined for equal-sized strips centered in each lane, rather than a rectangle encompassing the entire stained area, to minimize errors due to lane bending (Aldridge et al. 2008). The integrated optical density for each protein of interest was first normalized to the total amido black signal in its corresponding lane, and then to the normalized integrated optical density of the IM control protein, NK1R, from its corresponding membrane to control for intermembrane variability. NK1R bands were similarly normalized to the total amido black signal in corresponding lanes.

Samples were re-randomized and immunoblots were repeated with statistically similar results. Normalized data from the second set of immunoblots are presented.

Immunoblot analysis of TKE2 cells

TKE2 cells (ECACC 11033107; Sigma-Aldrich, St. Louis, MO, USA), a line of mouse corneal epithelial progenitors isolated from a CD-1 female mouse (Kawakita et al. 2008), were harvested at passage 3, incubated in 150 µL cold RIPA buffer with protease and phosphatase inhibitors (Halt Cocktail; Thermo Scientific), and sonicated on ice. After centrifugation at 13,000 g for 5 min at 4°C, the supernatant was collected and protein concentration was determined by BCA assay according to manufacturer's instructions.

Lysates containing equal amounts of protein (20 µg) were separated on a 10% Mini-PROTEAN TGX precast polyacrylamide gel (BioRad) and transferred to a nitrocellulose membrane with the BioRad Trans-Blot Turbo Transfer system. For detection of NEP and the loading control glyceraldehyde 3-phosphate dehydrogenase (GAPDH), membranes were cut at 70 kDa and blocked in 5% milk in TBST buffer at RT for 1.5 h. The upper half of the membrane (> 70 kDa) was incubated in goat anti-CD10 (NEP; PA5-47075; Invitrogen) at 1:1000, and the lower half (< 70 kDa) was incubated in mouse anti-GAPDH (MAB374; EMD Millipore) at 1:1000, both overnight at 4°C. After washing in TBST, membranes were incubated with HRP-conjugated secondary antibodies (Abcam) at 1:5000 for 1 h at RT and developed with SuperSignal West Femto Maximum Sensitivity Substrate (Thermo Scientific). Chemiluminescence was detected using a BioSpectrum 810 imaging system with CCD camera (Ultra-Violet Products).

TKE2 in vitro scratch assays

Scratch assays with TKE2 cells between passages 3 and 10 were used to determine whether thiorphan could promote wound closure *in vitro*. Cells were plated at a density of 62,500 cells/cm^2 and grown to confluence on uncoated 12-well Corning CellBIND plates (Corning Life Sciences, Corning, NY, USA) in Stemline Keratinocyte Medium II (S0196) with Stemline Keratinocyte Growth Supplement (S9945) and 2 mM glutamine (Sigma). The confluent monolayer was scratched with a 200 µL sterile pipette tip guided by a plastic ruler. Scratch-wounded monolayers were washed with prewarmed media to remove detached cells and debris before incubating in fresh media containing 1, 10, or 100 µM thiorphan (diluted from a 2 mM stock in water) or 10 µL of UltraPure water (Invitrogen, Carlsbad, CA, USA) in 0.5 mL of complete medium for 18 h. Conditions were assayed in triplicate wells, assigned at random on each plate.

Wound closure was monitored with time-lapse differential interference contrast (DIC) imaging on a custom-built Olympus IX-81 inverted microscope (Waltham, MA, USA) with a humidified, carbogenated (flow rate 0.5 - 1.0 L/min), 37°C environmental chamber at the University of Iowa Central Microscopy Research Facility. The motorized stage controller (ProScan II) and associated Olympus cellSens software allowed imaging of three pre-selected, "memorized" positions within each well. Images were collected at 4X every 15 min for the duration of the experiment. Scratch wound closure was analyzed in ImageJ software (NIH). The initial wound area (time 0) and remaining wound areas at 2 h intervals were manually outlined for quantification. Data are presented as average percent closure relative to initial wound area at each timepoint.

Statistics

Results are presented as mean ± SEM. A one-way ANOVA with *post hoc* Bonferroni correction for multiple comparisons was used to compare NEP activity and corneal rose bengal staining among groups. Student's unpaired *t* test was used to compare scratch wound closure between groups. All statistical analyses were performed in Graphpad Prism 6 or 7 (San Diego, CA, USA). Throughout, $P \leq 0.05$ was considered statistically significant.

Results

NEP deficiency promotes corneal epithelial wound healing in vivo

To evaluate the effect of NEP deficiency on corneal wound healing, we chemically injured the corneas of $NEP^{-/-}$ and WT mice with controlled application of sodium hydroxide to the ocular surface (Fig. 12). The acute phase of wound healing was tracked with slit lamp imaging at 1, 3, and 7 d after injury, with rose bengal retention serving as a

measure of the corneal defect at each timepoint. The corneas of sham-injured mice retained minor rose bengal stain after sham injury, typically in the central and/or nasal cornea. However, the pattern of dye retention was superficial compared to that observed in alkali-injured animals, and sham-injured corneas retained clarity and regularity of the ocular surface over the 7 days post-injury (Fig. 13a). There was also no significant difference in the area of positive staining between WT and $NEP^{-/-}$ sham groups at any timepoint (Fig. 13b).

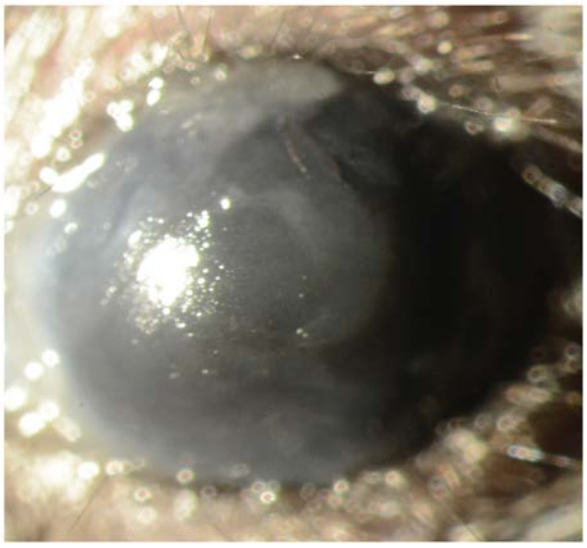

Figure 12. Broad-beam slit lamp image of the alkali-injured cornea. Representative image of the ocular surface 1 day after alkali injury, without rose bengal instillation to illustrate the density and area of corneal haze. Details of the iris and pupil are obscured, but the pupil remains distinguishable from the iris. This injury represents a grade III burn according to Roper-Hall criteria for corneal involvement. Limbal ischemia was not evaluated.

In the alkali-injured groups, corneas appeared diffusely opaque and edematous 1 day post-injury. At this acute time point, the area of corneal defect in alkali-injured $NEP^{-/-}$ mice was not significantly different from that in alkali-injured WT mice (Fig. 13b). However, at 3 and 7 days post-injury, the corneal defect area in $NEP^{-/-}$ mice was 42.72 ± 4.91% and 52.08 ± 7.19% smaller, respectively, than that in WT mice (Fig. 13b, $P < 0.0001$ at both time points).

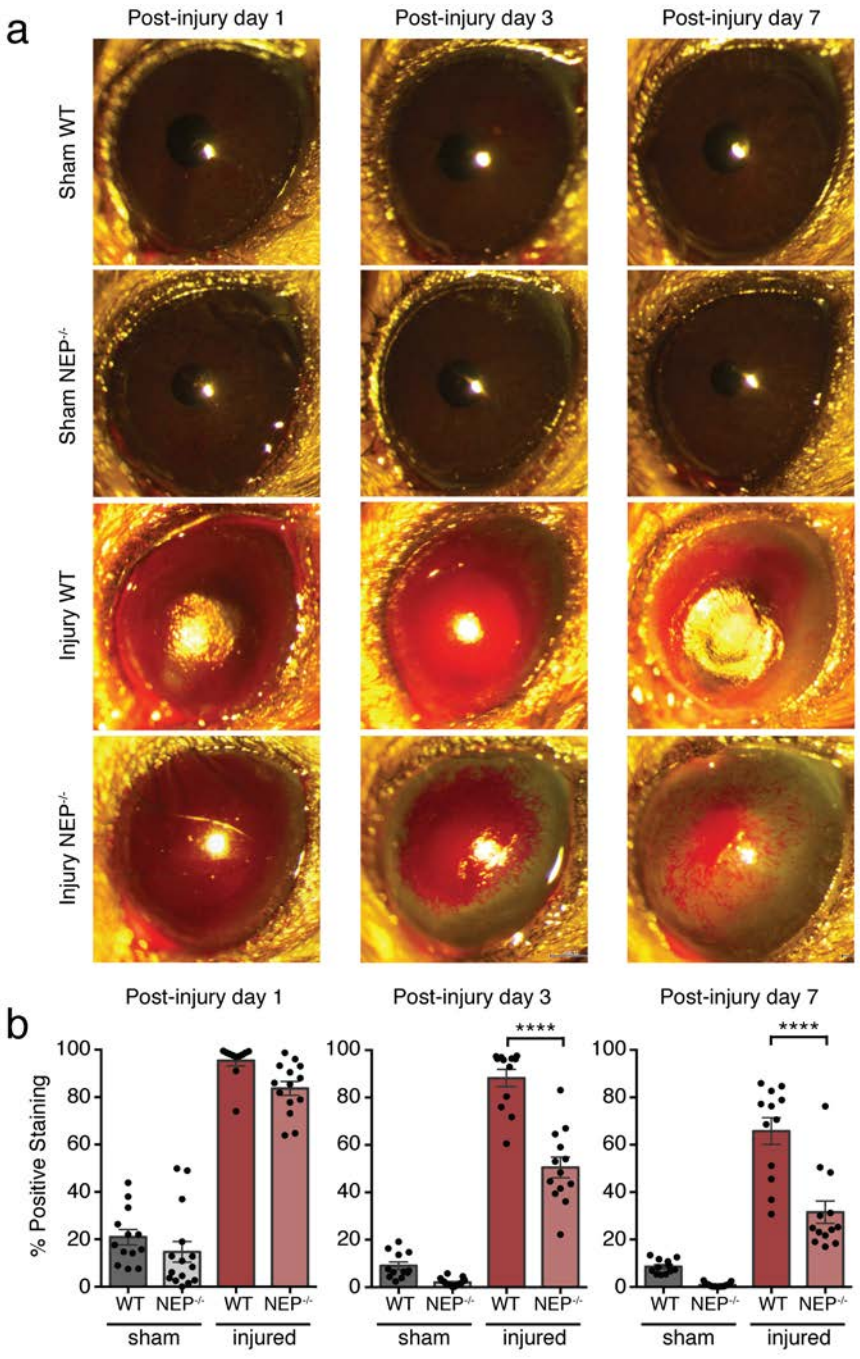

Figure 13. Corneal wound healing after alkali burn in WT and NEP$^{-/-}$ mice. (**a**) Representative broad beam slit lamp images obtained at 1, 3, and 7 days post-injury with rose bengal instillation to visualize corneal defects. (**b**) Quantification of positive rose bengal staining reported as a percentage of total corneal area at 1, 3, and 7 days post-injury (n = 12 - 18 mice/group at each timepoint; mean ± SEM; ****P < 0.0001; one-way ANOVA with Bonferroni correction).

Topical or systemic thiorphan inhibits corneal NEP

Based on the accelerated wound healing phenotype that we observed in NEP$^{-/-}$ mice, we next evaluated efficacy of the NEP inhibitor thiorphan on corneal wound healing in WT mice. First, to determine whether topical or *i.p.* thiorphan could inhibit NEP in the cornea, we assayed for NEP activity in whole cornea lysates from uninjured mice. We also isolated trigeminal ganglia from the same animals to determine whether thiorphan could inhibit NEP activity in the cell bodies of neurons innervating the cornea.

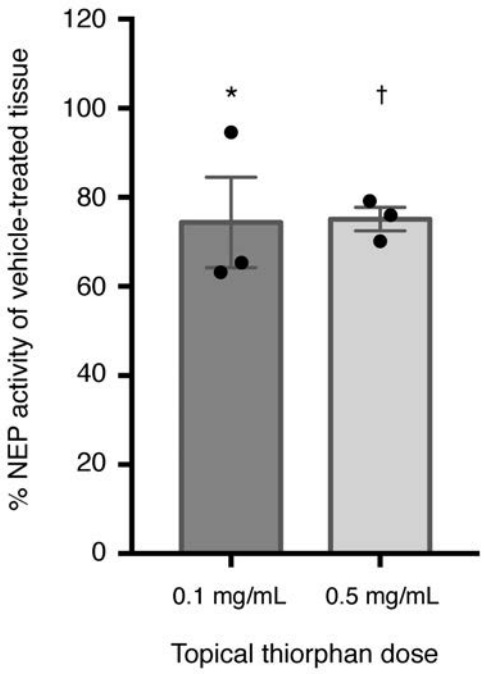

Figure 14. Effect of topical thiorphan on NEP activity in the cornea. NEP activity in corneas isolated from uninjured WT mice at 30 min after a single topical dose of 0.1 or 0.5 mg/mL thiorphan. Presented as % NEP activity of control, vehicle-treated tissue. At both doses, NEP activity was significantly lower than in vehicle-treated tissue (mean ± SEM; $^{*}P = 0.0394$; $^{+}P = 0.0445$; one-way ANOVA with Bonferroni correction).

A single 10 µL topical dose of 0.1 mg/mL thiorphan decreased NEP activity in the cornea by 26.05 ± 10.12% at 30 min after administration (n = 3 mice, *P* = 0.0394), compared to vehicle controls (Fig. 14, n = 4 mice). A single 10 µL topical dose of 0.5 mg/mL thiorphan similarly decreased NEP activity by 25.31 ± 2.64% at the same time point (Fig. 14, n = 3 mice, *P* = 0.0445). There was no significant difference in NEP inhibition between the 0.1 mg/mL and 0.5 mg/mL thiorphan groups (Fig. 14, *P* = 0.9962).

A single *i.p.* dose of 15 mg/kg thiorphan in an uninjured WT mouse decreased NEP activity in the cornea by 58.26 ± 8.96% at 1 h after administration (n = 3 mice, *P* = 0.0226) and by 34.14 ± 10.43% at 6 h after administration (n = 3 mice, *P* = 0.1407), compared to vehicle controls (Fig. 15). The same dose decreased NEP activity in the trigeminal ganglia by 28.39 ± 1.65% (n = 3 mice, *P* = 0.002) and 8.18 ± 4.24% (n = 3 mice, *P* = 0.3243) at 1 and 6 h after administration, respectively, compared to vehicle controls (Fig. 15). Based on these results, we proceeded with *i.p.* thiorphan dosing in our *in vivo* model of corneal wound healing.

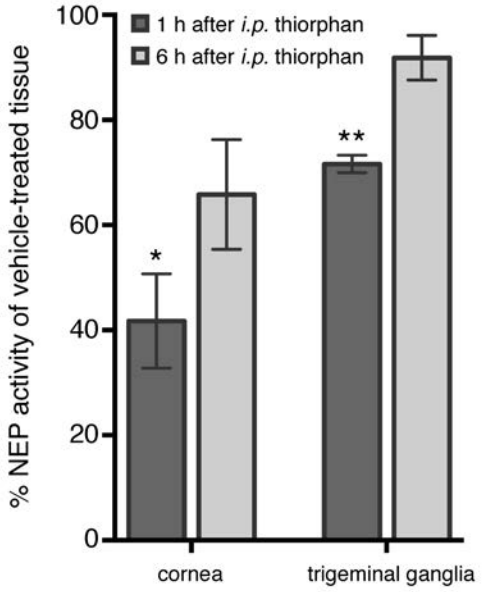

Figure 15. Effect of systemic thiorphan on NEP activity in the cornea and trigeminal ganglia. NEP activity in whole cornea and trigeminal ganglia isolated from uninjured WT mice at 1 h and 6 h after a single *i.p.* injection of 15 mg/kg thiorphan. Presented as % NEP activity of control, vehicle-treated tissue. In both tissues, NEP activity was significantly lower than in vehicle-treated tissue at 1 h, but not 6 h, after administration of *i.p.* thiorphan (mean ± SEM; **P* = 0.0226; ***P* = 0.002; one-way ANOVA with Bonferroni correction).

Thiorphan promotes corneal epithelial wound healing in vivo

In our chemical corneal injury model, we then administered *i.p.* thiorphan at 5 or 15 mg/kg daily to WT mice. Representative slit lamp images are shown in Fig. 16a. There were no significant differences in the area of positive rose bengal staining between vehicle, low dose, or high dose thiorphan-treated groups at the early time points of 1 or 3 days post-injury (Fig. 16b). At 7 days post-injury, however, the high dose thiorphan group had corneal defects 35.80 ± 4.20% smaller than those in vehicle-treated mice (Fig. 16b, $P = 0.0004$). There was no significant difference in corneal defect area between the low and high dose thiorphan groups ($P = 0.2305$), or between the low dose thiorphan and vehicle groups ($P > 0.999$). By 7 days post-injury, two mice in the vehicle-treated group (n = 8) and three in the low dose thiorphan-treated group (n = 8) required euthanization due to corneal perforation. None of the high dose thiorphan-treated mice (n = 10) developed corneal perforation (Fig. 17).

Though the cornea may initially undergo reepithelialization after corneal burn, severe injury may result in vision-compromising sequelae, including stromal opacity and abnormal vascular growth (Wagoner 1997). To determine if NEP inhibition acutely affects inflammation, corneal neovascularization, or fibrosis after alkali injury, we immunoblotted for markers of leukocytic infiltration (CD45), vascular endothelium (CD31), and myofibroblastic cells (alpha-smooth muscle actin) in corneas from alkali- and sham-injured mice treated with 15 mg/kg thiorphan or vehicle (Fig. 18). Expression of these markers at 1 week post-injury in thiorphan-treated mice (n = 7) did not significantly differ from vehicle-treated mice (n = 7; CD45, $P > 0.999$; CD31, $P = 0.080$; alpha-smooth muscle actin, $P = 0.769$). The immunoblots were repeated with similar results.

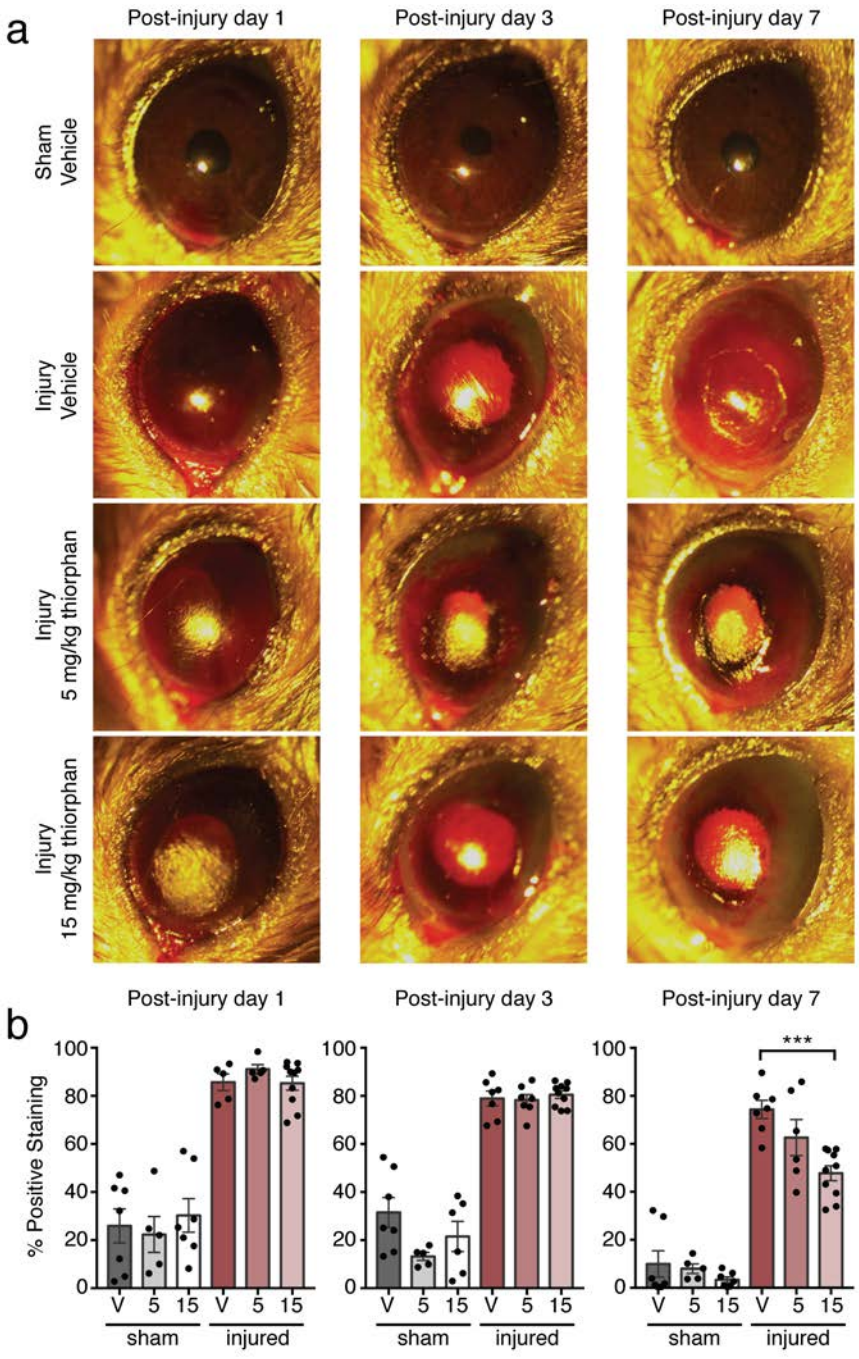

Figure 16. Corneal wound healing after alkali burn with thiorphan administration in WT mice. (**a**) Representative broad beam slit lamp images obtained at 1, 3, and 7 days post-injury with rose bengal instillation to visualize corneal defects. (**b**) Quantification of positive rose bengal staining reported as a percentage of total corneal area at 1, 3, and 7 days post-injury (n = 5 - 10 mice/group at each timepoint; mean ± SEM; ****P* = 0.0004; one-way ANOVA with Bonferroni correction). V, vehicle; 5, 5 mg/kg thiorphan; 15, 15 mg/kg thiorphan.

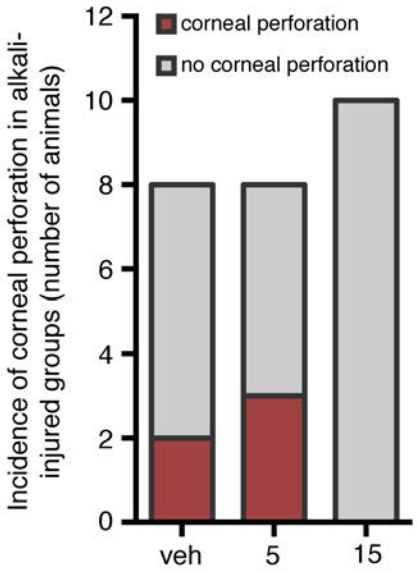

Figure 17. Corneal perforation in alkali-injured WT mice. Incidence of corneal perforation by day 7 post-injury. Veh, vehicle; 5, 5 mg/kg thiorphan; 15, 15 mg/kg thiorphan.

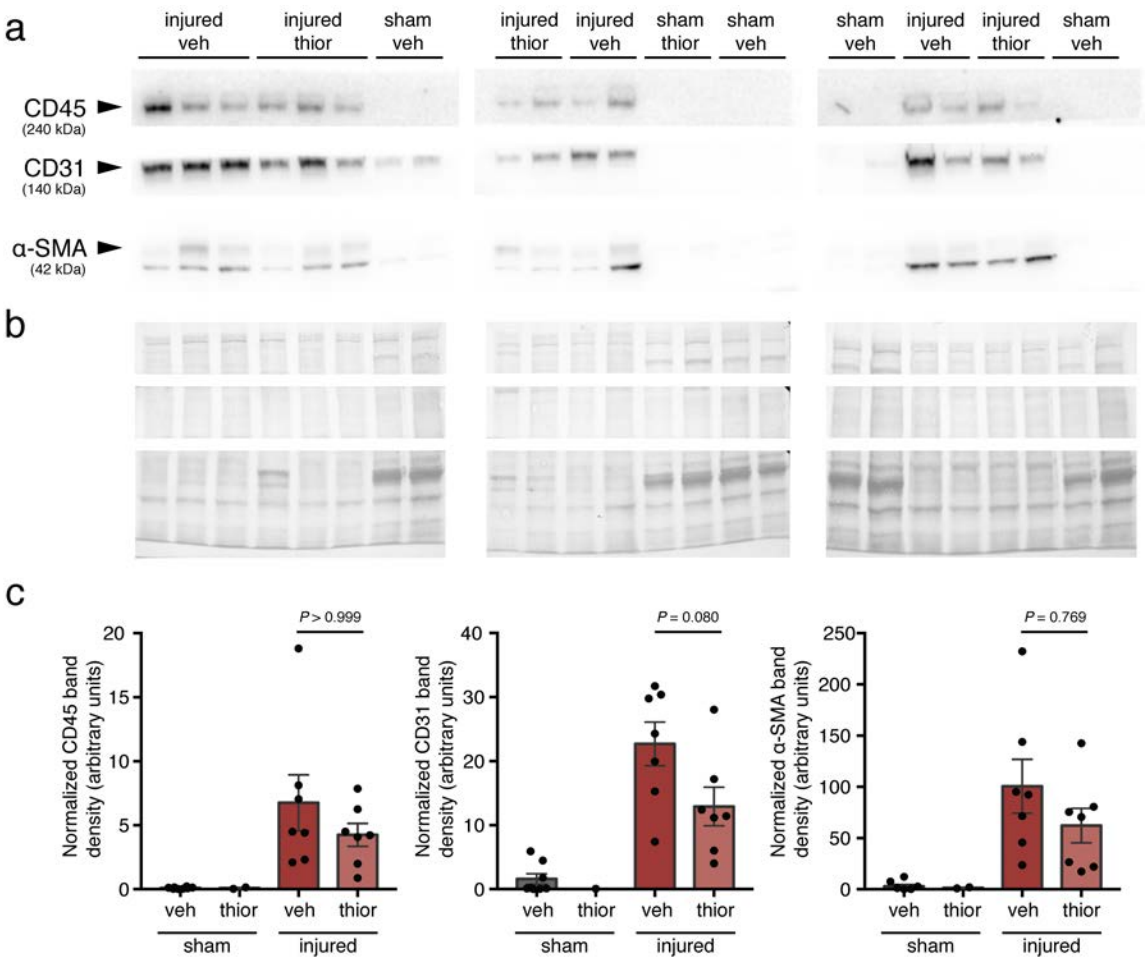

Figure 18. Thiorphan administration does not significantly affect CD45, CD31, or α-smooth muscle actin expression in alkali-injured WT corneas at one week. (**a**) Immunoblots showing expression of CD45, CD31, and α-smooth muscle actin in whole cornea lysates from WT mice at one week post-alkali or sham injury. Samples from each experimental group were randomized among three gels that were processed simultaneously. (**b**) Amido black stain for total protein on membranes corresponding to those shown in (**a**), utilized as a loading control. (**c**) Band intensities normalized to total protein and intermembrane reference protein. Each point represents expression in lysate from a single cornea (mean ± SEM; one-way ANOVA with Bonferroni correction). SMA, α-smooth muscle actin; veh, vehicle; thior, thiorphan (15 mg/kg).

Thiorphan does not affect migration of TKE2 cells after wounding in vitro

Based on the effects of thiorphan *in vivo*, we utilized an *in vitro* wound healing assay to begin dissecting the mechanism of accelerated corneal recovery with NEP inhibition. TKE2 expression of NEP was first confirmed by immunoblot (Fig. 19). Cultures were then grown to confluence, wounded, treated with thiorphan or vehicle, and imaged at intervals for 18 h (Fig 20a). In this cell migration-based assay, thiorphan did not enhance the rate of wound closure compared to vehicle controls (Fig. 20b, 20c; n = 5 wells per condition; $P = 0.6436$). Data are representative of two independent assays, but these experiments were performed four times with similar results, including with fibronectin-coated wells (data not shown).

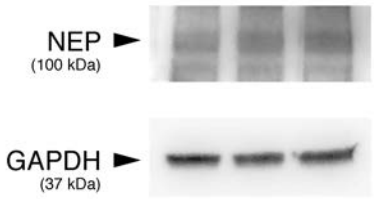

Figure 19. Expression of NEP protein in TKE2 cell line. Immunoblot of NEP (100 kDa) in lysates from confluent TKE2 cultures, with glyceraldehyde 3-phosphate dehydrogenase (GAPDH, 37 kDa) run as a loading control. Membrane was cut at 50 kDa.

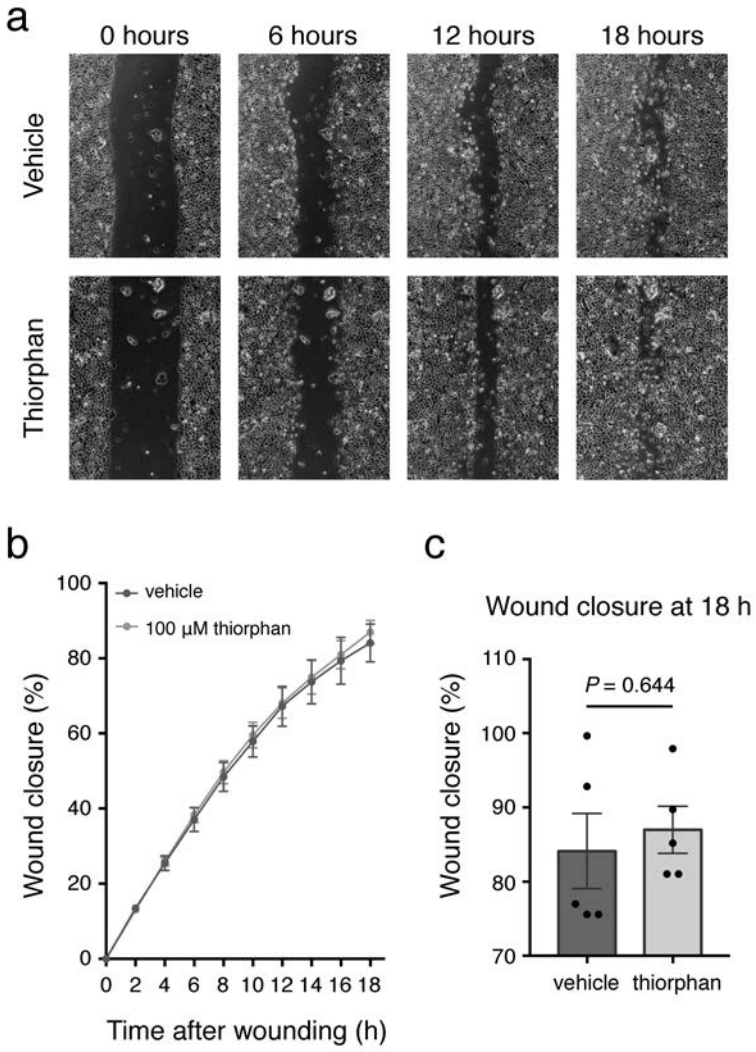

Figure 20. Thiorphan does not affect migration of TKE2 cells after wounding *in vitro*. (**a**) Representative images from *in vitro* scratch assays demonstrating that cell migration into the cell-free wound region does not vary with thiorphan treatment. (**b**) Summary graph of the course of wound healing over the duration of the assay. (**c**) Quantification of wound closure at the final timepoint (n = 5 wells per condition; two-tailed *t* test).

Discussion

Overview of findings

In this chapter, we report a critical role for NEP in corneal wound healing. Within the first week after severe chemical corneal injury, $NEP^{-/-}$ mice exhibited accelerated epithelial recovery relative to WT mice. We then evaluated therapeutic efficacy of the NEP inhibitor thiorphan in our corneal injury model. After establishing that thiorphan can be successfully delivered to the cornea and trigeminal ganglia with systemic administration, we demonstrated that pharmacologic NEP inhibition in WT mice similarly promotes corneal epithelial wound healing after chemical injury. Though the mechanism by which NEP inhibition accelerates recovery after corneal injury remains unknown, preliminary mechanistic work with the TKE2 corneal epithelial cell line suggests that thiorphan does not affect cell migration.

NEP deficiency accelerates recovery from chemical corneal injury

To investigate the effect of NEP deficiency on recovery from corneal injury, we applied a model of alkali burn, a severe form of chemical injury with an unmet need for improved pharmacologic treatments (Brodovsky et al. 2000; Rozenbaum et al. 1991). Alkaline agents are commonly found in various household cleaning products, including bleach, oven cleaners, and drain cleaners (McKenzie et al. 2010). Consequently, corneal alkali injuries occur more often and also cause more damage than their acid counterparts, with risk to young children substantially higher than previously estimated (Haring et al. 2016).

After chemical corneal injury, rapid reepithelialization is necessary to restore the protective barrier of tight junctions and limit recruitment of inflammatory cells, thereby reducing the risk of infection, scarring, persistent corneal defects, and other sight-threatening sequelae (Wagoner 1997). Indeed, the degree of corneal epithelial recovery

correlates with patient prognosis after chemical injury, with earlier resurfacing predictive of improved outcomes (Eslani et al. 2014; Wagoner 1997). Consequently, the first week after injury represents a “window of opportunity” during which medical interventions can limit potentially blinding sequelae and optimize the ocular surface for surgical reconstruction (Tuft and Shortt 2009). For this reason, we evaluated recovery in our mouse model of alkali corneal burn during the first week post-injury to coincide with the clinically-critical acute phase of corneal wound healing.

During this post-injury period, we observed that corneal epithelial wound healing in $NEP^{-/-}$ mice was significantly accelerated relative to WT mice as early as three days after wounding. One week post-injury, remaining corneal defects in $NEP^{-/-}$ mice were half the size of those in WT animals. However, the course of recovery beyond this timepoint was not within the scope of our study. In contrast to mechanical abrasions and other epithelial injuries that can resurface in a week, alkali injury is seldom restricted to the epithelium. Because their cationic form is lipophilic, alkaline chemicals rapidly penetrate the ocular surface and can result in damage all corneal layers, as well as the lens, ciliary body, and trabecular meshwork (Fish and Davidson 2010; Wagoner 1997). Recovery, if possible, occurs over weeks to months. This protracted course is also encountered in rodents. A recent study conducted in a rat model of alkali injury collected clinical, molecular, and histopathological data over 21 days, expanding on the typical week-long timeline seen in much of the literature (Choi et al. 2017). In congruence with clinical data, the authors reported development of corneal fibrosis and neovascularization at later time points, with persistent corneal opacity noted in injured animals throughout the duration of the study with little improvement. Thus, the effect of NEP on long-term outcomes of alkali injury is reserved for future investigation.

When comparing corneal epithelial recovery in WT animals to those with constitutive loss of NEP activity, a potential confounding factor is the increased density of corneal innervation observed in the $NEP^{-/-}$ mice (see Chapter 2). Because corneal nerves produce epitheliotrophic factors that promote physiological renewal as well as wound healing (Beuerman and Schimmelpfennig 1980; Lambiase et al. 1998; Mastropasqua et al. 2016), the accelerated corneal wound healing phenotype in $NEP^{-/-}$ mice may be related to increased innervation at baseline or to another unrecognized consequence of constitutive genetic disruption of NEP activity. However, thiorphan administration promotes recovery in WT mice within one week of corneal injury (see next subsection), an interval too brief for extensive reinnervation (Chan et al. 1990). This suggests that a difference in innervation, whether pre- or post-injury, is likely not the primary mechanism by which genetic or pharmacologic disruption of NEP activity supports corneal wound healing. Indeed, recapitulation of the accelerated wound healing phenotype of $NEP^{-/-}$ mice with thiorphan administration in WT mice supports that the findings in our genetic model are not due to compensatory mechanisms resulting from constitutive NEP inactivation. The pairing of a genetic study with a pharmacologic study is a major strength of this work.

NEP inhibition accelerates epithelial recovery from chemical corneal injury

Expanding upon findings in our genetic model of NEP deficiency, we demonstrated that pharmacologic NEP inhibition with thiorphan promotes corneal epithelial wound healing in WT animals. Thiorphan is a highly potent and specific NEP inhibitor, with an IC50 reported as low as 1.8 nM (Lambert et al. 1993; Roques et al. 1980). Though thiorphan also inhibits matrilysin, a small matrix metalloproteinase expressed by the basal corneal epithelium (Lu et al. 1999), the IC50 for matrilysin is reported near 10.5 µM (Oneda and

Inouye 2001), orders of magnitude lower than that for NEP. In addition, thiorphan is the active metabolite of racecadotril, an oral agent used clinically for hypersecretory diarrhea in Europe, Asia, and South America (Eberlin et al. 2012; Schwartz 2000). With a half-life of approximately 6 h with oral administration (Xu et al. 2007), racecadotril is well-tolerated and rapidly converted to thiorphan, the predominant species detected in plasma (Eberlin et al. 2012). Though racecadotril is not available for use in the United States, the NEP inhibitor sacubitril is currently approved for management of chronic heart failure (McMurray et al. 2014). This positions our basic science findings for rapid clinical translation.

In our evaluation of the *in vivo* efficacy of thiorphan, we compared the magnitude of NEP inhibition achieved in uninjured WT corneas through systemic and topical thiorphan administration. When targeting the cornea, the most common route of ocular drug delivery is topical administration due to ease of application, patient convenience, and low cost (Yavuz and Kompella 2017). However, as reflected in the modest NEP activity reduction achieved with topical thiorphan, efficient corneal drug delivery remains a challenge. Because the typical resident tear volume is approximately 7 µL in humans, the application of an ophthalmic solution to the ocular surface results in rapid clearance of excess volume through the nasolacrimal duct. Blinking, reflex tearing, and corneal permeability barriers further reduce bioavailability of most therapeutic agents, resulting in less than 5% dose delivery to the anterior segment (Yavuz and Kompella 2017). Frequent administration is a common strategy for achieving therapeutic doses with topical instillation.

Systemic administration, whether through oral or parenteral routes, faces similar permeability issues in the cornea, with the additional limitations of extensive drug dilution in the vascular system, hepatic metabolism, and renal clearance, all of which reduce

bioavailability of an agent prior to reaching the cornea. Potential off-target effects and toxicity must also be considered when systemically dosing for ocular drug delivery. A third route involves creating a depot in the subconjunctival space for sustained drug delivery. Unfortunately, periocular injection or implantation is invasive and uncomfortable for patients, and also technically challenging to administer in the context of acute ocular surface injury (Yavuz and Kompella 2017). Given these considerations and the results of our NEP enzyme activity assay, we pursued an intraperitoneal route of thiorphan administration in our *in vivo* model of corneal wound healing.

Mechanism of NEP inhibition in epithelial corneal repair

Corneal epithelial repair involves coordination of cellular, molecular, and functional changes in viable tissue at the wound margin. Local release of cytokines, growth factors, and neuropeptides facilitates reciprocal communication between the reparative epithelium and neighboring stromal keratocytes, corneal nerves, and immune cells to coordinate clearance of cellular debris from the wound bed, synthesis of adhesion proteins and extracellular matrix, and corneal epithelial cell migration and proliferation (Garcia-Hirschfeld et al. 1994; Imanishi et al. 2000; Ljubimov and Saghizadeh 2015; Reid et al. 1993).

The particular role of NEP in this intricate cascade is unknown. NEP acts on a diversity of peptides with pleiotropic actions (Kerr and Kenny 1974; Matsas et al. 1984; Turner et al. 1985), complicating identification of the specific mechanism by which this enzyme modulates corneal wound healing. Moreover, recent studies indicate that NEP, long considered an oligopeptidase (Turner et al. 2001), can inactivate substrates much larger than previously thought. The largest known substrate of NEP, fibroblast growth factor-2 (FGF-2; Goodman et al. 2006; Horiguchi et al. 2008), plus an assortment of

neuropeptides, are both involved in corneal wound healing and metabolized by NEP (Chikama et al. 1998; Imanishi et al. 2000; Sabatino et al. 2017). Inhibition of NEP could reduce the enzymatic degradation of these or other growth factors and neuropeptides, thereby prolonging their actions and accounting for the accelerated corneal wound healing observed in $NEP^{-/-}$ and thiorphan-treated WT mice.

As an initial step towards unraveling the mechanism of NEP inhibition in corneal wound healing, we employed an *in vitro* model of epithelial injury. Preliminary assays with the TKE2 mouse corneal epithelial cell line suggest that modulation of NEP activity does not alter cell migration after wounding. Alternatively, NEP inhibition may require the presence of other cell types, such as stromal keratocytes, immune cells, or sensory neurons, in order to alter epithelial behavior. An example of this interdependence is seen with substance P (SP) *in vivo*. Predominantly produced and released by sensory nerves in the cornea (Markoulli et al. 2017; Yamada et al. 2003), SP sensitizes the corneal epithelium to circulating trophic factors produced elsewhere in the body (Chikama et al. 1998; Nishida et al. 2007; Yamada et al. 2008). Loss of innervation, and thus the primary source of SP, renders the corneal epithelium unresponsive to physiologic concentrations of these agents (Nishida 2005). Conceivably, the negative *in vitro* data may therefore be an artifact of the isolated system in which thiorphan was tested. Still, this alternative interpretation presupposes that the therapeutic action of thiorphan occurs through direct interaction with corneal tissue. It may be that thiorphan acts peripherally on immune cells or the endothelium of pericorneal vasculature, thereby modulating the wound environment to indirectly support reepithelialization. Indeed, at one week post-injury, there was a trend for decreased expression of the vascular marker CD31 in corneas from thiorphan-treated mice, indicating delayed or reduced development of neovascularization after alkali burn. Given that nerves and neovessels reciprocally inhibit

each other in the cornea (Ferrari et al. 2013), thiorphan could indirectly support corneal nerve regrowth at later stages of repair through reduction of neovascularization. Further investigation is warranted to clarify the mechanism by which NEP participates in corneal wound healing.

Conclusions

Collectively, our data identify a previously unknown role of NEP in the injured cornea and provide preclinical support for a novel pharmacologic approach to management of corneal injury. Combination of NEP inhibitors with standard medical treatments for alkali burn, such as topical ascorbate, citrate, antibiotics, and steroids (Brodovsky et al. 2000), may assist in optimizing the corneal surface for reepithelialization, thereby mitigating the risk of sight-threatening complications in the later stages of wound healing. Furthermore, efficacy of thiorphan administration in this model of corneal alkali injury suggests that NEP inhibition may have therapeutic utility in other types of corneal injury, such as mechanical abrasions or damage associated with dry eye disease. These are avenues of future investigation.

CHAPTER 4: CONCLUSIONS AND FUTURE DIRECTIONS

Conclusions

With an array of etiologies and a complicated epidemiology, corneal trauma is an underreported, globally-significant cause of visual impairment. An estimated 55 million eye injuries occur each year (Négrel and Thylefors 1998), a small but clinically-significant fraction of which result from chemical exposure (Wagoner 1997). Because of the rapidity of ocular damage that occurs, corneal chemical injury confers a particularly high risk of permanent visual impairment, chronic complications, and life-long disability, even with aggressive medical and surgical rehabilitation (Burcu et al. 2014; Sharma et al. 2012). The development of improved therapeutic strategies is therefore critical.

In this work, we sought to increase our current understanding of corneal wound healing mechanisms that could be targeted to accelerate recovery and improve outcomes after injury. We focused on the enzyme NEP, demonstrating that constitutive NEP deficiency accelerates epithelial recovery in a mouse model of chemical corneal injury without affecting maintenance of corneal homeostasis. Furthermore, we evaluated the therapeutic efficacy of pharmacological NEP inhibition in chemical corneal injury. While further investigation is warranted to clarify the mechanism by which NEP modulates corneal wound healing, our *in vivo* findings provide novel preclinical support for a new pharmacologic approach to managing corneal injury, and potentially injury to other epithelial tissues, with promise for clinical translation using preexisting NEP inhibitors.

Future Directions

This thesis inspires several directions of further inquiry. Primarily, the mechanism by which NEP participates in corneal wound healing merits clarification. Here, we focus on potential effects of NEP on inflammation, both locally and systemically, and how this may promote recovery from corneal injury. We then consider additional corneal pathologies that may benefit from therapeutic NEP inhibition and potential implications for this approach in other epithelial tissues.

Inflammation

Corneal alkali burns progress through four phases: immediate, acute, early repair, and late repair (Wagoner 1997). The acute phase represents a “window of opportunity” during which medical interventions can prevent potentially blinding sequelae (Eslani et al. 2014; Tuft and Shortt 2009; Wagoner 1997). Because complications during this phase, such as neovascularization, delayed reepithelialization, ulceration, and perforation, are associated with inflammation (Bunker et al. 2014), many treatments for alkali burn attenuate the inflammatory reaction (Wagoner 1997). However, excessive dampening of inflammation can be detrimental to wound healing, as with prolonged steroid administration (Chung et al. 1998; Gritz et al. 1990; Leal et al. 2015; Saika 2007), emphasizing the importance of a balanced inflammatory response for optimal corneal wound healing.

NEP both generates and degrades vasoactive and proinflammatory peptides (Kerr and Kenny 1974; Matsas et al. 1984), and therefore has the potential to modulate the inflammatory landscape of the ocular surface and thereby influence corneal wound healing. IL-1β, one of the largest known substrates of NEP (Pierart et al. 1988), is an essential proinflammatory participant in peripheral nerve regeneration. Produced by

injury-activated macrophages, IL-1β stimulates NGF synthesis in myelin-forming Schwann cells associated with degenerating axons (Lindholm et al. 1987; Stoll and Müller 1986), but in excess can lead to neuropathic pain (Nadeau et al. 2011). This principle of balance also applies to corneal nerves: excessive or insufficient inflammation impedes regeneration (Namavari et al. 2012). The production of trophic factors, such as NGF, by Schwann cells is thought to contribute to restoration of stromal and subepithelial corneal nerves after injury, while a severely damaged corneal epithelium with deficient trophic activity may account for incomplete or delayed regrowth of epithelial nerves (Chan et al. 1990). Because axonal injury briefly induces NEP expression in myelin-forming Schwann cells (Kioussi et al. 1995), this enzyme may regulate local IL-1β availability and associated production of NGF after corneal injury. The effect of NEP inhibition on corneal nerve regeneration is therefore an important area of future investigation.

NEP inhibition also potentiates the biological effects of substance P (SP) in a variety of systems (Day et al. 2005; Lu et al. 1997; Mak et al. 2008; Medja et al. 2006; Scholzen et al. 2001). Except in the case of neurotrophic keratopathy, translational ophthalmic research has predominantly focused on the detrimental effects of SP in the cornea, including neovascularization, leukocyte infiltration, and intraocular inflammation (Bignami et al. 2014; Bignami et al. 2016). However, recent evidence suggests that SP may have novel therapeutic utility as an injury-inducible messenger for mobilization of CD29+ stromal-like cells and mesenchymal stem cells (MSCs). Hong et al. (2009) demonstrated that the peripheral blood level of SP, whether induced by alkali burn or exogenous administration, regulates recruitment of CD29+ stromal-like cells from the periphery to the injured cornea without affecting CD45+ monocyte cells. In a rabbit model of corneal burn, SP injection promoted earlier mobilization of CD29+ stromal-like

cells and accelerated restoration of corneal transparency during the acute phase of wound healing. Furthermore, SP stimulated *in vitro* proliferation and mobilization of bone marrow-derived MSCs, which can transdifferentiate into epithelial cells after tissue injury (Rojas et al. 2005; Sasaki et al. 2008; Sato et al. 2005).

In congruence with these findings, a more recent study by Lan et al. (2012) reported that mobilization of endogenous MSCs coincides with a rapid rise in peripheral SP after corneal injury, and that these cells home specifically to the injured cornea and promote corneal epithelial regeneration. Evidence from this study and others suggests that both MSCs and CD29+ stromal-like cells may reduce alkali-induced oxidative stress in the cornea, leading to the suppression of intracorneal inflammation and neovascularization during the acute phase of wound healing. These immunomodulatory effects may also attenuate loss of limbal stem cells, enabling more rapid epithelial recovery. In addition to immune effects, MSCs and CD29+ stromal-like cells may undergo mesenchymal-to-epithelial transdifferentiation and incorporate into regenerating corneal tissue to promote wound healing as well (Cejkova et al. 2013; Hong et al. 2009; Lan et al. 2012; Yao et al. 2012). Thus, modulation of systemic SP as a means of mobilizing these cell populations after corneal injury offers significant therapeutic potential. Unwanted neuroinflammatory effects must be considered, however. In contrast to exogenous SP administration, systemic NEP inhibition may produce a more modest elevation of endogenous SP. Whether NEP inhibition can alter peripheral SP levels after corneal injury remains a major question and future direction of this study.

Application of NEP inhibition in other injury models

Traumatic corneal abrasions are the leading cause of eye-related emergency department visits and can lead to permanent scarring and increase the risk of recurrent

epithelial erosions, even after surgical management (Channa et al. 2016; Reidy et al. 2000). Epithelial erosions can also manifest after refractive surgeries, including laser-assisted *in situ* keratomileusis (LASIK) and photorefractive keratectomy (PRK), two increasingly common procedures (Diez-Feijóo et al. 2014; Fattah et al. 2018). Whether traumatic or iatrogenic in origin, corneal epithelial erosions result from poor adhesion to the underlying matrix and would greatly benefit from an agent that could promote epithelial regeneration and fibronectin-integrin interactions (Nishida et al. 2015).

Persistent epithelial defects (PEDs), a severe corneal epithelial disturbance with various etiologies, would similarly benefit from an agent that could promote wound healing. PEDs most commonly develop in patients with dry eye disease (DED) but may also occur in those with trigeminal nerve damage, which can result from a myriad of local and systemic conditions, including infection, surgery, epilepsy, neoplasia, physical injury, chronic topical medication use, diabetes, and multiple sclerosis (Sacchetti and Lambiase 2014). In the case of both DED and trigeminal nerve pathology, the corneal epithelium fails to maintain homeostasis due to decreased growth factors, cytokines, and/or neuropeptides normally supplied by the tear film and corneal nerves (Meng and Kurose 2013). Furthermore, DED may itself modify the properties of corneal nerves, hindering their ability to regulate tear secretion and release epitheliotrophic factors directly (Meng and Kurose 2013).

Alteration of neuropeptide signaling is a promising strategy for management of these corneal epithelial pathologies. Accumulating evidence suggests that SP sensitizes the cornea to fibronectin, interleukin-6, and IGF-1 to stimulate corneal epithelial cell migration and attachment to various extracellular matrix proteins via induction of cadherin expression and activation of the integrin, FAK, and paxillin system (Araki-Sasaki et al. 2000; Nakamura et al. 1998; Nishida et al. 1996; Yamada et al. 2005).

However, SP is also associated with inflammation, vasodilation, plasma extravasation, and miosis (Bury and Mashford 1976; Soloway et al. 1981). To circumvent these unwanted effects of topical SP application, Yamada et al. isolated the minimum amino acid sequence required to stimulate corneal wound closure. This SP-derived peptide, FGLM-amide, combined with IGF-1 or its derivative peptide SSSR, has been used to successfully treat PEDs resulting from neurotrophic keratopathy (Chikama et al. 1998; Nishida et al. 2007; Yamada et al. 2008). Though we were unable to determine if NEP inhibition results in altered SP levels after corneal injury, investigation of alternative strategies for determination of SP and its fragments is a priority of future studies. However, we predict that NEP inhibition could facilitate moderate elevations in endogenous SP and/or other corneal neuropeptides to elicit beneficial wound healing actions in models of corneal epithelial pathology.

NEP inhibition may also benefit epithelial tissues outside the cornea, particularly skin, due to similarities in the cellular and molecular networks that coordinate wound healing in each (Bukowiecki et al. 2017). As in the cornea, a balanced inflammatory reaction is fundamental to skin wound healing. Prolonged inflammation may exacerbate tissue damage and lead to excessive fibrotic responses (Bignami et al. 2016; Okada et al. 2016; Scott et al. 2005) while impaired endogenous inflammation or therapeutic suppression of inflammation with steroids may delay epithelial wound closure or predispose to infection (Chung et al. 1998; Gritz et al. 1990; Leal et al. 2015; Saika 2007). Furthermore, both the skin and the cornea are densely innervated and express a similar medley of neuropeptides, neuropeptide receptors, and neuropeptide-degrading enzymes, including NEP (Olerud et al. 1999; Scholzen et al. 1998). Indeed, NEP activity is increased in diabetic skin ulcers in human patients, which likely contributes to diminished neuroinflammatory signaling and impaired wound healing (Antezana et al.

2002). This pattern of elevated NEP activity and delayed wound healing is recapitulated in the mutant db/db diabetic mouse, in which topical thiorphan improves wound closure kinetics after acute full-thickness cutaneous injury (Spenny et al. 2002). Modulation of NEP activity in other models of chronic, non-healing wounds, such as those that occur after cutaneous burns or prolonged immobility in the elderly (Mustoe 2004), may likewise prove beneficial.

Final Thoughts

NEP inhibitors as potential ophthalmic agents

In the translation of our findings, concerns regarding administration of NEP-inhibiting agents in humans may arise, given the accumulating evidence that NEP catalyzes the rate-limiting step of β-amyloid degradation (Iwata et al. 2000). Suppression of its activity may therefore contribute to the pathogenesis of Alzheimer's disease and age-related macular degeneration, a major cause of retinal blindness in the elderly (Luibl et al. 2006; Yasojima et al. 2001). Though additional work is needed to determine the optimal duration of NEP inhibition in corneal injury, we do not expect that prolonged administration of NEP inhibitors would be necessary in human patients, given the rapid therapeutic response in our mouse model. A short course of NEP inhibition would largely circumvent concerns about amyloid accumulation. Still, much of the evidence for these potential adverse consequences is based on animal studies, and the relevance of this evidence to humans is unknown (Becker et al. 2018; Campbell 2017). To address these uncertainties, the FDA approved a combined NEP inhibitor/angiotensin receptor blocker LCZ696 (valsartan/sacubitril) with the stipulation that Novartis conduct a study to examine its long-term effects on cognitive function (Unger 2015). The study is currently underway.

ABBREVIATIONS

aa	amino acid
ACE	angiotensin-converting enzyme
ANOVA	analysis of variance
ANP	atrial natriuretic peptide
BCA	bicinchoninic acid
CALLA	common acute lymphoblastic leukemia antigen
CCT	central corneal thickness
CEC	corneal epithelial cell
CESC	corneal epithelial stem cell
CGRP	calcitonin gene-related peptide
CNS	central nervous system
CSF	cerebrospinal fluid
DAPI	4′,6-diamidino-2-phenylindole
DED	dry eye disease
ECM	extracellular matrix
EGF	epidermal growth factor
ELISA	enzyme-linked immunosorbent assay
FGF-2	fibroblast growth factor-2
GAPDH	glyceraldehyde 3-phosphate dehydrogenase
HGF	hepatocyte growth factor
HRP	horseradish peroxidase
IEN	intraepithelial nerve
IGF-1	insulin-like growth factor-1
IL-1	interleukin-1
IM	intermembrane

i.p.	intraperitoneal
KGF	keratinocyte growth factor
LASIK	laser-assisted *in situ* keratomileusis
LESC	limbal epithelial stem cell
LSCD	limbal stem cell deficiency
MSC	mesenchymal stem cell
NEP	neprilysin
NGF	nerve growth factor
NKA	neurokinin A
NK1R	neurokinin-1 receptor
NPY	neuropeptide Y
PACAP	pituitary adenylate cyclase-activating peptide
PED	persistent epithelial defect
PRK	photorefractive keratectomy
RIPA	radioimmunoprecipitation assay
RT	room temperature
SD-OCT	spectral domain optical coherence tomography
SEM	standard error of the mean
SP	substance P
sVEGFR1	soluble vascular endothelial growth factor receptor-1
TAC	transit amplifying cell
TGF-β	transforming growth factor-beta
TNF-α	tumor necrosis factor-alpha
VEGF	vascular endothelial growth factor
VEGFR3	vascular endothelial growth factor receptor-3
VIP	vasoactive intestinal peptide
WT	wild type

REFERENCES

1. Aldridge GM, Podrebarac DM, Greenough WT, Weiler IJ. The use of total protein stains as loading controls: An alternative to high-abundance single-protein controls in semi-quantitative immunoblotting. J Neurosci Methods. 2008;172(2):250-4.
2. Alper MG. The anesthetic eye: An investigation of changes in the anterior ocular segment of the monkey caused by interrupting the trigeminal nerve at various levels along its course. Trans Am Ophthalmol Soc. 1975;73:323-65.
3. Ambati BK, Nozaki M, Singh N, et al. Corneal avascularity is due to soluble VEGF receptor-1. Nature. 2006;443(7114):993-7.
4. Ambati BK, Patterson E, Jani P, et al. Soluble vascular endothelial growth factor receptor-1 contributes to the corneal antiangiogenic barrier. Br J Ophthalmol. 2007;91(4):505-8.
5. Amitai-Lange A, Altshuler A, Bubley J, Dbayat N, Tiosano B, Shalom-Feuerstein R. Lineage tracing of stem and progenitor cells of the murine corneal epithelium. Stem Cells. 2015;33(1):230-9.
6. Anderson RA. Actin filaments in normal and migrating corneal epithelial cells. Invest Ophthalmol Vis Sci. 1977;16(2):161-6.
7. Antezana M, Sullivan SR, Usui M, et al. Neutral endopeptidase activity is increased in the skin of subjects with diabetic ulcers. J Invest Dermatol. 2002;119(6):1400-4.
8. Appelboom T, De Maertelaer V, De Prez E, Hauzeur JP, Deschodt-Lanckman M. Enkephalinase: A physiologic neuroimmunomodulator detected in the synovial fluid. Arthritis Rheum. 1991;34(8):1048-51.
9. Araki-Sasaki K, Aizawa S, Hiramoto M, et al. Substance P-induced cadherin expression and its signal transduction in a cloned human corneal epithelial cell line. J Cell Physiol. 2000;182(2):189-95.
10. Argüeso P, Gipson IK. Epithelial mucins of the ocular surface: structure, biosynthesis and function. Exp Eye Res. 2001;73(3):281-9.
11. Atallah MR, Palioura S, Perez VL, Amescua G. Limbal stem cell transplantation: current perspectives. Clin Ophthalmol. 2016;10:593-602.
12. Bahadir B, Behzatoglu K, Bektas S, Bozkurt ER, Ozdamar SO. CD10 expression in urothelial carcinoma of the bladder. Diagn Pathol. 2009;4:38.
13. Bakhtiari P, Djalilian A. Update on limbal stem cell transplantation. Middle East Afr J Ophthalmol. 2010;17(1):9-14.
14. Ban Y, Dota A, Cooper LJ, et al. Tight junction-related protein expression and distribution in human corneal epithelium. Exp Eye Res. 2003;76(6):663-9.

15. Baradaran-Rafii A, Eslani M, Haq Z, Shirzadeh E, Huvard MJ, Djalilian AR. Current and upcoming therapies for ocular surface chemical injuries. Ocul Surf. 2017;15(1):48-64.

16. Barbosa FL, Chaurasia SS, Cutler A, et al. Corneal myofibroblast generation from bone marrow-derived cells. Exp Eye Res. 2010;91(1):92-6.

17. Becker M, Moore A, Naughton M, Boland B, Siems WE, Walther T. Neprilysin degrades murine Aβ more efficiently than human Aβ: Further implication for species-specific amyloid accumulation. Neurosci Lett. 2018; S0304-3940(18):30574-3.

18. Beebe DC. Maintaining transparency: a review of the developmental physiology and pathophysiology of two avascular tissues. Semin Cell Dev Biol. 2008;19(2):125-33.

19. Belmonte C, Acosta MC, Gallar J. Neural basis of sensation in intact and injured corneas. Exp Eye Res. 2004;78(3):513-25.

20. Belmonte C, Acosta MC, Merayo-Lloves J, Gallar J. What Causes Eye Pain? Curr Ophthalmol Rep. 2015;3(2):111-121.

21. Belmonte C, Aracil A, Acosta MC, Luna C, Gallar J. Nerves and sensations from the eye surface. Ocul Surf. 2004;2(4):248-53.

22. Bettman JW. Nature of Bowman's layer. N Engl J Med. 1970;282(6):344.

23. Beuerman RW, Rózsa AJ. Collateral sprouts are replaced by regenerating neurites in the wounded corneal epithelium. Neurosci Lett. 1984;44(1):99-104.

24. Beuerman RW, Schimmelpfennig B. Sensory denervation of the rabbit cornea affects epithelial properties. Exp Neurol. 1980;69(1):196-201.

25. Bignami F, Rama P, Ferrari G. Substance P and its inhibition in ocular inflammation. Curr Drug Targets. 2016;17(11):1265-74.

26. Blanco-Mezquita JT, Hutcheon AE, Stepp MA, Zieske JD. αVβ6 integrin promotes corneal wound healing. Invest Ophthalmol Vis Sci. 2011;52(11):8505-13.

27. Bonini S, Rama P, Olzi D, Lambiase A. Neurotrophic keratitis. Eye (Lond). 2003;17(8):989-95.

28. Borson DB. Roles of neutral endopeptidase in airways. Am J Physiol. 1991;260(4 Pt 1):L212-25.

29. Bosler JS, Davies KP, Neal-Perry GS. Peptides in seminal fluid and their role in infertility: a potential role for opiorphin inhibition of neutral endopeptidase activity as a clinically relevant modulator of sperm motility: a review. Reprod Sci. 2014;21(11):1334-40.

30. Bourne WM, Nelson LR, Hodge DO. Central corneal endothelial cell changes over a ten-year period. Invest Ophthalmol Vis Sci. 1997;38(3):779-82.

31. Brodovsky SC, McCarty CA, Snibson G, et al. Management of alkali burns: An 11-year retrospective review. Ophthalmology. 2000;107(10):1829-35.

32. Brown G, Capellaro D, Greaves M. Leukemia-associated antigens in man. J Natl Cancer Inst. 1975;55(6):1281-9.

33. Buck RC. Cell migration in repair of mouse corneal epithelium. Invest Ophthalmol Vis Sci. 1979;18(8):767-84.

34. Bukowiecki A, Hos D, Cursiefen C, Eming SA. Wound healing studies in cornea and skin: Parallels, differences and opportunities. Int J Mol Sci. 2017;18(6)

35. Bunker DJ, George RJ, Kleinschmidt A, Kumar RJ, Maitz P. Alkali-related ocular burns: A case series and review. J Burn Care Res. 2014;35(3):261-8.

36. Bunnett NW, Wu V, Sternini C, et al. Distribution and abundance of neutral endopeptidase (EC 3.4.24.11) in the alimentary tract of the rat. Am J Physiol. 1993;264(3 Pt 1):G497-508.

37. Burcu A, Yalniz-Akkaya Z, Ozdemir MF, Erdem E, Onat MM, Ornek F. Surgical rehabilitation following ocular chemical injury. Cutan Ocul Toxicol. 2014;33(1):42-8.

38. Bury RW, Mashford ML. Biological activity of C-terminal partial sequences of substance P. J Med Chem. 1976;19(6):854-6.

39. Byrd JB, Touzin K, Sile S, et al. Dipeptidyl peptidase IV in angiotensin-converting enzyme inhibitor associated angioedema. Hypertension. 2008;51(1):141-7.

40. Campbell DJ, Anastasopoulos F, Duncan AM, James GM, Kladis A, Briscoe TA. Effects of neutral endopeptidase inhibition and combined angiotensin converting enzyme and neutral endopeptidase inhibition on angiotensin and bradykinin peptides in rats. J Pharmacol Exp Ther. 1998;287(2):567-77.

41. Campbell DJ. Long-term neprilysin inhibition: Implications for ARNIs. Nat Rev Cardiol. 2017;14(3):171-186.

42. Campbell DJ. The kallikrein-kinin system in humans. Clin Exp Pharmacol Physiol. 2001;28(12):1060-5.

43. Cejkova J, Trosan P, Cejka C, et al. Suppression of alkali-induced oxidative injury in the cornea by mesenchymal stem cells growing on nanofiber scaffolds and transferred onto the damaged corneal surface. Exp Eye Res. 2013;116:312-23.

44. Chan KY, Haschke RH. Action of a trophic factor(s) from rabbit corneal epithelial culture on dissociated trigeminal neurons. J Neurosci. 1981;1(10):1155-62.

45. Chan KY, Järveläinen M, Chang JH, Edenfield MJ. A cryodamage model for studying corneal nerve regeneration. Invest Ophthalmol Vis Sci. 1990;31(10):2008-21.

46. Chan-Ling T, Tervo K, Tervo T, Vannas A, Holden BA, Eranko L. Long-term neural regeneration in the rabbit following 180 degrees limbal incision. Invest Ophthalmol Vis Sci. 1987;28(12):2083-8.

47. Chang CY, Green CR, McGhee CN, Sherwin T. Acute wound healing in the human central corneal epithelium appears to be independent of limbal stem cell influence. Invest Ophthalmol Vis Sci. 2008;49(12):5279-86.

48. Channa R, Zafar SN, Canner JK, Haring RS, Schneider EB, Friedman DS. Epidemiology of eye-related emergency department visits. JAMA Ophthalmol. 2016;134(3):312-9.

49. Chen JJ, Tseng SC. Abnormal corneal epithelial wound healing in partial-thickness removal of limbal epithelium. Invest Ophthalmol Vis Sci. 1991;32(8):2219-33.

50. Chen JJ, Tseng SC. Corneal epithelial wound healing in partial limbal deficiency. Invest Ophthalmol Vis Sci. 1990;31(7):1301-14.

51. Chikama T, Fukuda K, Morishige N, Nishida T. Treatment of neurotrophic keratopathy with substance P-derived peptide (FGLM) and insulin-like growth factor I. Lancet. 1998;351(9118):1783-4.

52. Choi H, Phillips C, Oh JY, et al. Comprehensive modeling of corneal alkali injury in the rat eye. Curr Eye Res. 2017;42(10):1348-1357.

53. Chung EH, Hutcheon AE, Joyce NC, Zieske JD. Synchronization of the G1/S transition in response to corneal debridement. Invest Ophthalmol Vis Sci. 1999;40(9):1952-8.

54. Chung JH, Kang YG, Kim HJ. Effect of 0.1% dexamethasone on epithelial healing in experimental corneal alkali wounds: morphological changes during the repair process. Graefes Arch Clin Exp Ophthalmol. 1998;236(7):537-45.

55. Claerhout I, Beele H, Kestelyn P. Graft failure: I. Endothelial cell loss. Int Ophthalmol. 2008;28(3):165-73.

56. Connelly JC, Skidgel RA, Schulz WW, Johnson AR, Erdös EG. Neutral endopeptidase 24.11 in human neutrophils: cleavage of chemotactic peptide. Proc Natl Acad Sci USA. 1985;82(24):8737-41.

57. Cotsarelis G, Cheng SZ, Dong G, Sun TT, Lavker RM. Existence of slow-cycling limbal epithelial basal cells that can be preferentially stimulated to proliferate: implications on epithelial stem cells. Cell. 1989;57(2):201-9.

58. Crosson CE, Klyce SD, Beuerman RW. Epithelial wound closure in the rabbit cornea. A biphasic process. Invest Ophthalmol Vis Sci. 1986;27(4):464-73.

59. Cursiefen C, Chen L, Saint-Geniez M, et al. Nonvascular VEGF receptor 3 expression by corneal epithelium maintains avascularity and vision. Proc Natl Acad Sci USA. 2006;103(30):11405-10.

60. Cursiefen C, Masli S, Ng TF, et al. Roles of thrombospondin-1 and -2 in regulating corneal and iris angiogenesis. Invest Ophthalmol Vis Sci. 2004;45(4):1117-24.

61. D'Adamio L, Shipp MA, Masteller EL, Reinherz EL. Organization of the gene encoding common acute lymphoblastic leukemia antigen (neutral endopeptidase 24.11): Multiple miniexons and separate 5' untranslated regions. Proc Natl Acad Sci USA. 1989;86(18):7103-7.

62. Davanger M, Evensen A. Role of the pericorneal papillary structure in renewal of corneal epithelium. Nature. 1971;229(5286):560-1.

63. Davidson EP, Coppey LJ, Yorek MA. Early loss of innervation of cornea epithelium in streptozotocin-induced type 1 diabetic rats: improvement with ilepatril treatment. Invest Ophthalmol Vis Sci. 2012a;53(13):8067-74.

64. Davidson EP, Coppey LJ, Holmes A, Yorek MA. Effect of inhibition of angiotensin converting enzyme and/or neutral endopeptidase on vascular and neural complications in high fat fed/low dose streptozotocin-diabetic rats. Eur J Pharmacol. 2012b;677(1-3):180-7.

65. Day AL, Wick E, Jordan TH, et al. Neutral endopeptidase determines the severity of pancreatitis-associated lung injury. J Surg Res. 2005;128(1):21-7.

66. Daya SM, Watson A, Sharpe JR, et al. Outcomes and DNA analysis of ex vivo expanded stem cell allograft for ocular surface reconstruction. Ophthalmology. 2005;112(3):470-7.

67. De Leeuw AM, Chan KY. Corneal nerve regeneration. Correlation between morphology and restoration of sensitivity. Invest Ophthalmol Vis Sci. 1989;30(9):1980-90.

68. Devault A, Lazure C, Nault C, et al. Amino acid sequence of rabbit kidney neutral endopeptidase 24.11 (enkephalinase) deduced from a complementary DNA. EMBO J. 1987;6(5):1317-22.

69. Diez-Feijóo E, Grau AE, Abusleme EI, Durán JA. Clinical presentation and causes of recurrent corneal erosion syndrome: Review of 100 patients. Cornea. 2014;33(6):571-5.

70. Dorà NJ, Hill RE, Collinson JM, West JD. Lineage tracing in the adult mouse corneal epithelium supports the limbal epithelial stem cell hypothesis with intermittent periods of stem cell quiescence. Stem Cell Res. 2015;15(3):665-677.

71. Dua HS, Miri A, Alomar T, Yeung AM, Said DG. The role of limbal stem cells in corneal epithelial maintenance: Testing the dogma. Ophthalmology. 2009;116(5):856-63.

72. Dua HS, Miri A, Elalfy MS, Lencova A, Said DG. Amnion-assisted conjunctival epithelial redirection in limbal stem cell grafting. Br J Ophthalmol. 2017;101(7):913-919.

73. Dua HS, Shanmuganathan VA, Powell-Richards AO, Tighe PJ, Joseph A. Limbal epithelial crypts: A novel anatomical structure and a putative limbal stem cell niche. Br J Ophthalmol. 2005;89(5):529-32.

74. Dua HS. The conjunctiva in corneal epithelial wound healing. Br J Ophthalmol. 1998;82(12):1407-11.

75. Eberlin M, Mück T, Michel MC. A comprehensive review of the pharmacodynamics, pharmacokinetics, and clinical effects of the neutral endopeptidase inhibitor racecadotril. Front Pharmacol. 2012;3:93.

76. El-Brolosy MA, Stainier DYR. Genetic compensation: A phenomenon in search of mechanisms. PLoS Genet. 2017;13(7):e1006780.

77. Emoto I, Beuerman RW. Stimulation of neurite growth by epithelial implants into corneal stroma. Neurosci Lett. 1987;82(2):140-4.

78. Erdös EG, Schulz WW, Gafford JT, Defendini R. Neutral metalloendopeptidase in human male genital trac:. Comparison to angiotensin I-converting enzyme. Lab Invest. 1985;52(4):437-47.

79. Erdös EG, Skidgel RA. Neutral endopeptidase 24.11 (enkephalinase) and related regulators of peptide hormones. FASEB J. 1989;3(2):145-51.

80. Eslani M, Baradaran-Rafii A, Movahedan A, Djalilian AR. The ocular surface chemical burns. J Ophthalmol. 2014;2014:196827.

81. Estil S, Kravik K, Haaskjold E, Refsum SB, Bjerknes R, Wilson G. Pilot study on the time course of apoptosis in the regenerating corneal epithelium. Acta Ophthalmol Scand. 2002;80(5):517-23.

82. Farrell RA, McCally RL, Tatham PE. Wave-length dependencies of light scattering in normal and cold swollen rabbit corneas and their structural implications. J Physiol (Lond). 1973;233(3):589-612.

83. Fattah MA, Antonios R, Arba Mosquera S, Abiad B, Awwad ST. Epithelial erosions and refractive results after single-step transepithelial photorefractive keratectomy and alcohol-assisted photorefractive keratectomy in myopic eyes: A comparative evaluation over 12 months. Cornea. 2018;37(1):45-52.

84. Favrat B, Burnier M, Nussberger J, et al. Neutral endopeptidase versus angiotensin converting enzyme inhibition in essential hypertension. J Hypertens. 1995;13(7):797-804.

85. Ferrari G, Chauhan SK, Ueno H, et al. A novel mouse model for neurotrophic keratopathy: Trigeminal nerve stereotactic electrolysis through the brain. Invest Ophthalmol Vis Sci. 2011;52(5):2532-9.

86. Ferrari G, Hajrasouliha AR, Sadrai Z, Ueno H, Chauhan SK, Dana R. Nerves and neovessels inhibit each other in the cornea. Invest Ophthalmol Vis Sci. 2013;54(1):813-20.

87. Fini ME. Keratocyte and fibroblast phenotypes in the repairing cornea. Prog Retin Eye Res. 1999;18(4):529-51.

88. Fish R, Davidson RS. Management of ocular thermal and chemical injuries, including amniotic membrane therapy. Curr Opin Ophthalmol. 2010;21(4):317-21.

89. Foerster CG, Cursiefen C, Kruse FE. Persisting corneal erosion under cetuximab (Erbitux) treatment (epidermal growth factor receptor antibody). Cornea. 2008;27(5):612-4.

90. Foster CS, Azar DT, Dohlman CH. Smolin and Thoft's The Cornea: Scientific foundations and clinical practice. Philadelphia: Wolters Kluwer; 2015.

91. Friedenwald JS, Buschke W. Some factors concerned in the mitotic and wound healing activities of the corneal epithelium. Trans Am Ophthalmol Soc. 1944;42:371-83.

92. Friend J, Thoft RA. Functional competence of regenerating ocular surface epithelium. Invest Ophthalmol Vis Sci. 1978;17(2):134-9.

93. Fujikawa LS, Foster CS, Harrist TJ, Lanigan JM, Colvin RB. Fibronectin in healing rabbit corneal wounds. Lab Invest. 1981;45(2):120-9.

94. Fukami S, Watanabe K, Iwata N, et al. Abeta-degrading endopeptidase, neprilysin, in mouse brain: synaptic and axonal localization inversely correlating with Abeta pathology. Neurosci Res. 2002;43(1):39-56.

95. Fulcher IS, Matsas R, Turner AJ, Kenny AJ. Kidney neutral endopeptidase and the hydrolysis of enkephalin by synaptic membranes show similar sensitivity to inhibitors. Biochem J. 1982;203(2):519-22.

96. Gaddipati S, Rao P, Jerome AD, Burugula BB, Gerard NP, Suvas S. Loss of neurokinin-1 receptor alters ocular surface homeostasis and promotes an early development of herpes stromal keratitis. J Immunol. 2016;197(10):4021-4033.

97. Gallar J, Acosta MC, Moilanen JA, Holopainen JM, Belmonte C, Tervo TM. Recovery of corneal sensitivity to mechanical and chemical stimulation after laser in situ keratomileusis. J Refract Surg. 2004;20(3):229-35.

98. Garcia-Hirschfeld J, Lopez-Briones LG, Belmonte C. Neurotrophic influences on corneal epithelial cells. Exp Eye Res. 1994;59(5):597-605.

99. George SG, Kenny J. Studies on the enzymology of purified preparations of brush border from rabbit kidney. Biochem J. 1973;134(1):43-57.

100. Gipson IK, Spurr-Michaud S, Tisdale A, Elwell J, Stepp MA. Redistribution of the hemidesmosome components alpha 6 beta 4 integrin and bullous pemphigoid antigens during epithelial wound healing. Exp Cell Res. 1993;207(1):86-98.

101. Gipson IK, Spurr-Michaud S, Tisdale A, Keough M. Reassembly of the anchoring structures of the corneal epithelium during wound repair in the rabbit. Invest Ophthalmol Vis Sci. 1989;30(3):425-34.

102. Gipson IK, Spurr-Michaud SJ, Tisdale AS. Anchoring fibrils form a complex network in human and rabbit cornea. Invest Ophthalmol Vis Sci. 1987;28(2):212-20.

103. Gipson IK. Adhesive mechanisms of the corneal epithelium. Acta Ophthalmol Suppl. 1992;(202):13-7.

104. Goetzl EJ, Sreedharan SP, Turck CW, Bridenbaugh R, Malfroy B. Preferential cleavage of amino- and carboxyl-terminal oligopeptides from vasoactive intestinal polypeptide by human recombinant enkephalinase (neutral endopeptidase, EC 3.4.24.11). Biochem Biophys Res Commun. 1989;158(3):850-4.

105. Goldman A, Harper S, Speicher DW. Detection of Proteins on Blot Membranes. Curr Protoc Protein Sci. 2016;86:10.8.1-10.8.11.

106. Goodman OB, Febbraio M, Simantov R, et al. Neprilysin inhibits angiogenesis via proteolysis of fibroblast growth factor-2. J Biol Chem. 2006;281(44):33597-605.

107. Goyal S, Hamrah P. Understanding neuropathic corneal pain: Gaps and current therapeutic approaches. Semin Ophthalmol. 2016;31(1-2):59-70.

108. Greaves MF, Hariri G, Newman RA, Sutherland DR, Ritter MA, Ritz J. Selective expression of the common acute lymphoblastic leukemia (gp 100) antigen on immature lymphoid cells and their malignant counterparts. Blood. 1983;61(4):628-39.

109. Gritz DC, Lee TY, Kwitko S, McDonnell PJ. Topical anti-inflammatory agents in an animal model of microbial keratitis. Arch Ophthalmol. 1990;108(7):1001-5.

110. Hamrah P, Liu Y, Zhang Q, Dana MR. The corneal stroma is endowed with a significant number of resident dendritic cells. Invest Ophthalmol Vis Sci. 2003;44(2):581-9.

111. Hanna C, Bicknell DS, O'Brien JE. Cell turnover in the adult human eye. Arch Ophthalmol. 1961;65:695-8.

112. Hanna C, O'Brien JE. Cell production and migration in the epithelial layer of the cornea. Arch Ophthalmol. 1960;64:536-9.

113. Hanna C. Proliferation and migration of epithelial cells during corneal wound repair in the rabbit and the rat. Am J Ophthalmol. 1966;61(1):55-63.

114. Haring RS, Canner JK, Haider AH, Schneider EB. Ocular injury in the United States: Emergency department visits from 2006-2011. Injury. 2016;47(1):104-8.

115. Haring RS, Sheffield ID, Channa R, Canner JK, Schneider EB. Epidemiologic trends of chemical ocular burns in the United States. JAMA Ophthalmol. 2016;134(10):1119-1124.

116. Hasby EA, Saad HA. Immunohistochemical expression of Fas ligand (FasL) and neprilysin (neutral endopeptidase/CD10) in keratoconus. Int Ophthalmol. 2013;33(2):125-31.

117. Hashimoto S, Amaya F, Oh-Hashi K, Kiuchi K, Hashimoto S. Expression of neutral endopeptidase activity during clinical and experimental acute lung injury. Respir Res. 2010;11:164.

118. Hayashi S, Osawa T, Tohyama K. Comparative observations on corneas, with special reference to Bowman's layer and Descemet's membrane in mammals and amphibians. J Morphol. 2002;254(3):247-58.

119. He Y, Zhao H, Su G. Ginsenoside Rg1 decreases neurofibrillary tangles accumulation in retina by regulating activities of neprilysin and PKA in retinal cells of AD mice model. J Mol Neurosci. 2014;52(1):101-6.

120. Heigle TJ, Pflugfelder SC. Aqueous tear production in patients with neurotrophic keratitis. Cornea. 1996;15(2):135-8.

121. Hirsch M, Prenant G, Renard G. Three-dimensional supramolecular organization of the extracellular matrix in human and rabbit corneal stroma, as revealed by ultrarapid-freezing and deep-etching methods. Exp Eye Res. 2001;72(2):123-35.

122. Hirst LW, Fogle JA, Kenyon KR, Stark WJ. Corneal epithelial regeneration and adhesion following acid burns in the rhesus monkey. Invest Ophthalmol Vis Sci. 1982;23(6):764-73.

123. Hirst LW, Kenyon KR, Fogle JA, Hanninen L, Stark WJ. Comparative studies of corneal surface injury in the monkey and rabbit. Arch Ophthalmol. 1981;99(6):1066-73.

124. Hoang MV, Sansom CE, Turner AJ. Mutagenesis of Glu403 to Cys in rabbit neutral endopeptidase-24.11 (neprilysin) creates a disulphide-linked homodimer: analogy with endothelin-converting enzyme. Biochem J. 1997;327 (Pt 3):925-9.

125. Hodson S, Miller F. The bicarbonate ion pump in the endothelium which regulates the hydration of rabbit cornea. J Physiol (Lond). 1976;263(3):563-77.

126. Hong HS, Lee J, Lee E, et al. A new role of substance P as an injury-inducible messenger for mobilization of CD29(+) stromal-like cells. Nat Med. 2009;15(4):425-35.

127. Hooper NM. Families of zinc metalloproteases. FEBS Lett. 1994;354(1):1-6.

128. Horiguchi A, Chen DY, Goodman OB, et al. Neutral endopeptidase inhibits prostate cancer tumorigenesis by reducing FGF-2-mediated angiogenesis. Prostate Cancer Prostatic Dis. 2008;11(1):79-87.

129. Howell S, Nalbantoglu J, Crine P. Neutral endopeptidase can hydrolyze beta-amyloid(1-40) but shows no effect on beta-amyloid precursor protein metabolism. Peptides. 1995;16(4):647-52.

130. Huang AJ, Tseng SC. Corneal epithelial wound healing in the absence of limbal epithelium. Invest Ophthalmol Vis Sci. 1991;32(1):96-105.

131. Hull DS, Green K, Boyd M, Wynn HR. Corneal endothelium bicarbonate transport and the effect of carbonic anhydrase inhibitors on endothelial permeability and fluxes and corneal thickness. Invest Ophthalmol Vis Sci. 1977;16(10):883-92.

132. Ikeda K, Emoto N, Raharjo SB, et al. Molecular identification and characterization of novel membrane-bound metalloprotease, the soluble secreted form of which hydrolyzes a variety of vasoactive peptides. J Biol Chem. 1999;274(45):32469-77.

133. Imanishi J, Kamiyama K, Iguchi I, Kita M, Sotozono C, Kinoshita S. Growth factors: importance in wound healing and maintenance of transparency of the cornea. Prog Retin Eye Res. 2000;19(1):113-29.

134. Iwamoto I, Yamazaki H, Tomioka H, Yoshida S. Inhibitory effect of tranilast on substance P-induced plasma extravasation in rat skin. Immunopharmacol Immunotoxicol. 1991;13(1-2):65-71.

135. Iwata N, Tsubuki S, Takaki Y, et al. Identification of the major Abeta1-42-degrading catabolic pathway in brain parenchyma: suppression leads to biochemical and pathological deposition. Nat Med. 2000;6(2):143-50.

136. Jackman HL, Tan FL, Tamei H, et al. A peptidase in human platelets that deamidates tachykinins. Probable identity with the lysosomal "protective protein". J Biol Chem. 1990;265(19):11265-72.

137. Jester JV, Budge A, Fisher S, Huang J. Corneal keratocytes: Phenotypic and species differences in abundant protein expression and in vitro light-scattering. Invest Ophthalmol Vis Sci. 2005;46(7):2369-78.

138. Jester JV, Moller-Pedersen T, Huang J, et al. The cellular basis of corneal transparency: Evidence for 'corneal crystallins'. J Cell Sci. 1999;112 (Pt 5):613-22.

139. Johnson AR, Ashton J, Schulz WW, Erdös EG. Neutral metalloendopeptidase in human lung tissue and cultured cells. Am Rev Respir Dis. 1985;132(3):564-8.

140. Johnson AR, Coalson JJ, Ashton J, Larumbide M, Erdös EG. Neutral endopeptidase in serum samples from patients with adult respiratory distress syndrome. Comparison with angiotensin-converting enzyme. Am Rev Respir Dis. 1985;132(6):1262-7.

141. Johnson KS, Levin F, Chu DS. Persistent corneal epithelial defect associated with erlotinib treatment. Cornea. 2009;28(6):706-7.

142. Jones MA, Marfurt CF. Peptidergic innervation of the rat cornea. Exp Eye Res. 1998;66(4):421-35.

143. Joyce NC, Harris DL, Mello DM. Mechanisms of mitotic inhibition in corneal endothelium: Contact inhibition and TGF-beta2. Invest Ophthalmol Vis Sci. 2002;43(7):2152-9.

144. Joyce NC. Proliferative capacity of the corneal endothelium. Prog Retin Eye Res. 2003;22(3):359-89.

145. Katayama M, Nadel JA, Bunnett NW, Di maria GU, Haxhiu M, Borson DB. Catabolism of calcitonin gene-related peptide and substance P by neutral endopeptidase. Peptides. 1991;12(3):563-7.

146. Kaufman PL, Adler FH, Levin LA et al. Adler's Physiology of the Eye. Elsevier Health Sciences; 2011.

147. Kawakita T, Higa K, Shimmura S, Tomita M, Tsubota K, Shimazaki J. Fate of corneal epithelial cells separated from limbus in vivo. Invest Ophthalmol Vis Sci. 2011;52(11):8132-7.

148. Kawakita T, Shimmura S, Hornia A, Higa K, Tseng SC. Stratified epithelial sheets engineered from a single adult murine corneal/limbal progenitor cell. J Cell Mol Med. 2008;12(4):1303-16.

149. Kenny AJ, Bourne A. Cellular reorganisation of membrane peptidases in Wallerian degeneration of pig peripheral nerve. J Neurocytol. 1991;20(11):875-85.

150. Kenyon KR, Fogle JA, Stone DL, Stark WJ. Regeneration of corneal epithelial basement membrane following thermal cauterization. Invest Ophthalmol Vis Sci. 1977;16(4):292-301.

151. Kenyon KR, Tseng SC. Limbal autograft transplantation for ocular surface disorders. Ophthalmology. 1989;96(5):709-22.

152. Kenyon KR. Recurrent corneal erosion: Pathogenesis and therapy. Int Ophthalmol Clin. 1979;19(2):169-95.

153. Kerr MA, Kenny AJ. The molecular weight and properties of a neutral metallo-endopeptidase from rabbit kidney brush border. Biochem J. 1974a;137(3):489-95.

154. Kerr MA, Kenny AJ. The purification and specificity of a neutral endopeptidase from rabbit kidney brush border. Biochem J. 1974b;137(3):477-88.

155. Khodadoust AA, Green K. Physiological function of regenerating endothelium. Invest Ophthalmol. 1976;15(2):96-101.

156. Khodadoust AA, Silverstein AM, Kenyon DR, Dowling JE. Adhesion of regenerating corneal epithelium. The role of basement membrane. Am J Ophthalmol. 1968;65(3):339-48.

157. Kim M, Kim JK, Lee HK. Corneal endothelial decompensation after iris-claw phakic intraocular lens implantation. J Cataract Refract Surg. 2008;34(3):517-9.

158. Kioussi C, Crine P, Matsas R. Endopeptidase-24.11 is suppressed in myelin-forming but not in non-myelin-forming Schwann cells during development of the rat sciatic nerve. Neuroscience. 1992;50(1):69-83.

159. Kioussi C, Mamalaki A, Jessen K, Mirsky R, Hersh LB, Matsas R. Expression of endopeptidase-24.11 (common acute lymphoblastic leukaemia antigen CD10) in the

sciatic nerve of the adult rat after lesion and during regeneration. Eur J Neurosci. 1995;7(5):951-61.

160. Kioussi C, Matsas R. Endopeptidase-24.11, a cell-surface peptidase of central nervous system neurons, is expressed by Schwann cells in the pig peripheral nervous system. J Neurochem. 1991;57(2):431-40.

161. Ko JA, Mizuno Y, Ohki C, Chikama T, Sonoda KH, Kiuchi Y. Neuropeptides released from trigeminal neurons promote the stratification of human corneal epithelial cells. Invest Ophthalmol Vis Sci. 2014;55(1):125-33.

162. Ko JA, Yanai R, Nishida T. Up-regulation of ZO-1 expression and barrier function in cultured human corneal epithelial cells by substance P. FEBS Lett. 2009;583(12):2148-53.

163. Kokkonen JO, Kuoppala A, Saarinen J, Lindstedt KA, Kovanen PT. Kallidin- and bradykinin-degrading pathways in human heart: Degradation of kallidin by aminopeptidase M-like activity and bradykinin by neutral endopeptidase. Circulation. 1999;99(15):1984-90.

164. Konomi K, Zhu C, Harris D, Joyce NC. Comparison of the proliferative capacity of human corneal endothelial cells from the central and peripheral areas. Invest Ophthalmol Vis Sci. 2005;46(11):4086-91.

165. Kostis JB, Packer M, Black HR, Schmieder R, Henry D, Levy E. Omapatrilat and enalapril in patients with hypertension: The Omapatrilat Cardiovascular Treatment vs. Enalapril (OCTAVE) trial. Am J Hypertens. 2004;17(2):103-11.

166. Kuckelkorn R, Kottek A, Reim M. [Intraocular complications after severe chemical burns--incidence and surgical treatment]. Klin Monbl Augenheilkd. 1994;205(2):86-92.

167. Kuckelkorn R, Schrage N, Keller G, Redbrake C. Emergency treatment of chemical and thermal eye burns. Acta Ophthalmol Scand. 2002;80(1):4-10.

168. Kuwabara T, Perkins DG, Cogan DG. Sliding of the epithelium in experimental corneal wounds. Invest Ophthalmol. 1976;15(1):4-14.

169. Lafrance MH, Vézina C, Wang Q, Boileau G, Crine P, Lemay G. Role of glycosylation in transport and enzymic activity of neutral endopeptidase-24.11. Biochem J. 1994;302 (Pt 2):451-4.

170. Lambert DM, Mergen F, Poupaert JH, Dumont P. Analgesic potency of S-acetylthiorphan after intravenous administration to mice. Eur J Pharmacol. 1993;243(2):129-34.

171. Lambiase A, Rama P, Bonini S, Caprioglio G, Aloe L. Topical treatment with nerve growth factor for corneal neurotrophic ulcers. N Engl J Med. 1998;338(17):1174-80.

172. Lan Y, Kodati S, Lee HS, Omoto M, Jin Y, Chauhan SK. Kinetics and function of mesenchymal stem cells in corneal injury. Invest Ophthalmol Vis Sci. 2012;53(7):3638-44.

173. Lavail JH, Johnson WE, Spencer LC. Immunohistochemical identification of trigeminal ganglion neurons that innervate the mouse cornea: Relevance to intercellular spread of herpes simplex virus. J Comp Neurol. 1993;327(1):133-40.

174. Leal EC, Carvalho E, Tellechea A, et al. Substance P promotes wound healing in diabetes by modulating inflammation and macrophage phenotype. Am J Pathol. 2015;185(6):1638-48.

175. Lee BH, McLaren JW, Erie JC, Hodge DO, Bourne WM. Reinnervation in the cornea after LASIK. Invest Ophthalmol Vis Sci. 2002;43(12):3660-4.

176. Lehrer MS, Sun TT, Lavker RM. Strategies of epithelial repair: Modulation of stem cell and transit amplifying cell proliferation. J Cell Sci. 1998;111 (Pt 19):2867-75.

177. Li Z, Burns AR, Miller SB, Smith CW. CCL20, γδ T cells, and IL-22 in corneal epithelial healing. FASEB J. 2011;25(8):2659-68.

178. Liang L, Sheha H, Li J, Tseng SC. Limbal stem cell transplantation: New progresses and challenges. Eye (Lond). 2009;23(10):1946-53.

179. Lindholm D, Heumann R, Meyer M, Thoenen H. Interleukin-1 regulates synthesis of nerve growth factor in non-neuronal cells of rat sciatic nerve. Nature. 1987;330(6149):658-9.

180. Ljubimov AV, Saghizadeh M. Progress in corneal wound healing. Prog Retin Eye Res. 2015;49:17-45.

181. Llorens-Cortes C, Huang H, Vicart P, Gasc JM, Paulin D, Corvol P. Identification and characterization of neutral endopeptidase in endothelial cells from venous or arterial origins. J Biol Chem. 1992;267(20):14012-8.

182. Lu B, Figini M, Emanueli C, et al. The control of microvascular permeability and blood pressure by neutral endopeptidase. Nat Med. 1997;3(8):904-7.

183. Lu B, Gerard NP, Kolakowski LF, et al. Neutral endopeptidase modulation of septic shock. J Exp Med. 1995;181(6):2271-5.

184. Lu PC, Ye H, Maeda M, Azar DT. Immunolocalization and gene expression of matrilysin during corneal wound healing. Invest Ophthalmol Vis Sci. 1999;40(1):20-7.

185. Luibl V, Isas JM, Kayed R, Glabe CG, Langen R, Chen J. Drusen deposits associated with aging and age-related macular degeneration contain nonfibrillar amyloid oligomers. J Clin Invest. 2006;116(2):378-85.

186. Mackie IA. Role of the corneal nerves in destructive disease of the cornea. Trans Ophthalmol Soc U K. 1978;98(3):343-7.

187. Majo F, Rochat A, Nicolas M, Jaoudé GA, Barrandon Y. Oligopotent stem cells are distributed throughout the mammalian ocular surface. Nature. 2008;456(7219):250-4.

188. Mak IT, Kramer JH, Chmielinska JJ, Khalid MH, Landgraf KM, Weglicki WB. Inhibition of neutral endopeptidase potentiates neutrophil activation during Mg-deficiency in the rat. Inflamm Res. 2008;57(7):300-5.

189. Malfroy B, Schofield PR, Kuang WJ, Seeburg PH, Mason AJ, Henzel WJ. Molecular cloning and amino acid sequence of rat enkephalinase. Biochem Biophys Res Commun. 1987;144(1):59-66.

190. Malfroy B, Swerts JP, Guyon A, Roques BP, Schwartz JC. High-affinity enkephalin-degrading peptidase in brain is increased after morphine. Nature. 1978;276(5687):523-6.

191. Mapp PI, Walsh DA, Kidd BL, Cruwys SC, Polak JM, Blake DR. Localization of the enzyme neutral endopeptidase to the human synovium. J Rheumatol. 1992;19(12):1838-44.

192. Marfurt CF, Jones MA, Thrasher K. Parasympathetic innervation of the rat cornea. Exp Eye Res. 1998;66(4):437-48.

193. Marfurt CF, Kingsley RE, Echtenkamp SE. Sensory and sympathetic innervation of the mammalian cornea: A retrograde tracing study. Invest Ophthalmol Vis Sci. 1989;30(3):461-72.

194. Markoulli M, You J, Kim J, et al. Corneal nerve morphology and tear film substance P in diabetes. Optom Vis Sci. 2017;94(7):726-731.

195. Mastropasqua L, Massaro-Giordano G, Nubile M, Sacchetti M. Understanding the pathogenesis of neurotrophic keratitis: The role of corneal nerves. J Cell Physiol. 2017;232(4):717-724.

196. Matsas R, Fulcher IS, Kenny AJ, Turner AJ. Substance P and [Leu]enkephalin are hydrolyzed by an enzyme in pig caudate synaptic membranes that is identical with the endopeptidase of kidney microvilli. Proc Natl Acad Sci USA. 1983;80(10):3111-5.

197. Matsas R, Kenny AJ, Turner AJ. An immunohistochemical study of endopeptidase-24.11 ("enkephalinase") in the pig nervous system. Neuroscience. 1986;18(4):991-1012.

198. Matsas R, Kenny AJ, Turner AJ. The metabolism of neuropeptides. The hydrolysis of peptides, including enkephalins, tachykinins and their analogues, by endopeptidase-24.11. Biochem J. 1984;223(2):433-40.

199. Matsas R, Rattray M, Kenny AJ, Turner AJ. The metabolism of neuropeptides. Endopeptidase-24.11 in human synaptic membrane preparations hydrolyses substance P. Biochem J. 1985;228(2):487-92.

200. Matsuda M, Sawa M, Edelhauser HF, Bartels SP, Neufeld AH, Kenyon KR. Cellular migration and morphology in corneal endothelial wound repair. Invest Ophthalmol Vis Sci. 1985;26(4):443-9.

201. Matsuda M, Ubels JL, Edelhauser HF. A larger corneal epithelial wound closes at a faster rate. Invest Ophthalmol Vis Sci. 1985;26(6):897-900.

202. Maurice DM. The location of the fluid pump in the cornea. J Physiol (Lond). 1972;221(1):43-54.

203. Maurice DM. The structure and transparency of the cornea. J Physiol (Lond). 1957;136(2):263-86.

204. McCartney MD, Cantu-Crouch D. Rabbit corneal epithelial wound repair: tight junction reformation. Curr Eye Res. 1992;11(1):15-24.

205. McKenzie LB, Ahir N, Stolz U, Nelson NG. Household cleaning product-related injuries treated in US emergency departments in 1990-2006. Pediatrics. 2010;126(3):509-16.

206. McMurray JJ, Packer M, Desai AS, et al. Angiotensin-neprilysin inhibition versus enalapril in heart failure. N Engl J Med. 2014;371(11):993-1004.

207. Medeiros Mdos S, Turner AJ. Metabolism and functions of neuropeptide Y. Neurochem Res. 1996;21(9):1125-32.

208. Medja F, Lelièvre V, Fontaine RH, et al. Thiorphan, a neutral endopeptidase inhibitor used for diarrhoea, is neuroprotective in newborn mice. Brain. 2006;129(Pt 12):3209-23.

209. Meek KM, Knupp C. Corneal structure and transparency. Prog Retin Eye Res. 2015;49:1-16.

210. Meng ID, Kurose M. The role of corneal afferent neurons in regulating tears under normal and dry eye conditions. Exp Eye Res. 2013;117:79-87.

211. Michael-Titus AT, Fernandes K, Setty H, Whelpton R. *In vivo* metabolism and clearance of substance P and co-expressed tachykinins in rat striatum. Neuroscience. 2002;110(2):277-86.

212. Morrison JC, Fraunfelder FW, Milne ST, Moore CG. Limbal microvasculature of the rat eye. Invest Ophthalmol Vis Sci. 1995;36(3):751-6.

213. Morrison JC, Van Buskirk EM. Anterior collateral circulation in the primate eye. Ophthalmology. 1983;90(6):707-15.

214. Müller LJ, Marfurt CF, Kruse F, Tervo TM. Corneal nerves: structure, contents and function. Exp Eye Res. 2003;76(5):521-42.

215. Müller LJ, Pels L, Vrensen GF. Ultrastructural organization of human corneal nerves. Invest Ophthalmol Vis Sci. 1996;37(4):476-88.

216. Müller LJ, Vrensen GF, Pels L, Cardozo BN, Willekens B. Architecture of human corneal nerves. Invest Ophthalmol Vis Sci. 1997;38(5):985-94.

217. Murakami J, Nishida T, Otori T. Coordinated appearance of beta 1 integrins and fibronectin during corneal wound healing. J Lab Clin Med. 1992;120(1):86-93.

218. Mustoe T. Understanding chronic wounds: A unifying hypothesis on their pathogenesis and implications for therapy. Am J Surg. 2004;187(5A):65S-70S.

219. Nadeau S, Filali M, Zhang J, et al. Functional recovery after peripheral nerve injury is dependent on the pro-inflammatory cytokines IL-1β and TNF: Implications for neuropathic pain. J Neurosci. 2011;31(35):12533-42.

220. Nadel JA, Borson DB. Modulation of neurogenic inflammation by neutral endopeptidase. Am Rev Respir Dis. 1991;143(3 Pt 2):S33-6.

221. Nakamura M, Chikama T, Nishida T. Synergistic effect with Phe-Gly-Leu-Met-NH2 of the C-terminal of substance P and insulin-like growth factor-1 on epithelial wound healing of rabbit cornea. Br J Pharmacol. 1999;127(2):489-97.

222. Nakamura M, Nagano T, Chikama T, Nishida T. Up-regulation of phosphorylation of focal adhesion kinase and paxillin by combination of substance P and IGF-1 in SV-40 transformed human corneal epithelial cells. Biochem Biophys Res Commun. 1998;242(1):16-20.

223. Nakamura M, Ofuji K, Chikama T, Nishida T. The NK1 receptor and its participation in the synergistic enhancement of corneal epithelial migration by substance P and insulin-like growth factor-1. Br J Pharmacol. 1997;120(4):547-52.

224. Namavari A, Chaudhary S, Ozturk O, et al. Semaphorin 7a links nerve regeneration and inflammation in the cornea. Invest Ophthalmol Vis Sci. 2012;53(8):4575-85.

225. Namavari A, Chaudhary S, Sarkar J, et al. In vivo serial imaging of regenerating corneal nerves after surgical transection in transgenic thy1-YFP mice. Invest Ophthalmol Vis Sci. 2011;52(11):8025-32.

226. Négrel AD, Thylefors B. The global impact of eye injuries. Ophthalmic Epidemiol. 1998;5(3):143-69.

227. Netto MV, Mohan RR, Sinha S, Sharma A, Dupps W, Wilson SE. Stromal haze, myofibroblasts, and surface irregularity after PRK. Exp Eye Res. 2006;82(5):788-97.

228. Nishida T, Chikama T, Morishige N, Yanai R, Yamada N, Saito J. Persistent epithelial defects due to neurotrophic keratopathy treated with a substance P-derived peptide and insulin-like growth factor 1. Jpn J Ophthalmol. 2007;51(6):442-7.

229. Nishida T, Inui M, Nomizu M. Peptide therapies for ocular surface disturbances based on fibronectin-integrin interactions. Prog Retin Eye Res. 2015;47:38-63.

230. Nishida T, Nakagawa S, Ohashi Y, Awata T, Manabe R. Fibronectin in corneal wound healing: Appearance in cultured rabbit cornea. Jpn J Ophthalmol. 1982;26(4):410-5.

231. Nishida T, Nakamura M, Ofuji K, Reid TW, Mannis MJ, Murphy CJ. Synergistic effects of substance P with insulin-like growth factor-1 on epithelial migration of the cornea. J Cell Physiol. 1996;169(1):159-66.

232. Nishida T, Yanai R. Advances in treatment for neurotrophic keratopathy. Curr Opin Ophthalmol. 2009;20(4):276-81.

233. Nishida T. Neurotrophic mediators and corneal wound healing. Ocul Surf. 2005;3(4):194-202.

234. O'Connell JE, Jardine AG, Davidson G, Connell JM. Candoxatril, an orally active neutral endopeptidase inhibitor, raises plasma atrial natriuretic factor and is natriuretic in essential hypertension. J Hypertens. 1992;10(3):271-7.

235. Obata H, Tsuru T. Corneal wound healing from the perspective of keratoplasty specimens with special reference to the function of the Bowman layer and Descemet membrane. Cornea. 2007;26(9 Suppl 1):S82-9.

236. Ohkubo K, Okuda M, Kaliner MA. Immunological localization of neuropeptide-degrading enzymes in the nasal mucosa. Rhinology. 1994;32(3):130-3.

237. Okada Y, Shirai K, Miyajima M, et al. Loss of TRPV4 function suppresses inflammatory fibrosis induced by alkali-burning mouse corneas. PLoS ONE. 2016;11(12):e0167200.

238. Olerud JE, Usui ML, Seckin D, et al. Neutral endopeptidase expression and distribution in human skin and wounds. J Invest Dermatol. 1999;112(6):873-81.

239. Oliveira-Soto L, Efron N. Morphology of corneal nerves using confocal microscopy. Cornea. 2001;20(4):374-84.

240. Oneda H, Inouye K. Interactions of human matrix metalloproteinase 7 (matrilysin) with the inhibitors thiorphan and R-94138. J Biochem. 2001;129(3):429-35.

241. Painter RG, Dukes R, Sullivan J, Carter R, Erdös EG, Johnson AR. Function of neutral endopeptidase on the cell membrane of human neutrophils. J Biol Chem. 1988;263(19):9456-61.

242. Park KS, Lim CH, Min BM, et al. The side population cells in the rabbit limbus sensitively increased in response to the central cornea wounding. Invest Ophthalmol Vis Sci. 2006;47(3):892-900.

243. Parthasarathy R, Chow KM, Derafshi Z, et al. Reduction of amyloid-beta levels in mouse eye tissues by intra-vitreally delivered neprilysin. Exp Eye Res. 2015;138:134-44.

244. Pellegrini G, Traverso CE, Franzi AT, Zingirian M, Cancedda R, De Luca M. Long-term restoration of damaged corneal surfaces with autologous cultivated corneal epithelium. Lancet. 1997;349(9057):990-3.

245. Peterson JL, Phelps ED, Doll MA, Schaal S, Ceresa BP. The role of endogenous epidermal growth factor receptor ligands in mediating corneal epithelial homeostasis. Invest Ophthalmol Vis Sci. 2014;55(5):2870-80.

246. Pierart ME, Najdovski T, Appelboom TE, Deschodt-Lanckman MM. Effect of human endopeptidase 24.11 ("enkephalinase") on IL-1-induced thymocyte proliferation activity. J Immunol. 1988;140(11):3808-11.

247. Rama P, Matuska S, Paganoni G, Spinelli A, De Luca M, Pellegrini G. Limbal stem-cell therapy and long-term corneal regeneration. N Engl J Med. 2010;363(2):147-55.

248. Reid TW, Murphy CJ, Iwahashi CK, Foster BA, Mannis MJ. Stimulation of epithelial cell growth by the neuropeptide substance P. J Cell Biochem. 1993;52(4):476-85.

249. Reidy JJ, Paulus MP, Gona S. Recurrent erosions of the cornea: Epidemiology and treatment. Cornea. 2000;19(6):767-71.

250. Reins RY, Courson J, Lema C, Redfern RL. MyD88 contribution to ocular surface homeostasis. PLoS ONE. 2017;12(8):e0182153.

251. Rissler K. Sample preparation, high-performance liquid chromatographic separation and determination of substance P-related peptides. J Chromatogr B, Biomed Appl. 1995;665(2):233-70.

252. Rojas M, Xu J, Woods CR, et al. Bone marrow-derived mesenchymal stem cells in repair of the injured lung. Am J Respir Cell Mol Biol. 2005;33(2):145-52.

253. Ronco P, Pollard H, Galceran M, Delauche M, Schwartz JC, Verroust P. Distribution of enkephalinase (membrane metalloendopeptidase, E.C. 3.4.24.11) in rat organs. Detection using a monoclonal antibody. Lab Invest. 1988;58(2):210-7.

254. Roques BP, Fournié-Zaluski MC, Soroca E, et al. The enkephalinase inhibitor thiorphan shows antinociceptive activity in mice. Nature. 1980;288(5788):286-8.

255. Rose C, Voisin S, Gros C, Schwartz JC, Ouimet T. Cell-specific activity of neprilysin 2 isoforms and enzymic specificity compared with neprilysin. Biochem J. 2002;363(3):697-705.

256. Rossi A, Kontarakis Z, Gerri C, et al. Genetic compensation induced by deleterious mutations but not gene knockdowns. Nature. 2015;524(7564):230-3.

257. Rozenbaum D, Baruchin AM, Dafna Z. Chemical burns of the eye with special reference to alkali burns. Burns. 1991;17(2):136-40.

258. Rózsa AJ, Guss RB, Beuerman RW. Neural remodeling following experimental surgery of the rabbit cornea. Invest Ophthalmol Vis Sci. 1983;24(8):1033-51.

259. Sabatino F, Di zazzo A, De Simone L, Bonini S. The intriguing role of neuropeptides at the ocular surface. Ocul Surf. 2017;15(1):2-14.

260. Sacchetti M, Lambiase A. Diagnosis and management of neurotrophic keratitis. Clin Ophthalmol. 2014;8:571-9.

261. Saika S. Yin and yang in cytokine regulation of corneal wound healing: Roles of TNF-alpha. Cornea. 2007;26(9 Suppl 1):S70-4.

262. Sandvig KU, Haaskjold E, Bjerknes R, Refsum SB, Kravik K. Cell kinetics of conjunctival and corneal epithelium during regeneration of different-sized corneal epithelial defects. Acta Ophthalmol (Copenh). 1994;72(1):43-8.

263. Sasaki M, Abe R, Fujita Y, Ando S, Inokuma D, Shimizu H. Mesenchymal stem cells are recruited into wounded skin and contribute to wound repair by transdifferentiation into multiple skin cell type. J Immunol. 2008;180(4):2581-7.

264. Sato Y, Araki H, Kato J, et al. Human mesenchymal stem cells xenografted directly to rat liver are differentiated into human hepatocytes without fusion. Blood. 2005;106(2):756-63.

265. Schmid E, Leierer J, Doblinger A, et al. Neurokinin a is a main constituent of sensory neurons innervating the anterior segment of the eye. Invest Ophthalmol Vis Sci. 2005;46(1):268-74.

266. Scholzen T, Armstrong CA, Bunnett NW, Luger TA, Olerud JE, Ansel JC. Neuropeptides in the skin: Interactions between the neuroendocrine and the skin immune systems. Exp Dermatol. 1998;7(2-3):81-96.

267. Scholzen TE, Steinhoff M, Bonaccorsi P, et al. Neutral endopeptidase terminates substance P-induced inflammation in allergic contact dermatitis. J Immunol. 2001;166(2):1285-91.

268. Schultz RO, Van Horn DL, Peters MA, Klewin KM, Schutten WH. Diabetic keratopathy. Trans Am Ophthalmol Soc. 1981;79:180-99.

269. Schulz WW, Hagler HK, Buja LM, Erdös EG. Ultrastructural localization of angiotensin I-converting enzyme (EC 3.4.15.1) and neutral metalloendopeptidase (EC 3.4.24.11) in the proximal tubule of the human kidney. Lab Invest. 1988;59(6):789-97.

270. Schwartz JC, De la Baume S, Malfroy B, et al. "Enkephalinase", a newly characterised dipeptidyl carboxypeptidase: properties and possible role in enkephalinergic transmission. Int J Neurol. 1980;14(2-4):195-204.

271. Schwartz JC, Malfroy B, De la Baume S. Biological inactivation of enkephalins and the role of enkephalin-dipeptidyl-carboxypeptidase ("enkephalinase") as neuropeptidase. Life Sci. 1981;29(17):1715-40.

272. Schwartz JC. Racecadotril: A new approach to the treatment of diarrhoea. Int J Antimicrob Agents. 2000;14(1):75-9.

273. Scott JR, Muangman PR, Tamura RN, et al. Substance P levels and neutral endopeptidase activity in acute burn wounds and hypertrophic scar. Plast Reconstr Surg. 2005;115(4):1095-102.

274. Shapiro MS, Friend J, Thoft RA. Corneal re-epithelialization from the conjunctiva. Invest Ophthalmol Vis Sci. 1981;21(1 Pt 1):135-42.

275. Sharma A, Coles WH. Kinetics of corneal epithelial maintenance and graft loss. A population balance model. Invest Ophthalmol Vis Sci. 1989;30(9):1962-71.

276. Sharma N, Singh D, Sobti A, et al. Course and outcome of accidental sodium hydroxide ocular injury. Am J Ophthalmol. 2012;154(4):740-749.e2.

277. Sharpe JR, Daya SM, Dimitriadi M, Martin R, James SE. Survival of cultured allogeneic limbal epithelial cells following corneal repair. Tissue Eng. 2007;13(1):123-32.

278. Sherwin T, McGhee CN. Corneal epithelial homeostasis. Ophthalmology. 2010;117(1):190-1.

279. Shimada K, Takahashi M, Turner AJ, Tanzawa K. Rat endothelin-converting enzyme-1 forms a dimer through Cys412 with a similar catalytic mechanism and a distinct substrate binding mechanism compared with neutral endopeptidase-24.11. Biochem J. 1996;315 (Pt 3):863-7.

280. Shipp MA, Stefano GB, Switzer SN, Griffin JD, Reinherz EL. CD10 (CALLA)/neutral endopeptidase 24.11 modulates inflammatory peptide-induced changes in neutrophil morphology, migration, and adhesion proteins and is itself regulated by neutrophil activation. Blood. 1991;78(7):1834-41.

281. Sigelman S, Friedenwald JS. Mitotic and wound-healing activities of the corneal epithelium; effect of sensory denervation. AMA Arch Ophthalmol. 1954;52(1):46-57.

282. Skryzdło-Radomańska B, Pollard H, Schabowski J, et al. [Activity of enkephalinase (EC.3.4.24.11). Neutral endopeptidase (NEP) in human digestive tract epithelial cells]. Wiad Lek. 1994;47(1-2):13-7.

283. Słoniecka M, Le Roux S, Boman P, Byström B, Zhou Q, Danielson P. Expression profiles of neuropeptides, neurotransmitters, and their receptors in human keratocytes in vitro and in situ. PLoS ONE. 2015;10(7):e0134157.

284. Soloway MR, Stjernschantz J, Sears M. The miotic effect of substance P on the isolated rabbit iris. Invest Ophthalmol Vis Sci. 1981;20(1):47-52.

285. Soong HK. Vinculin in focal cell-to-substrate attachments of spreading corneal epithelial cells. Arch Ophthalmol. 1987;105(8):1129-32.

286. Spenny ML, Muangman P, Sullivan SR et al. Neutral endopeptidase inhibition in diabetic wound repair. Wound Repair Regen. 2002;10(5):295-301.

287. Spillantini MG, Sicuteri F, Salmon S, Malfroy B. Characterization of endopeptidase 3.4.24.11 ("enkephalinase") activity in human plasma and cerebrospinal fluid. Biochem Pharmacol. 1990;39(8):1353-6.

288. Stepp MA, Tadvalkar G, Hakh R, Pal-Ghosh S. Corneal epithelial cells function as surrogate Schwann cells for their sensory nerves. Glia. 2017;65(6):851-863.

289. Stewart JR, Kenny AJ. Proteins of the kidney microvillar membrane. Effects of monensin, vinblastine, swainsonine and glucosamine on the processing and assembly of endopeptidase-24.11 and dipeptidyl peptidase IV in pig kidney slices. Biochem J. 1984;224(2):559-68.

290. Stiemke MM, Edelhauser HF, Geroski DH. The developing corneal endothelium: Correlation of morphology, hydration and Na/K ATPase pump site density. Curr Eye Res. 1991;10(2):145-56.

291. Stoll G, Müller HW. Macrophages in the peripheral nervous system and astroglia in the central nervous system of rat commonly express apolipoprotein E during development but differ in their response to injury. Neurosci Lett. 1986;72(3):233-8.

292. Stramer BM, Zieske JD, Jung JC, Austin JS, Fini ME. Molecular mechanisms controlling the fibrotic repair phenotype in cornea: Implications for surgical outcomes. Invest Ophthalmol Vis Sci. 2003;44(10):4237-46.

293. Sun TT, Tseng SC, Lavker RM. Location of corneal epithelial stem cells. Nature. 2010;463(7284):E10-1.

294. Suuronen EJ, Nakamura M, Watsky MA, et al. Innervated human corneal equivalents as in vitro models for nerve-target cell interactions. FASEB J. 2004;18(1):170-2.

295. Suzuki K, Tanaka T, Enoki M, Nishida T. Coordinated reassembly of the basement membrane and junctional proteins during corneal epithelial wound healing. Invest Ophthalmol Vis Sci. 2000;41(9):2495-500.

296. Teranishi S, Kimura K, Nishida T. Role of formation of an ERK-FAK-paxillin complex in migration of human corneal epithelial cells during wound closure in vitro. Invest Ophthalmol Vis Sci. 2009;50(12):5646-52.

297. Tervo K, Tervo T, Eränkö L, Vannas A, Cuello AC, Eränkö O. Substance P-immunoreactive nerves in the human cornea and iris. Invest Ophthalmol Vis Sci. 1982;23(5):671-4.

298. Thoft RA, Friend J. The X, Y, Z hypothesis of corneal epithelial maintenance. Invest Ophthalmol Vis Sci. 1983;24(10):1442-3.

299. Tran-Paterson R, Boileau G, Giguère V, Letarte M. Comparative levels of CALLA/neutral endopeptidase on normal granulocytes, leukemic cells, and transfected COS-1 cells. Blood. 1990;76(4):775-82.

300. Tuft SJ, Shortt AJ. Surgical rehabilitation following severe ocular burns. Eye (Lond). 2009;23(10):1966-71.

301. Turner AJ, Isaac RE, Coates D. The neprilysin (NEP) family of zinc metalloendopeptidases: genomics and function. Bioessays. 2001;23(3):261-9.

302. Turner AJ, Matsas R, Kenny AJ. Endopeptidase-24.11 and neuropeptide metabolism. Biochem Soc Trans. 1985;13(1):39-42.

303. Twardy BS, Channappanavar R, Suvas S. Substance P in the corneal stroma regulates the severity of herpetic stromal keratitis lesions. Invest Ophthalmol Vis Sci. 2011;52(12):8604-13.

304. Ueda A, Nishida T, Otori T, Fujita H. Electron-microscopic studies on the presence of gap junctions between corneal fibroblasts in rabbits. Cell Tissue Res. 1987;249(2):473-5.

305. Unger, E. F. Approval letter — US Food and Drug Administration. FDA http://www.accessdata.fda.gov/ drugsatfda_docs/appletter/2015/ 207620Orig1s000ltr.pdf (2015).

306. Vanneste Y, Michel A, Dimaline R, Najdovski T, Deschodt-Lanckman M. Hydrolysis of alpha-human atrial natriuretic peptide in vitro by human kidney membranes and purified endopeptidase-24.11: Evidence for a novel cleavage site. Biochem J. 1988;254(2):531-7.

307. Varnell RJ, Freeman JY, Maitchouk D, Beuerman RW, Gebhardt BM. Detection of substance P in human tears by laser desorption mass spectrometry and immunoassay. Curr Eye Res. 1997;16(9):960-3.

308. Wagoner MD. Chemical injuries of the eye: current concepts in pathophysiology and therapy. Surv Ophthalmol. 1997;41(4):275-313.

309. Waksman G, Hamel E, Delay-Goyet P, Roques BP. Neutral endopeptidase-24.11, mu and delta opioid receptors after selective brain lesions: an autoradiographic study. Brain Res. 1987;436(2):205-16.

310. Watanabe M, Nakayasu K, Iwatsu M, Kanai A. Endogenous substance P in corneal epithelial cells and keratocytes. Jpn J Ophthalmol. 2002;46(6):616-20.

311. Wei ZG, Wu RL, Lavker RM, Sun TT. In vitro growth and differentiation of rabbit bulbar, fornix, and palpebral conjunctival epithelia: Implications on conjunctival epithelial transdifferentiation and stem cells. Invest Ophthalmol Vis Sci. 1993;34(5):1814-28.

312. West-Mays JA, Dwivedi DJ. The keratocyte: corneal stromal cell with variable repair phenotypes. Int J Biochem Cell Biol. 2006;38(10):1625-31.

313. Whitcher JP, Srinivasan M, Upadhyay MP. Corneal blindness: A global perspective. Bull World Health Organ. 2001;79(3):214-21.

314. Whyteside AR, Turner AJ. Human neprilysin-2 (NEP2) and NEP display distinct subcellular localisations and substrate preferences. FEBS Lett. 2008;582(16):2382-6.

315. Wiley L, Sundarraj N, Sun TT, Thoft RA. Regional heterogeneity in human corneal and limbal epithelia: An immunohistochemical evaluation. Invest Ophthalmol Vis Sci. 1991;32(3):594-602.

316. Williams K, Watsky M. Gap junctional communication in the human corneal endothelium and epithelium. Curr Eye Res. 2002;25(1):29-36.

317. Wilson SE, Chaurasia SS, Medeiros FW. Apoptosis in the initiation, modulation and termination of the corneal wound healing response. Exp Eye Res. 2007;85(3):305-11.

318. Wilson SE, He YG, Weng J, et al. Epithelial injury induces keratocyte apoptosis: hypothesized role for the interleukin-1 system in the modulation of corneal tissue organization and wound healing. Exp Eye Res. 1996;62(4):325-7.

319. Wilson SE, He YG, Weng J, Zieske JD, Jester JV, Schultz GS. Effect of epidermal growth factor, hepatocyte growth factor, and keratinocyte growth factor, on proliferation, motility and differentiation of human corneal epithelial cells. Exp Eye Res. 1994;59(6):665-78.

320. Wilson SE, Hong JW. Bowman's layer structure and function: critical or dispensable to corneal function? A hypothesis. Cornea. 2000;19(4):417-20.

321. Wilson SE, Kim WJ. Keratocyte apoptosis: Implications on corneal wound healing, tissue organization, and disease. Invest Ophthalmol Vis Sci. 1998;39(2):220-6.

322. Wilson SE, Liu JJ, Mohan RR. Stromal-epithelial interactions in the cornea. Prog Retin Eye Res. 1999;18(3):293-309.

323. Wilson SE, Mohan RR, Netto M, et al. RANK, RANKL, OPG, and M-CSF expression in stromal cells during corneal wound healing. Invest Ophthalmol Vis Sci. 2004;45(7):2201-11.

324. Wilson SE, Pedroza L, Beuerman R, Hill JM. Herpes simplex virus type-1 infection of corneal epithelial cells induces apoptosis of the underlying keratocytes. Exp Eye Res. 1997;64(5):775-9.

325. Wilson SE. Corneal myofibroblast biology and pathobiology: generation, persistence, and transparency. Exp Eye Res. 2012;99:78-88.

326. Wolter JR. Regeneration and hyper-regeneration of corneal nerves. Ophthalmologica. 1966;151(5):588-603.

327. Woodlief NF. Initial observations on the ocular microcirculation in man. I. The anterior segment and extraocular muscles. Arch Ophthalmol. 1980;98(7):1268-72.

328. Xu Y, Huang J, Liu F, Gao S, Guo Q. Quantitative analysis of racecadotril metabolite in human plasma using a liquid chromatography/tandem mass spectrometry. J Chromatogr B Analyt Technol Biomed Life Sci. 2007;852(1-2):101-7.

329. Yamada M, Mashima Y, Tsubota K. Scanning electron microscopic observation of basal cells following corneal epithelial abrasion. Eye (Lond). 1996;10 (Pt 5):569-74.

330. Yamada M, Ogata M, Kawai M, Mashima Y, Nishida T. Substance P and its metabolites in normal human tears. Invest Ophthalmol Vis Sci. 2002;43(8):2622-5.

331. Yamada M, Ogata M, Kawai M, Mashima Y, Nishida T. Substance P in human tears. Cornea. 2003;22(7 Suppl):S48-54.

332. Yamada N, Matsuda R, Morishige N, et al. Open clinical study of eye-drops containing tetrapeptides derived from substance P and insulin-like growth factor-1 for treatment of persistent corneal epithelial defects associated with neurotrophic keratopathy. Br J Ophthalmol. 2008;92(7):896-900.

333. Yamada N, Yanai R, Inui M, Nishida T. Sensitizing effect of substance P on corneal epithelial migration induced by IGF-1, fibronectin, or interleukin-6. Invest Ophthalmol Vis Sci. 2005;46(3):833-9.

334. Yandle T, Richards M, Smith M, Charles C, Livesey J, Espiner E. Assay of endopeptidase-24.11 activity in plasma applied to in vivo studies of endopeptidase inhibitors. Clin Chem. 1992;38(9):1785-91.

335. Yao L, Li ZR, Su WR, et al. Role of mesenchymal stem cells on cornea wound healing induced by acute alkali burn. PLoS ONE. 2012;7(2):e30842.

336. Yasojima K, Akiyama H, McGeer EG, McGeer PL. Reduced neprilysin in high plaque areas of Alzheimer brain: A possible relationship to deficient degradation of beta-amyloid peptide. Neurosci Lett. 2001;297(2):97-100.

337. Yavuz B, Kompella UB. Ocular Drug Delivery. Handb Exp Pharmacol. 2017;242:57-93.

338. Yee RW, Geroski DH, Matsuda M, Champeau EJ, Meyer LA, Edelhauser HF. Correlation of corneal endothelial pump site density, barrier function, and morphology in wound repair. Invest Ophthalmol Vis Sci. 1985;26(9):1191-201.

339. Yoon JJ, Ismail S, Sherwin T. Limbal stem cells: Central concepts of corneal epithelial homeostasis. World J Stem Cells. 2014;6(4):391-403.

340. Yorek MS, Obrosov A, Lu B, Gerard C, Kardon RH, Yorek MA. Effect of inhibition or deletion of neutral endopeptidase on neuropathic endpoints in high fat fed/low dose streptozotocin-treated mice. J Neuropathol Exp Neurol. 2016;

341. You L, Kruse FE, Völcker HE. Neurotrophic factors in the human cornea. Invest Ophthalmol Vis Sci. 2000;41(3):692-702.

342. Zhang L, Anderson MC, Liu CY. The role of corneal stroma: A potential nutritional source for the cornea. J Nat Sci. 2017;3(8)

343. Zhang W, Magadi S, Li Z, Smith CW, Burns AR. IL-20 promotes epithelial healing of the injured mouse cornea. Exp Eye Res. 2017;154:22-29.

344. Zhao M, Song B, Pu J, Forrester JV, McCaig CD. Direct visualization of a stratified epithelium reveals that wounds heal by unified sliding of cell sheets. FASEB J. 2003;17(3):397-406.